REPUBLIC OF TÜRKİYE

ALTINBAS UNIVERSITY

Institute of Graduate Studies

Mechanical Engineering

A COMPARATIVE INVESTIGATION FOR PV MODULES PERFORMANCE EQUIPPED WITH A BACK SURFACE COOLING SYSTEM

Ahmed Taha Yas AL-JUMAILI

Master's Thesis

Supervisor

Asst. Prof. Dr. Yaser ALAIWI

Istanbul, 2023

A COMPARATIVE INVESTIGATION FOR PV MODULES PERFORMANCE EQUIPPED WITH A BACK SURFACE COOLING SYSTEM

Ahmed Taha Yas AL-JUMAILI

Mechanical Engineering

Master’s Thesis

ALTINBAŞ UNIVERSITY

2023

The thesis titled A COMPARATIVE INVESTIGATION FOR PV MODULES PERFORMANCE EQUIPPED WITH A BACK SURFACE COOLING SYSTEM prepared by AHMED TAHA YAS AL-JUMAILI and submitted on 25/04/2023 has been **accepted unanimously** for the degree of Master of Science in Mechanical Engineering.

Asst. Prof. Dr. Yaser ALAIWI

Supervisor

Thesis Defense Jury Members:

Asst. Prof. Dr. Yaser AL-AIWI	Department of Mechanical Engineering, Altınbaş University	_____
Asst. Prof. Dr. Serdar AY	Department of Mechanical Engineering, Altınbaş University	_____
Asst. Prof. Dr. Ahmed SADIK	Department of Mechanical Engineering, Hasan Kalyoncu University	_____

I hereby declare that this thesis meets all format and submission requirements of a Master's Thesis.

Submission date of the thesis to Institute of Graduate Studies: ___/___/___

I hereby declare that all information and data presented in this graduation project has been obtained in full accordance with academic rules and ethical conduct. I also declare all unoriginal materials and conclusions have been cited in the text and all references mentioned in the Reference List have been cited in the text, and vice versa as required by the abovementioned rules and conduct.

Ahmed Taha Yas AL-JUMAILI

Signatur

DEDICATION

To my parents, family, friends, and all those who have contributed to my academic journey, I extend my heartfelt gratitude. Your unwavering support and encouragement have been instrumental in shaping my love of learning and passion for knowledge. Your belief in me has served as a constant source of motivation and has driven me to achieve this work. I dedicate this thesis to you with immense love and appreciation, in recognition of all that you have done for me.

PREFACE

I would like to extend my sincere thanks to Asst. Prof. Dr. Yaser ALAIWI, lecturer at Altınbaş University, Department of Mechanical Engineering, who was my supervisor during the writing of this research and who gave me the right direction by providing much correct advice, instructions, and information. Would also like to thank Assoc. Prof. Dr. Süleyman BAŞTÜRK, Head of the Mechanical Engineering Department at Altınbaş University, who in turn assisted immediately to solve all technical problems from laboratories and others. Also thanks to all the friends who supported, encouraged me and gave me valuable advice and information.

ABSTRACT

A COMPARATIVE INVESTIGATION FOR PV MODULES PERFORMANCE EQUIPPED WITH A BACK SURFACE COOLING SYSTEM

AL-JUMAILI, Ahmed Taha Yas

M.Sc., Mechanical Engineering, Altınbaş University,

Supervisor: Asst. Prof. Dr. Yaser ALAIWI

Date: April / 2023

Pages: 103

The operating temperature is the most important factor impacting PV module performance. When it exceeds 25 °C, the electrical power and efficiency decrease. The purpose of this research is to improve thermal performance and compare the performance of two common crystalline PV panel types (Mono and poly). Modules with a back-cooling system were designed and numerically analyzed with SolidWorks and ANSYS Fluent 2021 R2 for the simulation under Baghdad weather at noon. The cooling system used consists of a phase-change material, paraffin wax (RT55), with a thickness of 5 cm and a heatsink with 33 fins with heights of 10, 20, and 30 mm and thicknesses of 2, 4, and 6 mm. to select the best height of the wax 1-3-5-10-20 cm examined. The result showed for polycrystalline panel temperature reduced by 8.4 °C using PCM and by 11.9°C using PCM- fins. Also output power enhanced to 200.6 W by 10.2 W, and its efficiency improved by 5%. Similarly, the use of PCM and PCM-fins lowered the temperature of the monocrystalline by 8.3 and 12.5 °C, respectively. Therefore, raising the output power to 202.4 W by 10.7 W and improving the electrical efficiency by 5.2%. The results of the study showed that mono had better performance than poly. This result is acceptable and is in good agreement with previous

studies. The proposed cooling system also had an effective role in reducing the temperature and improving performance.

Keywords: Mono-Poly Crystalline, Paraffin wax, Heat dissipation, Ansys.

TABLE OF CONTENTS

Pages

LIST OF TABLES

Pages

LIST OF FIGURES

Pages

ABBREVIATIONS

ISC	:	Short Circuit Current
VOC	:	Voltage Open Current
Rs	:	Series Resistance
R-SH	:	Shunt Resistance
PCM	:	Phase Change Material
RT55	:	Paraffins Wax
N	:	Diode Factor
EGO	:	Band Cap Silicon
FF	:	Performance Factor
T cell	:	Cell Temperature
T_m	:	Ambient Temperature
TR	:	Reference Temperature
A	:	Area Of Model
G	:	Solar Radiation
μ	:	Kinematic Viscosity
h	:	Enthalpy
ΔH	:	Latent Heat
β	:	Liquid Fraction Of PCM
$\vec{V}$	:	Fluid Velocity

FB	:	Buoyancy Force
VP	:	Solid Velocity
Q_i	:	Internal Heat Production
GIT	:	Grid Independence
T_sky	:	Sky Temperature
T_g	:	Glass Temperature
K	:	Thermal Conductivity
Cp	:	Specific Heat
h	:	Convection Heat Transfer Coefficient
PV	:	Photovoltaic Panel
EVE	:	Ethylene Vinyl Acetate
TPT	:	Back Sheet Tedlar

LIST OF SYMBOLS

Cp	:	Specific Heat At Constant Pressure
H	:	Specific Enthalpy, Or Total Energy
P	:	Pressure
T	:	Temperature (Temp)
ŋ	:	Efficiency
ρ	:	Density
C	:	Specific Heat
W	:	Weight
τ	:	Transmissivity
α	:	Absorptivity
ε	:	Emissivity
Si	:	Silicon Cell
P	:	Power
V	:	Voltage
I	:	Current

1. INTRODUCTION

1.1 GENERAL

Clean energy is used to describe energy sources that regenerate themselves spontaneously and may be utilized repeatedly. Solar, wind, geothermal, hydropower, and bioenergy are some of these energy sources. In general, renewable energy sources are seen as more ecologically responsible and sustainable than non-renewable power sources, such as fossil fuels, which are limited and emit greenhouse gases when burned [1]. The use of renewable energy sources has several advantages. For instance, they can lessen our dependence on fossil fuels, which play a significant role in climate change. Additionally, renewable energy sources can offer a more consistent and predictable energy supply and often have lower long-term operational expenses. Additionally, the utilization of renewable energy may foster employment growth and local economic development [2]. Although the UN globalist agenda emphasised the necessity of developing green power and lowering pollution (CO_2 or NOx), facts indicate that these targets are not achievable under the existing structure. If global coal and natural gas usage continues at its present rate, the heat of the earth is expected to increase by 4–6 °C above what it was before industrialization.

A rise of this magnitude would be disastrous for the production of food, people's health, as well as biodiversity. It would jeopardise the existence of communities in so many places on the globe [3]. Solar energy has the potential to fulfill the world’s energy needs if it is exploited efficiently. Energy from the sun can be converted directly to electricity by photovoltaic cells (PV) or it can be converted thermally by concentrated solar power. In recent years, PV technology has become more attractive thanks to a considerable reduction in its costs. Solar energy system operating costs are frequently cheaper than those of non-renewable energy sources. However, PV cells cannot convert all of the energy in the solar spectrum due to their inability to utilize low-energy photons and the thermal energy produced through thermalization by high-energy photons [4].

The sun produces enormous amounts of energy, with the planet receiving about 1.8 x 1014 kW each day. This accounts for a large fraction of the sun's total solar power, which is calculated to be 3.8 x 1023 kW. Solar energy is a renewable resource that may be used to

power a variety of devices, such as solar water heaters, concentrated solar power plants, and solar panels [5].

The two crucial factors that affected a solar photovoltaic company's effectiveness were the dispersion and intensity of solar radiation. The two factors differ greatly across countries. Asia has the highest potential for solar radiation absorption compared to other warm countries since their year-round sunshine duration is greater figure (1.1) shows variation of solar radiation in Middle East. It's important to understand that a lot of solar energy is wasted since it isn't used [6]. Using semiconducting materials that show the photovoltaic effect, the process known as photovoltaic (PV) transforms light into electricity. When photons (light particles) from the sun or other light sources dislodge electrons from their atoms, a current of electricity is produced. Typically constructed of silicon, PV cells are organized in panels or modules that may be put on buildings such as walls or roofs. Since it has been around for a while, photovoltaic PV technology has grown in popularity as a method of producing power for use in homes, companies, and other purposes [7]. As shown in Figure1.2.

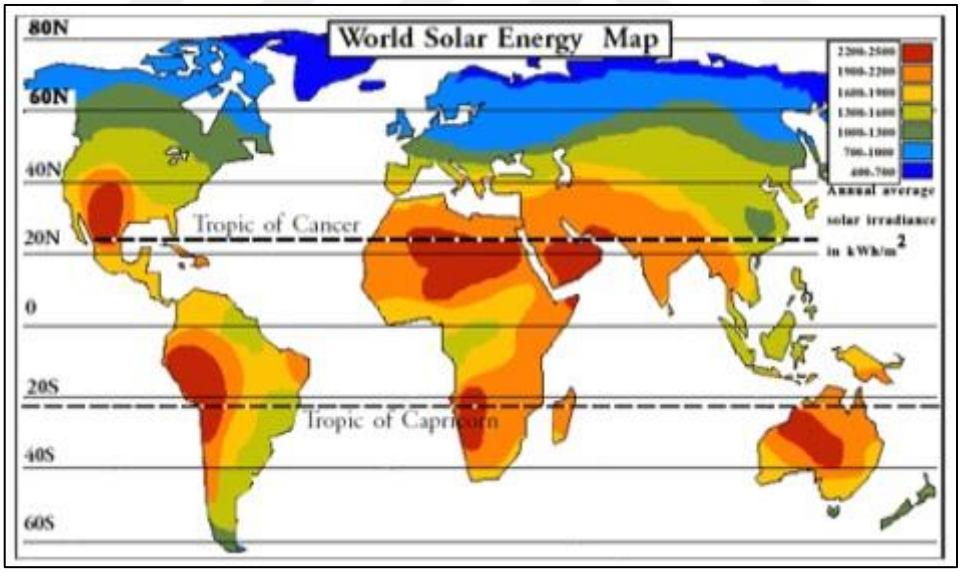

Figure 1.1: Solar Radiation [8].

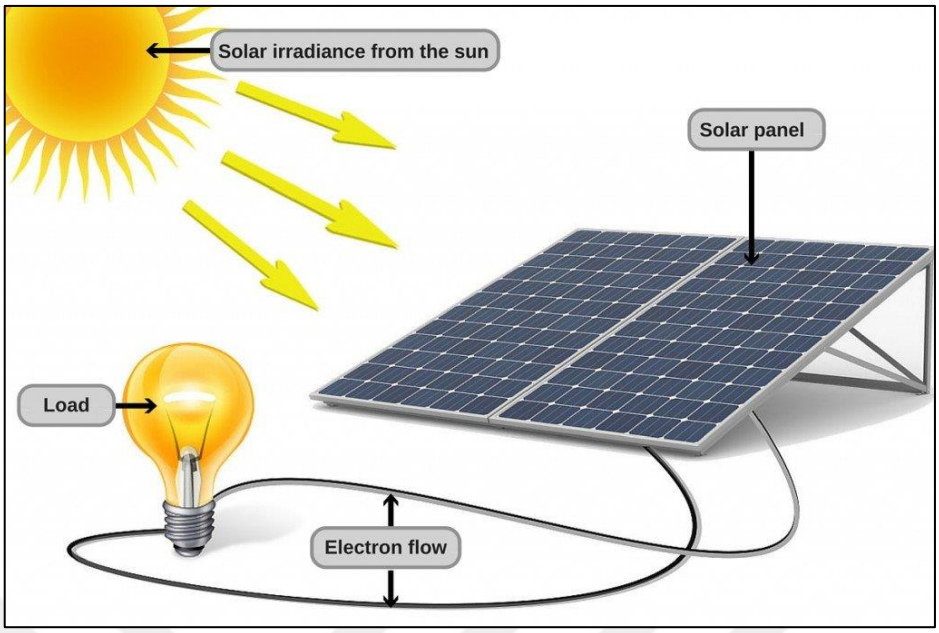

Figure 1.2: Converting Sunlight Into Electricity [9].

Because of their capacity to transform solar irradiation into direct current power, solar photovoltaic cells are commonly used as one of the most substantial green energy sources [10] [11]. The PV influence was discovered by Becquerel while researching the influence of sunlight on electrolytic cells in 1839. However, it took some time to achieve high enough efficiency for practical use. Solar cells saw significant progress in the 1950s due to their use in space programs, initially achieving efficiencies of 6–10 % with polycrystalline Si and C-Si solar cells.

The renewable energy movement of the 1970s also drove a lot of research and development in photovoltaic technology. Compound semiconductor solar cells, which are made from III-V and II-VI materials, were first researched in the 1960s [12]. Solar cells, which are used to convert sunlight into electricity, are not 100% efficient. In fact, only about 20% of the radiation coming in is transformed into electricity, while the rest is wasted as heat. This is because solar cells lose strength and efficiency as their temperature increases. High heat can also damage the silicon surface of the solar cell, which can affect the cell's performance. To maximize the productivity of solar cells, it is significant to keep them cool and protected from extreme heat [13].

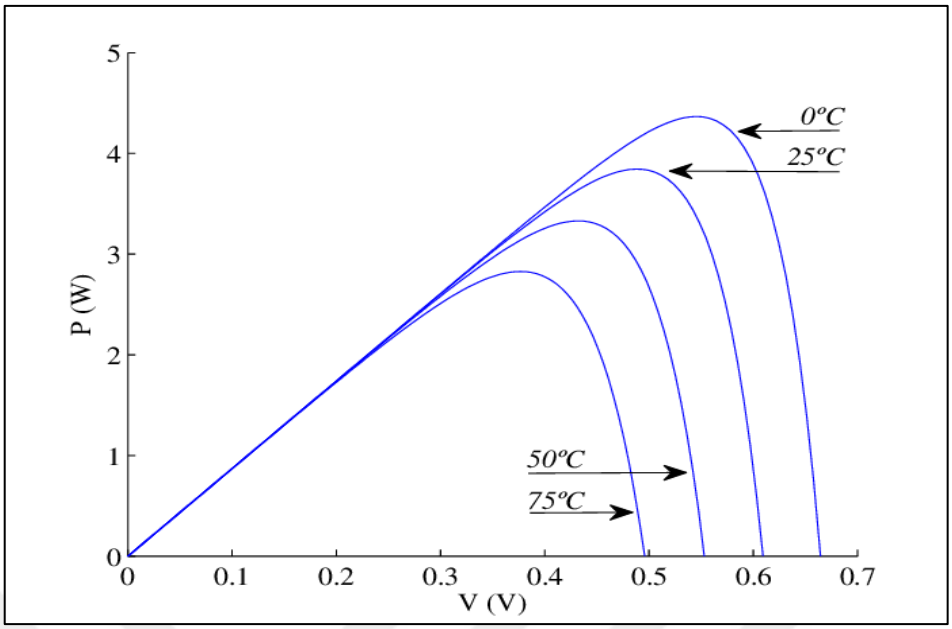

Figure 1.3: P–V Properties The Temperature Range Of The Module Is From 0 To 75 Celsius [13].

1.2 THE ORIGIN OF THE ISSUE

PV modules are quite sensitive to rising ambient temperatures. The power and performance of PV modules are reduced when the ambient temperature rises [14]. Solar cell power output P and voltage output V are connected through the P–V characteristic, assuming constant solar irradiance (E) and panel temperature (T_m). If Tm or E are modified in any way, the entire collection of attributes is modified. Figure (1-3) shows a temperature increase in a cell. The maximum current of solar cells decreases as the temperature increases. For every 1 degree Celsius increase, the output power of the cells drops by 0.5%. This means that overheating can significantly impact the production of solar cells [15].

Solar PV cells are the primary element of PV systems and are mainly semiconductor devices that can convert solar radiation into DC electricity when exposed to sunlight. Such an optical cell consists of a P-N junction formed on a thin light-sensitive material, primarily silicon. The P-N junction of the cell is formed by doping a silicon wafer with impurities, thereby creating two layers with different electrical properties. The physical process through which solar cells convert solar radiation into electricity is known as the PV effect [16]. As shown in figure 1–4. This demonstrates the science of transforming the absorbed light from the silicon cell into a current.

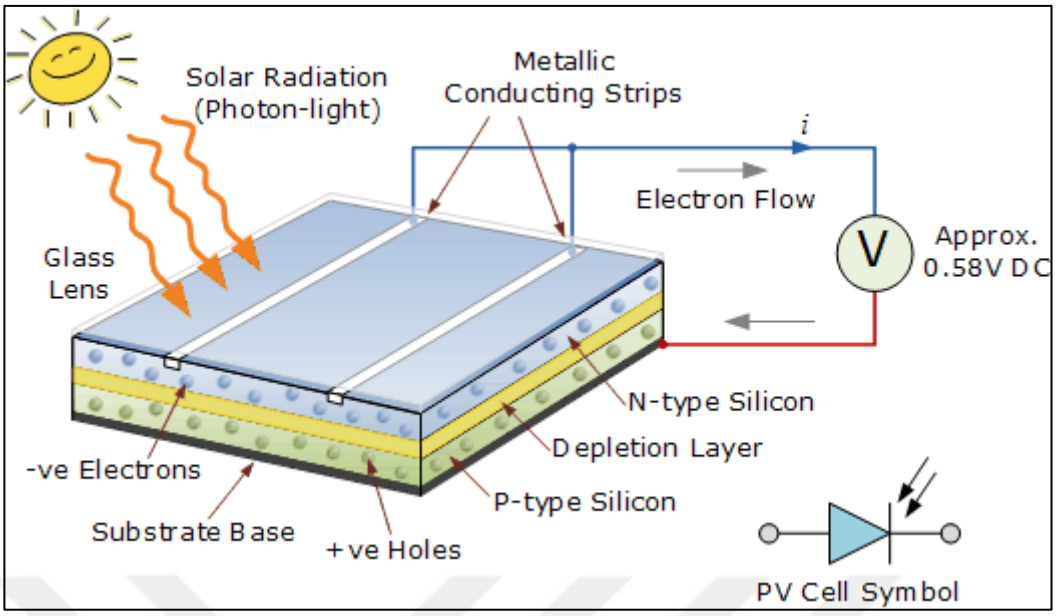

Figure 1.4: P-N Junction For Solar Cell [17].

A typical PV panel has layers of glass, silica, EVA, and PVF. Figure 1-6. Predicting the amount of heat absorbed by photovoltaic cells can be difficult due to the varying absorptivity coefficients of various materials. The heat output of photovoltaic cells is difficult to accurately determine due to factors such as cell efficiency, the environment in which the cells are used, and the material of the cells. Among other things, has an impact on the temperature of the cells. Of day, the tilt angle, and a material's emissivity and reflectivity. The amount of heat is determined by the amount of emissivity lost to the surrounding environment, but reflectivity determines how much heat is absorbed from the backside and frame of the model. The temperature of photovoltaics is generally higher than the ambient air temperature, leading to greater dissipation through heat loss rather than absorption through diffuse irradiance. Figure (1-5) [18].

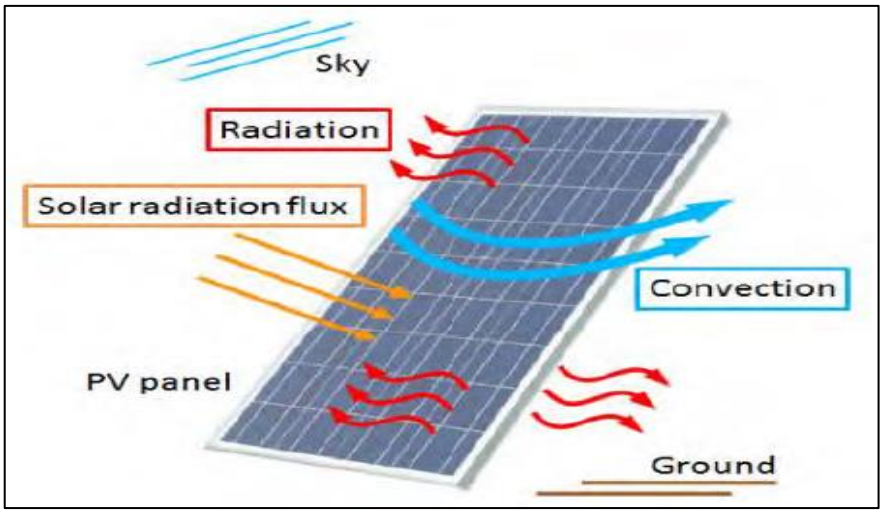

Figure 1.5: Heat Transfer In PV Panel [19].

In recent times, the efficiency of photovoltaic panels has significantly improved, with some reaching more than 16%. However, panels with an efficiency rate of 11.7 percent are still widely available and have been shown to experience a decline in performance when their cell temperatures reach 25 °C [20].

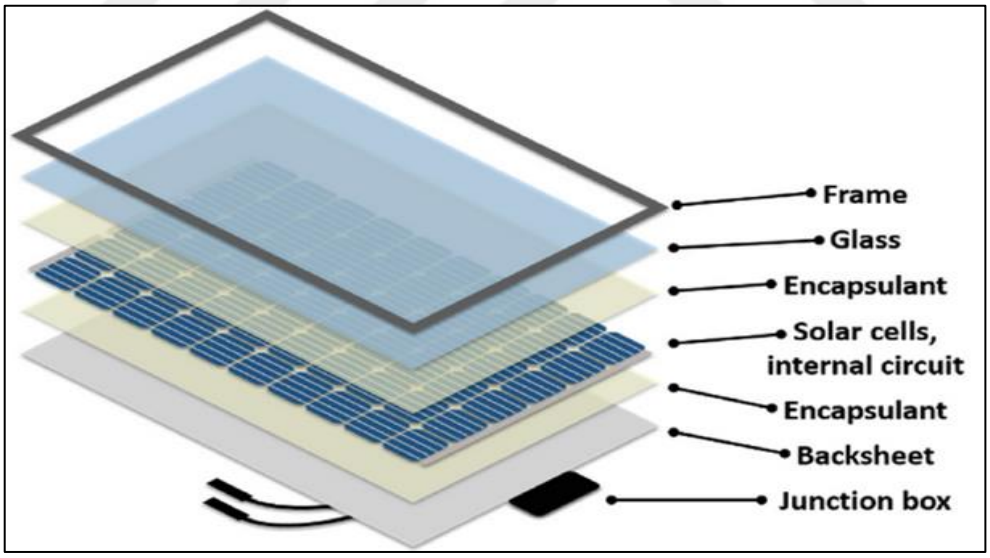

Figure 1.6: PV Panel Structures [21].

1.3 THE MOST COMMON TYPES OF SOLAR CELLS AND METHODS OF MANUFACTURING

The most popular types of panels are monocrystalline and polycrystalline solar panels figure (1.7), as well as silicon thin panels, and mono panels generally appear black because of more receptive to sunlight. This type of cell is more complicated to make and has a higher production cost than other panels since it is made by cutting a cylindrical silicon crystal into little pieces. The polycrystalline material is frequently blue, and the light reflection on the surface of the cell pieces is slightly varied. Polycrystals are created by melting and recrystallizing silicon metal. After re-cutting, the crystals are gathered in the shape of cells [22].

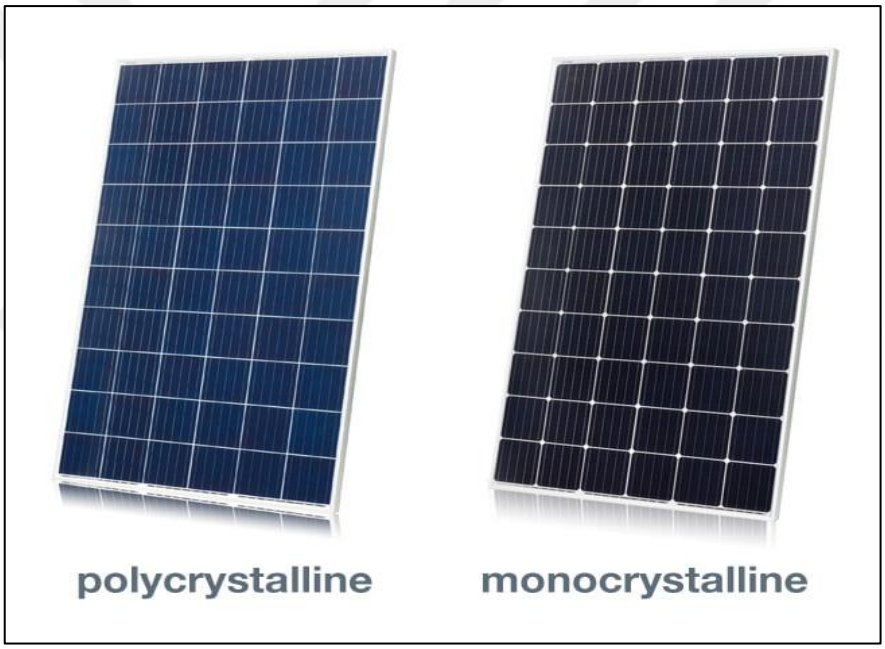

Figure 1.7: Mono-Polycrystalline Panels [23].

Photovoltaic items are available in a broad range of forms, dimensions, and hues. PV modules are produced by hundreds of businesses worldwide, each with a unique set of efficiency and cost restrictions. In addition, installation prices vary depending on the project and the equipment. According to Figures 1.8, there are three types of PV materials: crystal-clear silicon, tinny film machinery, and rapidly innovative technologies. One of the materials used most frequently in solar photovoltaic technology is silicon.

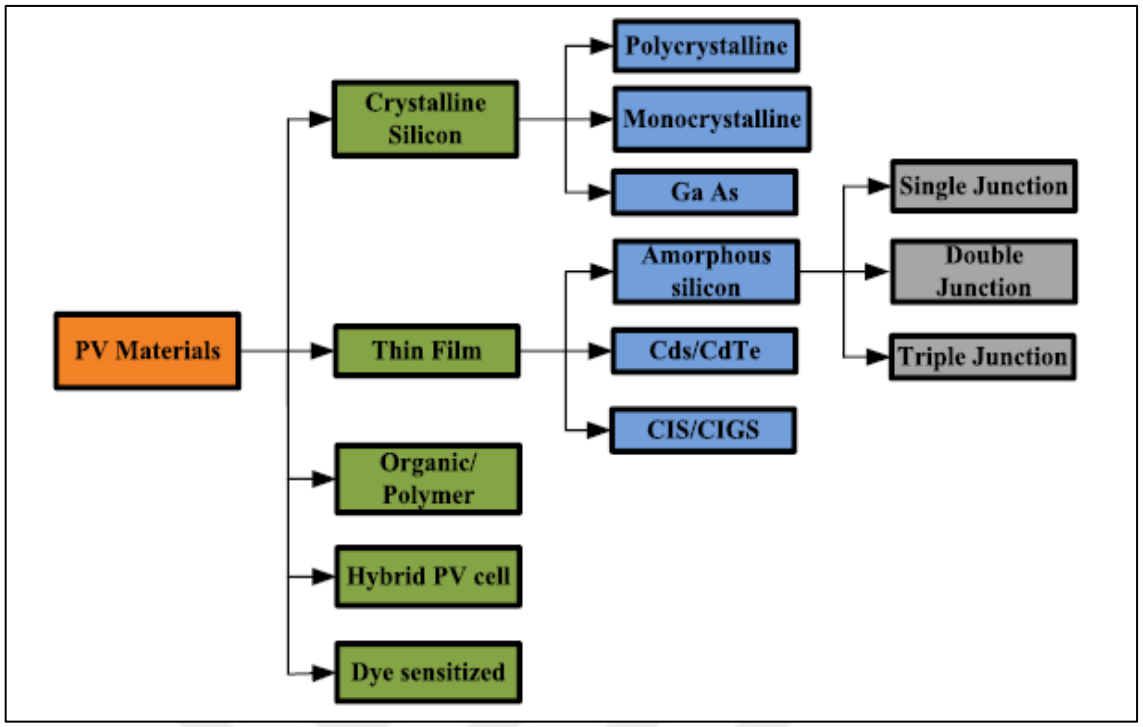

Figure 1.8: Solar Panels According To The Material Of Manufacture [24].

1.4 ENVIRONMENTAL INFLUENCES ON PHOTOVOLTAIC PANEL PERFORMANCE

1.4.1 Dust

Dust accumulating on the PV system due to gravity limits transmittance significantly, resulting in decreased performance of modern technology SPVs. Environmental dust, sand, and pollutants include both small and large particles of micro-to macro-diameters. The amount of dust that covers SPV is determined by geographical factors such as wind velocity, level above ground, soil characteristics, humidity, and temperature. The inevitable performance-lowering element of SPV is air pollution. Cleaning solutions like time-based washing, mechanical cleaning, as well as a dust-free coating on the SPV may all help to increase electric performance. The yearly mean concentration of particles has a diameter of 2:5 microns in the who data [25]. As shown the figure 1.9 cause Dust accumulation in the three main causes:

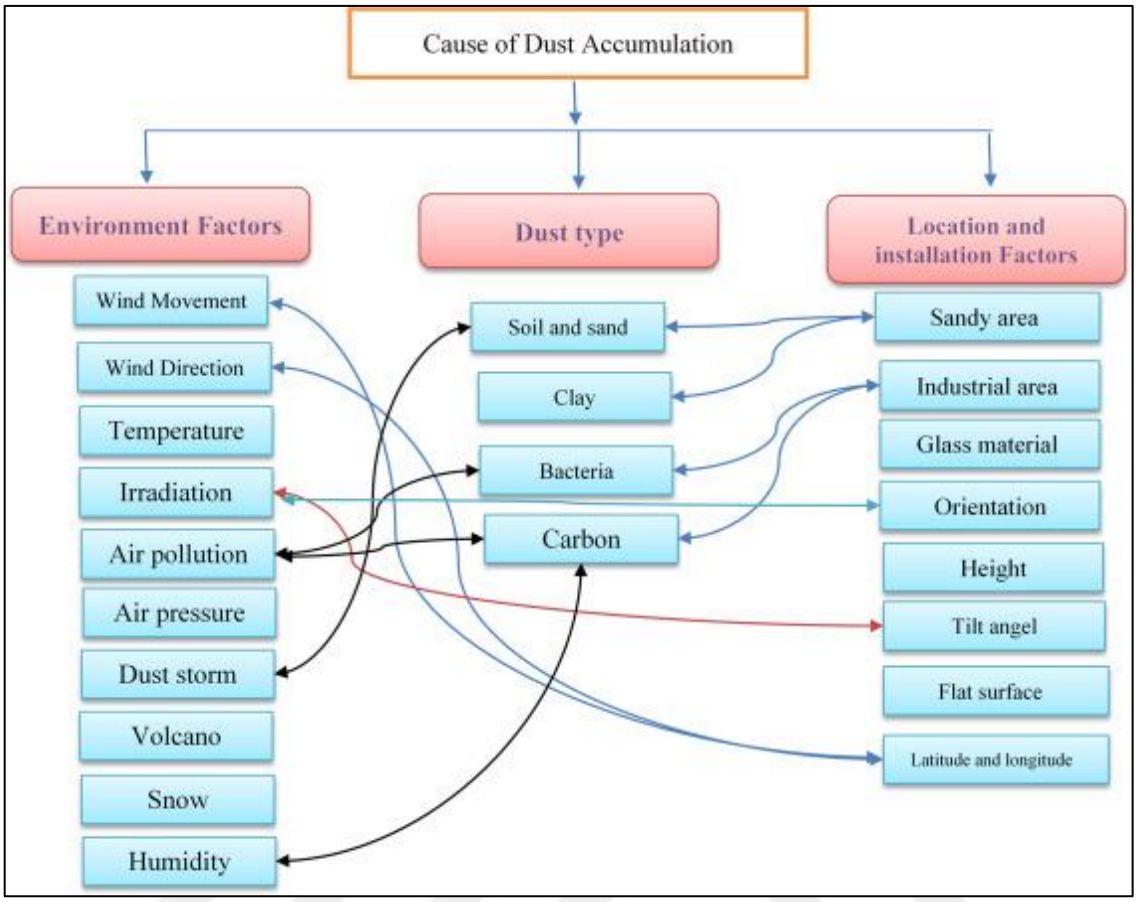

Figure 1.9: Shows Causes Of Dust Growth On Solar Modules' Surfaces [26].

1.4.2 Irradiance

The quantity of sunlight that strikes a specific surface is measured by irradiance. The quantity of energy a photovoltaic cell will generate depends on its irradiance. More sunshine equals more power. If only the sun was always shining. Irradiance fluctuates during the day; it is a fact. Irradiance rates can be impacted by the sun's angle, moving clouds, cloudy conditions, and air pollution. But the overall amount of energy the system takes in from the sun stays mostly unchanged throughout time. Typically, the sun's energy barely changes by 5 to 10% on an annual average [27].

1.4.3 Humidity

When a PV panel is exposed to high humidity for an extended length of time, part of the moisture level enters the panel's glass and begins to delaminate the cells. As a result, the panel's life span shortens, affecting the photovoltaic panel system's performance. It was

discovered that increasing the humidity by 50.15 percent reduces the solar radiation landing on the module surface by 24.05 percent. Furthermore, the panel's output current was decreased by 36.22 percent due to a 50.15 percent rise in humidity [28].

1.4.4 Location Geography

Since locations with different geographical and climatic circumstances have a substantial impact on the productivity of the solar board, location is a crucial factor when installing photovoltaic panels. The findings demonstrate that geographical location and climatic conditions have an impact on the appropriate tilt angle as well as the direction of a solar power system. Research shows that in the northern latitudes, photovoltaic modules oriented south with a slope angle comparable to the latitude achieved the system's greatest annual efficiency. In trials conducted in diverse geographical locations, tracking panels frequently produce more energy than stationary panels. An orientation tracking (one-axis) panel generated 20% greater daily energy production than a stationary panel, according to research done in Damascus, Syria [29].

1.4.5 Snow and Ice

A significant barrier to widespread solar photovoltaic adoption in cold areas such as Canada is coping with the impact of snow and ice building on the panels' faces. Photovoltaic plate production is contingent upon keeping photovoltaic surfaces clear of impediments like snow and ice. The issue is serious since even a small amount of snow on PV panels can dramatically lower the output of an entire string of photovoltaic panels. Snow damage to a photovoltaic system is estimated to be between 2.7 and 17 percent for a structure with a low-profile in Turkey, Californian, and 0.3-2.7 percent for an uncovered high-ceiling mount system in Germany. It depends on the tilt angle of the model, and weather conditions of the photovoltaic modules [30].

1.4.6 Shading

Shade can greatly affect the efficiency of PV model. When a single cell within the module is covered, it can lead to imbalances in the current production and a reduction in the panel's overall output power. This is because a shaded cell produces less electricity than an unshaded one, and since all the cells in a module are linked in series, the same quantity of

each cell must have electricity flowing through it. If the shaded cell is unable to handle the current passing through it, it may become overheated and potentially cause damage. It is therefore crucial to minimize shading as much as possible so as to optimize the effectiveness of solar panels [31].

1.5 PROBLEM STATEMENT

The heat of the photovoltaic modules is a crucial aspect that determines the amount of power they will produce. While more sunlight can be beneficial, it also results in a rise in the panel's temperature, which can offset some of the benefits. In reality, the most efficient solar photovoltaic panels only transform about 20% of the incident solar irradiance into straight current energy, with the majority of the remaining irradiation being reflected or absorbed by the module material as heat [25]. When the temperature of the environment rises by one degree Celsius, the panel's efficiency falls by 0.5% and its voltage falls by 2.2 mV. The high heat of the cell will have a detrimental influence on the model's ability to produce power [26]. There is a strong motivation to decrease cell base temperature through heat transfer and removal methods in the fastest and simplest technique possible.

1.6 OVERCOMING THE CHALLENGE OF HIGH TEMPERATURE IN PHOTOVOLTAIC PANELS

To deal with the issue of photovoltaic cells overheating, a number of assisted cooling methods may be used. However, choosing the best cooling system is crucial since it is mostly determined by the kind of PV production materials used and also by the climatic conditions in the locations where photovoltaic cells are installed, particularly during the summer months. Solar PV cooling systems may be separated into two groups: passive and active. Machines like air compressors or water pumps can be used to cool down PV modules without using more energy.

This method is called "active cooling," and it can be used on both the front and back of PV modules. Passive cooling involves removing or reducing the extra temperature of the PV board without ingesting extra energy, as well as naturally dissipating it to the ambient as shown in figure 1.10 [9]. Applying a layer of water over a solar module to reduce its temperature is one approach to cooling it. Water can lower the Temperature of cells by taking away the heat that the module generates during the day [22]. A cooling system

developed based on passive cooling induced by fans as cooling mechanism. A DC fan attached to the back side of the PV panel will extract the heat energy distributed and cool down the PV panel. As a result, it is concluded that there is an optimum number of DC fans required as a cooling mechanism for producing efficient electrical output from a PV panel [32]. In addition, the PV module may be cooled using a finned PCM container. The research allowed for an increase in efficiency of about 4.8 percent and 5.3%, respectively [24].

The working temperature of a photovoltaic (PV) unit has the biggest influence on its performance. A considerable percentage of the heat created by the board is dissipated into the environment, affecting the board's performance and efficiency. A comparison of two photovoltaic cells (mono and poly) will be performed. Both versions will have a back-cooling system that comprises paraffin wax (RT55) and a heatsink with aluminum fins to assist better thermal transfer of the module and release heat to the environment. Using the package ANSYS (fluent flow).

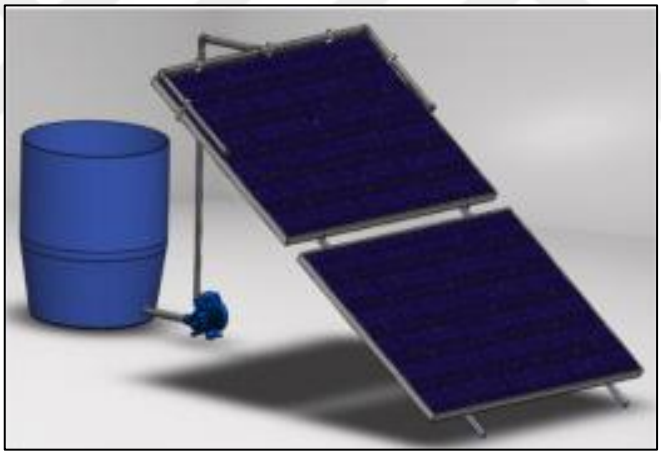

Figure 1.10: Active Cooling Methods [33].

1.7 AIMS AND OBJECTIVES

The current project aims to enhance the performance and output electrical power of two types of photovoltaic panels, monocrystalline and polycrystalline, by reducing the temperature of the solar cells, which are made of semiconductor materials such as silicon. As temperatures above 25 °C negatively impact the efficiency of the cells, reducing the temperature of the panels is of utmost importance. It has been established that there is a decrease in efficiency of 0.4% for every degree above 25°C. The study will involve a

comparative analysis of the performances of the two types of panels under challenging weather conditions, specifically in Baghdad City during the noon period, where temperatures are known to be high. The research will employ a cooling system that integrates phase change material (PCM) and a heatsink and use simulation software, Ansys Fluent, to predict the thermal behavior and performance of the panels.

1.8 THESIS STRUCTURE

The structure of the thesis was separated into five chapters.

Chapter 1. Comprises basic information about solar panel, problem statement, aim, and objectives.

Chapter 2. Give description of the heatsink process and PCM, and ways of improvement with a relevant literature survey of the current work.

Chapter 3. Contains the description of the electrical and thermal analysis, the electrical components, which include all of the electrical equations needed in power and electrical efficiency calculations, and the governing equations about energy, mass, and momentum for the liquid and solid phases.

Chapter 4. Describes finite element analysis for PV panel and represent the results obtained from (ANSYS software programs) and the discussion of those results.

Chapter 5. Conclusions and scope for future work have been stated finally.

2. LITERATURE REVIEW

2.1 INTRODUCTION

Photovoltaics is one of the most widely employed clean energy sources on earth. However, when the temperature of the PV cell rises, its electrical power decreases [31]. Which makes it important to find ways to develop the module's efficiency in high-temperature situations. One of the techniques used to raise efficiency and performance is cooling. A variety of ways of cooling solar PV panels have been used by researchers, including active and passive methods. Researchers used a forced air stream, PCM, a heat exchanger, water, and many other methods to make a solar PV thermal system work better. The major purpose of this chapter is to look at the significant information that the researchers found in their research about how to improve the efficiency as well as the performance of PV cells, how to cool them, and other reasons that affect the output of solar cells.

2.2 PHASE CHANGE MATERIALS (PCM)

In recent years, PCM have been used in a variety of applications, the most significant of which are cooling applications that utilise water and air because of their capacity to store enormous amounts of heat and then dissipate it through melting, despite their small size. While it comes in a variety of shapes and sizes, its primary applications include energy conservation in buildings and heat storage applications such as hot water tanks, as well as protecting food from extreme heat during shipping and storage. Finally, it was used in photovoltaic (PV-PCM) applications to raise the efficiency of solar panels, an area in which researchers have made tremendous progress, and the rise in panel efficiency was noticed when phase-changing materials were used [34].

Phase change materials are categorized into two fundamental types of organic materials: paraffin compounds (amino acids) and non-paraffin compounds, which have high thermal stability and are employed in low-temperature applications. Inorganic materials, like salt hydrates, are more common than their predecessors. To use in low and moderate temperature uses. The usage of (PCM) in house heating and cooling applications has been investigated. PCMs are adaptable, melting and solidifying across a wide temperature range,

making them appropriate for a variety of applications. Furthermore, such technologies benefit people and save energy as shown in figure 2-1.

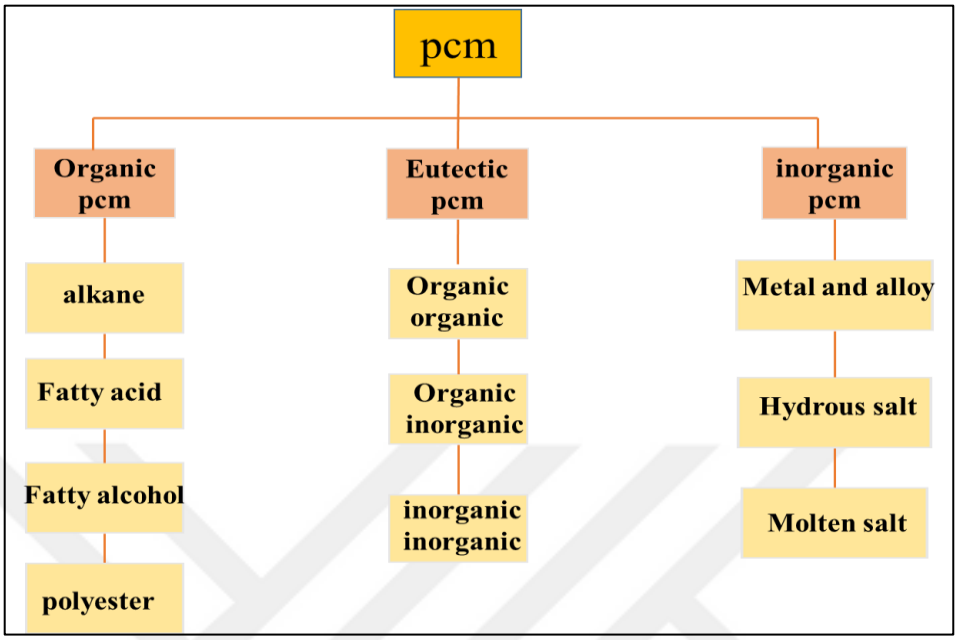

Figure 2.1: PCM Are Classified According To Their Properties.

Table 2.1: Type Of Commercial PCM [28].

Organic	Commercial PCM
Paraffin c 18	S27
Tetradecanol	RT30
Paraffin c 16-28	TH29
Paraffin c 13	RT25
Dodecanol	STL27
Paraffin wax	RT40- RT50-RT58

PCM are utilized for temperature regulation in several photovoltaic systems so as to decrease temperature-dependent photovoltaic efficiency loss. At three different degrees of insolation, the performance of each PCM was determined by evaluating four distinct PV/PCM systems. Modifying the mass and thermal conductivity of PCM was essential for the adjustment of PV temperature. The highest temperature drop of 18 degrees Celsius was obtained in 30 minutes, and a temperature drop of 10 degrees Celsius was maintained continuously for 5 hours [35].

A PV/PCM hybrid with two types of PCMs has been studied, and it can keep the PV at its normal working temperature of 25°C, improving solar energy conversion efficiency during varying diurnal insolation. The incoming energy is captured as heat by the photovoltaic and transferred to the PCMs via the high thermal cell wall. The PCMs' thermal management properties may keep the PV temperature lower for longer [36]. (PCMs) have been studied as a way to regulate the temperature of solar panels. By incorporating PCMs into the design of solar panels, it is potential to keep the temperature of the cells closer to the ambient temperature for longer periods of time when exposed to high levels of solar radiation. For example, research has shown that the use of PCMs can allow solar panels to maintain a temperature below 40 degrees Celsius for an additional 80 minutes when subjected to 1000 W/m^2 of solar radiation over a prolonged period [37].

Investigated on a global scale, the yearly growth in energy production provided by a photovoltaic structure with a phase change material core. PCM functions as a heatsink. In regions with little intra-annual climatic fluctuation, the PCM provides the cooling effects. When the ideal PCM melting point is used, yearly photovoltaic energy production increases by more than 6% in Mexico and eastern Africa, and by more than 5% in several other regions [38]. The study specifically aimed on the thermal characteristics of three separate PCM classes. The thermophysical characteristics of five solid–liquid phase transition materials were analyzed for usage in photovoltaic heat regulation applications. The components were separated into three major categories: wax, salt hydrates, and fatty acid mixtures. It is essential to examine the link between the thermophysical characteristics of PCMs and their usage as temperature managers and the external operation of PV systems [39].

A comprehensive heat transport analysis of the photovoltaic panel in conjunction with the PCM was done. This study determined the convection influences on the melted PCM, the wind velocity, and the PV board's slope angle. Then noted the panel's maximum working temperature when conduction and convection effects are combined is 54.90 °C, as well as 58.5 °C when convection in melted PCM is not included (just conduction mode). Additionally, higher wind velocity or a higher tilt angle have been shown to minimize the functioning temperature of PV panels [40].

The impact of adding phase-changing materials on power conversion efficiency, as well as increased lifetime in building-integrated photovoltaic, was examined. The primary purpose is to assess the operating temperature regulation for BIPV with and without PCMs under different climate conditions. The finding showed that PCM applications have a beneficial environmental effect because of used fewer resources to make BIPV. This is because PCMs can store heat and avoid major damage to the BIPV early in its life cycle [41]. The computational analysis and scientific experiment demonstrate that the use of PCM is capable of regulating the temperature of the PV model by ten degrees Celsius for around six hours in Malaysian conditions. These temperature decreases greatly enhance the productivity of the photovoltaic module [42].

The efficiency of solar panels was investigated by utilizing a variety of cooling configurations that included a variety of thermal absorber designs, coolants, and PCMs. According to this study, PV panels incorporating PCM are effective options for solar panel cooling [43]. After doing significant research on a number of natural and forced cooling methods for solar photovoltaics, previously employed systems have been deemed superior. For cooling, inactive cooling uses PCM paraffins such as wax, eutectics, natural material, cotton wick, etc., whereas active cooling uses gas, water, nanofluids, etc. Then noticed that the ambient temperature of the panel affects the conversion process, which has an effect on both electrical performance and efficiency. As the temperature of the cell rises, its performance degrades [44].

Figure 2.2: Melted PCM Pouring On The Rear Part Of PV [42].

The thermodynamic photovoltaic-PCM model was investigated to determine the mass, heat, and energy transfer mechanisms of a PCM positioned under a photovoltaic panel. The

appropriate PCM increases the created output energy to a high of 12.7 W. The highest functional temperature of the photovoltaic cell was lowered from 70.36 °C to 56 °C because the PCM's thickness increased from 1 cm to 3 cm [45]. To create a simplified model to calculate and analyze both the effectiveness and thermal functionality of the PCM system, in which they examined different PCMs' melting points and latent temperatures to select the appropriate PCM, and based on previous reviews, then discovered that the plate temperature decreased by about 10.1 °C and the efficiency increased by up to 3.73 percent [34].

PCM was applied to the backside of a photovoltaic panel. PV thermal management (PCM) is designed to absorb the excess heat of the PV panel, which allows for PV thermal control and energy power efficiency enhancement. The findings show that the PV temperature differential between photovoltaic systems without PCM and PV-PCM systems can reach 23 degrees Celsius, resulting in a 5.18 percent increase in the PV-PCM system's energy production [46]. To create a model to evaluate the PCM's functionality throughout the year and under different situations. Five modules were simulated, and the findings suggest that PCM performs well in the summer with a high melting point [47]. To improve the effectiveness of photovoltaic panels, PCM are used as a cooling technique. The influence of PCM physical properties, ambient conditions, and encapsulation design has been computed and empirically investigated. It can be demonstrated that the use of a suitable PCM can enhance the productivity of photovoltaic panels and PV thermal systems.

Then employed PCM to decrease the solar plate's heat and enhance the structure's ability to convert solar energy into usable power [48]. An analytical and experimental investigation was undertaken to calculate the impact of inclination angles on the efficacy of the solution. Procedure properties of a substance (PCM) when it is used as a heatsink behind a solar panel. Based on the data, when the angle of tilt went from 0 to 90 degrees, the melting time went down and the plate temperature went down by 0.4% to 12.0% [49]. Then investigated methods for cooling a solar panel with PCM on the backside of the PV model. Compared with the efficiency of free cooling and evaporative cooling with the PCM, they discovered that free cooling is more effective in hot conditions [50].

2.3 HEATSINK

Heat sinks are used to passively or actively cool a method, with or without the expenditure of other power. Heatsinks are constructed of heat-absorbing and heat-distributing materials. Because of their excellent thermal conductivity, copper and aluminum are often used in heatsinks. Heatsinks use variously sized and shaped fins to dissipate heat [51]. The dispersants were employed in conjunction with solar cells and had a considerable effect on lowering the panel's temperature, as the dispersants aid in heat dispersion to the surrounding region Figure (2-3) shows one type of heatsink and its operation [52].

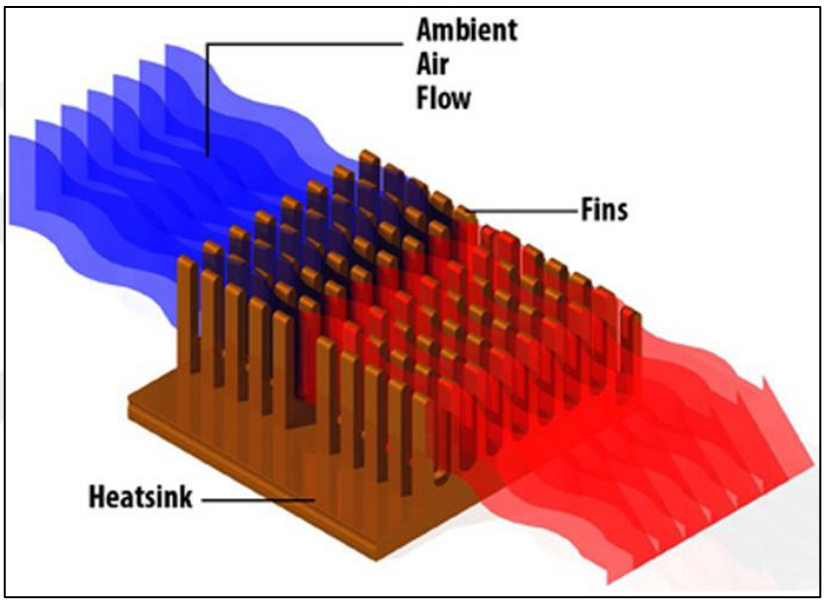

Figure 2.3: Heat Sink.

Researchers were able to study the impacts of four alternative thermal management methods on the thermal efficiency, point-based efficiency, and overall efficiency of a solar panel by mixing experimentally injected graphite with an externally finned heatsink. According to the findings of this study, this strategy was the most efficient way to improve the capacity of a solar panel by 12.97%. As a result, including graphite and an externally finned heatsink in the design of solar panels may be an efficient strategy to increase their performance and efficiency [53].The effectiveness of a solar cell coupled to a thermal sink cooling system was evaluated under varying levels of solar radiation as well as passive and active air cooling over the heatsink. As compared to a solar cell cooled by natural convection, the temperature of a solar panel dropped by convective heat transfer at 500 W/m^2 of incoming

heat flux increased as the solar irradiation increased. 5.4% of the solar panel heat is dissipated when the heatsink is cooled by natural convection, while 11% is dissipated when it is cooled by forced convection. This is because forced air flow has a higher heat transfer coefficient than natural air flow [7].

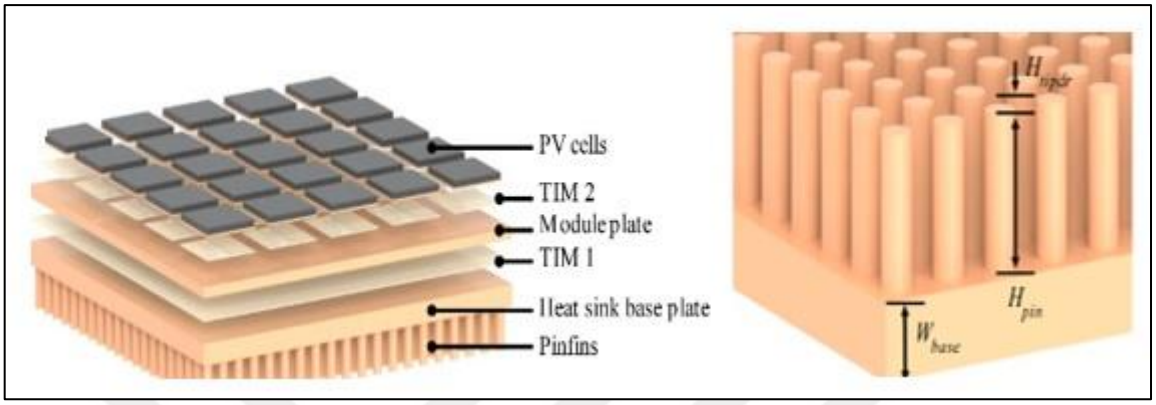

Figure 2.4: Heat Sink With Pin Fins [54].

Looked for a link between lowering the heat of a cell and variations in its performance and productivity in cells during normal operation circumstances and those with thermoelectric panel. According to the findings, the combination of a heat sink and a thermoelectric module lowers the heat of the PV panels, increasing their efficiency as well as output power. The cooling performance was optimum. In an ideal situation, the thermoelectric heat transfer cells could increase solar panel performance and power output by 10.50% [55].

In an effort to design a more effective method for cooling the cell, they evaluated the output of a PV cell using a finned mini-channel heat sink exposed to a high concentration ratio. The thermal conductivity of water was improved by introducing nanoparticles of alumina and silicon dioxide. Furthermore, there was a substantial improvement when the temperature of the fluid was increased. At a Re of 8.25 and a concentration level of 500, the system's overall efficiency improved by 3.82 percent [56].

Thermal control is achieved through the use of two layers of heat sink and a CPV cell. The cooling orientations of air in parallel flow and counter flow were examined. When the concentration ratio (CR) was 5, 10, 15, and 20, ethanol was used as a coolant to prevent the CPV from overheating. According to the experiments, when the inlet flow rate is raised, temperatures drop significantly [57]. According to the research, a heat sink was used to cool

a solar panel. The heat sink was cooled by two Nano fluids. The heat sink comprises an aluminum cover and two zigzag-channeled components.

At various Reynolds numbers, the heat sink and PV performance were evaluated for nanoparticle concentration. The introduction of alumina nanoparticles improves the thermal performance of solar cells. Increasing the (Re) number from 50 to 150 resulted in a 7% increase in thermal efficiency [58]. Analyzed cooling a solar cell module by increasing the back surface's heat transfer factor. The efficiency of a heat sink engaged on the backside of a panel is studied, as is the impact of fin height on heatsink performance. The panel's front and back surfaces achieved 62 °C as well as 51 °C, respectively, with a 20 mm heatsink fin height. When the fins were 300 mm long, temperatures dropped to 45 °C as well as 30 °C, respectively. The figure below shows a heatsink with a fin length of 20 mm

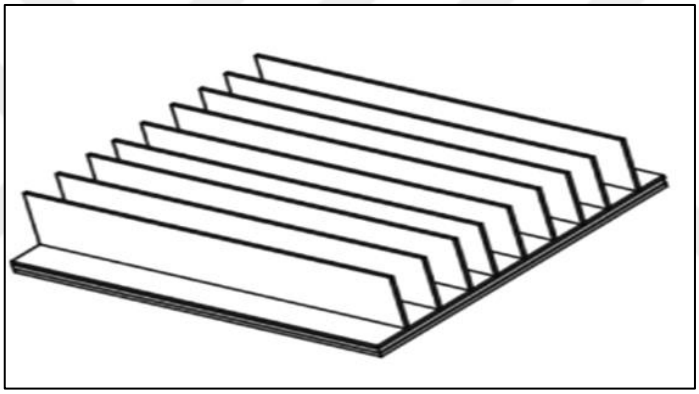

Figure 2.5: Heatsink With 20 Mm Fin Height [59].

They looked at the effect of cooling on solar model efficiency. They tested the efficiency of pv cells using a flat cooling channel as well as a finned channel placed at the rear of the model, and they discovered that the presence of fins increased the output of the model by 18.92%, and a drop in the panel temperature was recorded of 39.82 °C, after it was 57.91 °C without cooling [60].

To improve thermal efficiency, a passive cooling system comprised of a heatsink with aluminum and copper fins and a number of them (5–10–15) positioned at the bottom of the panel was applied. They found that increasing the number of blades increased the thermal effectiveness of the board, with 15 blades and an aluminum base yielding the best results. Finally, the board's temperature decreased by 10.2 C, and its productivity improved by 2.74 % [51]. It is possible to enhance a solar cell's efficiency by using numerical calculations

and air channels with varying air speeds fitted with a heat sink in the shape of a hexagonal pin-fin placed at the bottom of the panel. Thermal efficiency increased by 60.8 percent, and electrical efficiency increased by 13.1 percent as a result [61].

2.4 HEATSINK AND PCM

The effect of PCMs on reducing the temperature increase in integrated PV cells in buildings was investigated. Two particular PCMs were used to mitigate the overheating of PV cells. Thermal performance was offered to improve the thermal conductivity of the PCM for different inner fin arrangements by using paraffin wax RT25 with inner fins. The temperature rise of the PV/PCM system could be decreased by more than 30 °C as compared to a single flat aluminum sheet rest through a phase change [62]. Figure (2-6) shows PCM and heatsink for cooling electronic devices.

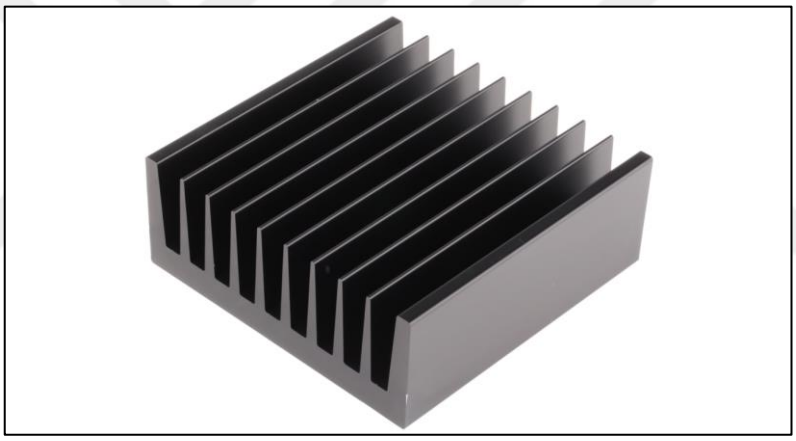

Figure 2.6: PCM With Heatsink [63].

The majority of the investigated natural cooling techniques are PCM-built, followed by air-based, liquid-based (water, nanofluids, etc.), and finally radiative-based. Based on the obtained results and known technical solutions, the air-based cooling option using Alfins installed on the PV plate back surface is currently the greatest practical passive cooling alternative, both technically and economically [64]. To forecast the transient temperature variation, a 2D model of the PV layers was constructed and connected with a stage change material and heatsink. When compared to single-hole and three- holes series heatsink arrangements, heatsink geometries with three also five equivalent cavities were shown to dramatically lower panel heat. Furthermore, it was discovered that using a five-parallel-hole heatsink considerably improved the solar cell's temperature uniformity [65].

In order to enhance the photovoltaic system and make the panel work better, a container with a phase-changing material and a heatsink was made and fastened to the posterior of the panel. In order to figure out how deep the container should be, the effects of the environment on wind speed, melting point, and ambient temperature, as well as the depth of the fin and the distance between them, were studied [66]. A new method to improve the efficiency of solar PV panels by using PCMs and aluminum panels such as TCE was proposed. They used two 5 W PVs; one was combined with an aluminum plate at the rear of the panel. The panel was compared to one combined with a naturally ventilated plate without PCM and aluminum. It was experimentally verified that the aluminum plate at the back of the panel enhanced its efficiency by an average of 24.4%. With a decrease in average temperature of 10.35 °C, the electrical efficiency of the plate increased by 2%. The maximum decrease in temperature was 13 °C for the first day and 7.7 °C for the second day [67].

Investigated Heatsinks with fins coupled with PCM substances were produced to generate an effective heat load and improve the efficiency of thermal conductivity. A big drop in temperature was seen, especially when there was a lot of heat flux [68]. The research looked at the numerical enhancement in photovoltaic cooling achieved by employing finned PCM (FPCM) heatsinks. The PV, PCM, and FPCM methodologies were tested in the Southeast of England's atmospheric conditions. Experience has shown that PCM heatsinks may reduce the maximum PV temperature by about 13 K, while FPCM heatsinks can enhance PV cooling by 19 K.

Figures demonstrate that PCM heat sinks may boost PV output energy from 13% to 14%. Figure (2–7) [69]. Assembled and examined three distinct PCM containers, including grooved, tubed, and finned containers, to increase the output power of a PV structure (PV). The finned container proved to be the best in terms of cooling. the outcome, the heat of the PV units dropped a lot, allowing them to produce the most electricity possible [70]. A numerical study was done to lower the temperature. Of electrical devices by using a mixture of phase-changing materials and heat dissipators of various shapes and sizes to raise the bad conductivity of phase-changing materials, and a significant improvement in thermal performance was observed [71].

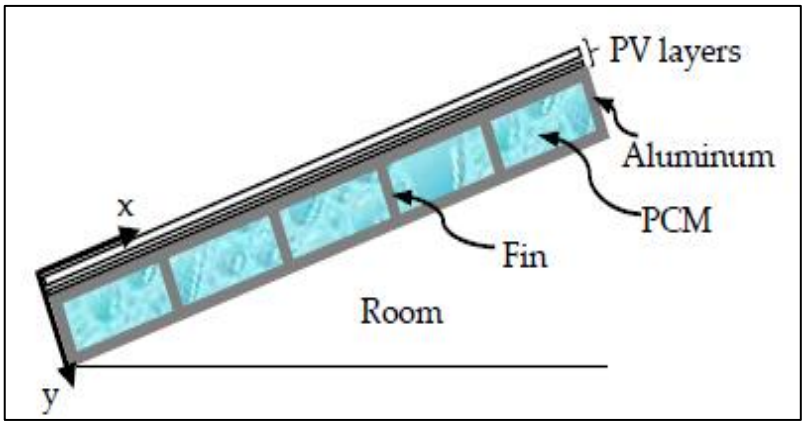

Figure 2.7: Components Of The Heatsink With PCM [69].

2.5 COOLING STRATEGIES THAT CAN BOOST THE EFFECTIVENESS OF PV MODULES

The adoption of a unique micro-pipe array enhances the cooling of the solar model. Natural convection cooling devices in both air and water were evaluated. When the average radiation amount is 26.3 MJ, the largest variations in photoelectric conversion efficiency (2.6 percent), maximum temperature drop (4.7 °C), and maximum output power (8.4 percent) are observed. When average radiation is 21.9 MJ, the water-cooled solar plate with heat pipe surpasses the air-cooled type by a maximum of 3% in photoelectric conversion efficiency, 8% in temperature reduction, and 13.9 percent in output power increase [72].

A new study on a hybrid solar energy system combining thermal and photovoltaic technology to actively cool photovoltaic cells revealed that a series of channels with only an entrance and exit were placed to the back of the photovoltaic board to ensure equal airflow distribution. In certain tests, active cooling was utilized. Temperature and efficiency are linear. Without active cooling, the module becomes extremely hot, limiting the solar cells' efficiency to 8–9%. When solar cells are operated with active cooling, their efficiency increases to between 12 and 14% [71]. Then worked to cool the photovoltaic panel by using a wind-powered roof-top turbine blower. Solar cell cooling and ventilation were accomplished in the same process. The wind-turbine ventilator was powered by a dynamo. To improve the productivity of the solar cell, air was circulated beneath it using a blade. Along with the ventilator's normal breathing, this combination increased the output power of the photovoltaic cell by 46.54 percent [73].

Active evaporative cooling is utilized to reduce the PV heat. Increase caused by solar irradiance absorption on PV modules was tested. He coated the rear of the panel with synthetic clay and allowed a thin layer of water to evaporate. The findings indicate that the suggested technique is technically possible, as it achieves an output voltage gain of 19.4% at its maximum. as well as 19.1% in output energy [74]. To boost the effectiveness of PV plates, they have created a unique method. This entails adding a thin layer of oil to the front side of the PV plates to improve the quantity of sunlight that the plates receive and, consequently, their efficiency. To examine several oils, including mineral oils and natural oils. The output of the photovoltaic panel has been examined. Labovac oil lets more light through than other oils, so it has been found that covering modules with a thin film of Labovac oil, about 1 mm thick, makes the model more than 20% more efficient [75].

In Egypt, an alternative cooling method for PV panels was evaluated. Instead of a compressor, a heat exchanger uses a soil heat exchanger to cool the rear of a panel. The thermally pre-cooled airflow across the back of the panel at an ideal ratio of 0.0288 m3/s was successful in moderate the board's temperature from 55 °C (without cooling) to 42 °C. The photovoltaic panel's electrical output improved from around 18.90% to 22.98% at this optimal flow rate[11]. The experiment to cool solar panels with saturated activated alumina and saline water is presented. At varying radiation levels. In the 6-hour test, two irradiation levels of 800 W/m2 and 1000 W/m^2 were used.

The salt influence, mostly on activated alumina tablets, was monitored for four months. Internal and exterior design changes recommended increased system cooling by 3–4 Cover previous configurations [76]. They developed a novel cooling method that works with solar panels. The thermo-magneto-generator system operates as both a thermal dissipater and an electrical generator. The cooling technique improved efficiency by over 99%. The peak generation is 1.6 mW/m^2 [77]. A cotton fiber mesh is used to make the plate's back surface cooler; this mesh takes in water from a pipe and transmits it down the slope of the device by capillary action. During the experiment, the temperature decreased by 23.55 degrees Celsius. As a result, the power of the panel increased by approximately 30.3 percent [78].

To used hydrogel beads soaked with Al_2O_3 liquid nanofluid to cool solar panels. With 0.5 percent wt., the surface temperature dropped from 17.9 degrees Celsius to 17.1 degrees

Celsius. From a performance standpoint, 0.5 percent wt. provided the best results, but due to the cost of nanomaterial's, 0.25 percent wt. concentrations are the most cost-effective option [79]. A smart water spraying approach that ineffectively solves a critical gap faced by the PV cell during hot weather situations. The use of an Arduino board to implement a microcontroller temperature control water spray device improved the effectiveness of the solar cell. The study used a temperature control feedback system and made a cooling algorithm for solar collectors. This made the PV panel array about 16.65% more efficient [80].

Investigated was the effectiveness of polycrystalline photovoltaic cells when cooled by evaporation. Under similar circumstances, cooled PV panels outperformed uncooled PV panels in terms of efficiency and output. Evaporative convective cooling uses a wetted cloth on the cooling channel's bottom surface. When a 120 mm air gap was used to cool the solar model, it increased daily energy output and efficiency by about 1.7 and 1.2 percent, respectively [13]. Water-based photovoltaic systems. This technology reduces the photovoltaic panels' temperature by 5–6 °C. From a thermal and electrical energy production standpoint, the solar PV absorber system is perhaps the most economically advantageous. Self-contained PV systems might benefit from water evaporation on the rear of the panels by utilising mud and cotton wicks. Solar panels in dry climates benefit from dual cooling [81].

2.6 VARIABLES THAT INFLUENCE SOLAR CELLS' PRODUCTIVITY

The impact of a variety of reasons on the panel temperature of selected PV methods in Singapore was examined, including material, ventilation, module frame, and other ambient circumstances. The monitoring findings revealed that the temperature rose between the lowest and highest temperatures. Readings varied due to three factors. When the temperature of silicon wafer-based modules is increased by one degree, power consumption decreases by 0.45% [82]. Modified initial conditions such as clear conductors, metallic pattern conductivity, and low light intensity allowed for grid design as well as finger size optimization. The results show that a metal grid with 20-lm broad lines would enhance the performance effectiveness of the solar board by 11.7% [83].

The impacts of external influences on the module's temperature were explored. The sun, wind, temperature, and distance between neighboring cells were all taken into account. The solar panel layer reached a maximum temperature of 331.76 kelvin. Additionally, lighter irradiation facilitates the solar module's thermal dissipation, hence increasing its temperature. When the wind speed goes from 0 meters per second to 1 meters per second, the efficiency of a solar module also goes up [84]. The influence of humidity on solar panel output was tested in a lab. After measurement of PV output (voltages and currents), solar radiation incident studies show that when humidity increases, solar irradiance and panel power production decline. The panel's output power decreases by 34.22 percent for every 50 percent increase in humidity [28].

The distance between the panels and the roof impacted the ability of free airflow to detect the temperature of the panels. It was discovered that the performance of the panels was influenced by the natural airflow beneath them. The amount of solar irradiation, distance between solar models, and so on were also investigated. The average temperature of a PV group without an air cavity is about 12 c greater than that of a PV array with an air gap of more than 200 millimeters and about 18 c higher widened to 250 millimeters [85].The influence of dust depletion on the electrical output of the SPV was examined, as well as an experimental examination of the output power sensitivity throughout dust depletion. Sand storms, levels of pollution, and snow quantity all have a significant influence on SPV's performance. These difficulties reduce solar panel efficiency and have a detrimental influence on electrical performance [25].

Snowfall on photovoltaic panels can significantly reduce power output, as shown in figure 2-8. This effect must be precisely anticipated to be considered a reliable source of energy. There were other topics they investigated. To examine both engaged and cumulative solar irradiance, Furthermore to the thermal capacitance of the PV panels [86]. Hand scrubbing, vacuuming, and electrostatic precipitation are some of the cleaning techniques used. This cleaning procedure has the potential to increase the panel's efficiency by 15-20% [87]. Then found that the dust reduces the adequate sunlight received by the solar cells, lowering the output. So cleaning routines are implemented to increase panel performance. The more frequently you clean, the better, though this may require more energy and the gain may be insufficient [88].

Figure 2.8: The Effect Of The Snow On The Model [89].

3. THEORETICAL ANALYSIS

3.1 INTRODUCTION

This chapter will go through all of the governing equations and boundary conditions utilized in the numerical work. There are two sections in the chapter. The first is the electrical components, which includes all of the electrical equations needed in power and electrical efficiency calculations, and the second is the thermal model. Understanding solar panel thermal and electrical performance with Ansys Fluent 2021 R2 software

3.2 ELECTRICAL AND THERMAL ANALYSIS

The ability of solar panels to produce energy is influenced by a number of factors. We will talk about two of the most crucial elements in this simulation study: solar radiation and panel temperature. A solar panel's variations in voltage, power, and electrical efficiency are accompanied by variations in panel radiation and temperature. To display the generation current, use the following formula (3.1):

$$I = I_{LG} - I_{OS}\exp\left(\frac{q}{nkT_P}\left(V + IR_f\right)\right) - 1\Bigg] - \frac{V + IR_S}{R_{SH}} \tag{3.1}$$

Where:

The charge of an electron is a well-known value, designated as q, and it is equal to 1.602*10^-19.There are several factors that can have an impact on performance of PV panel, including the air temperature (TP), the resistance within the panel's electrical circuit (Rs and R-SH), the energy of the silicon band gap (EGO), and the size of the panel (A).Coulomb's constant (n) is a factor that determines the efficiency of the diode within the panel, and it can range from 1 (for an ideal diode) to 2 (for practical diodes) [90].

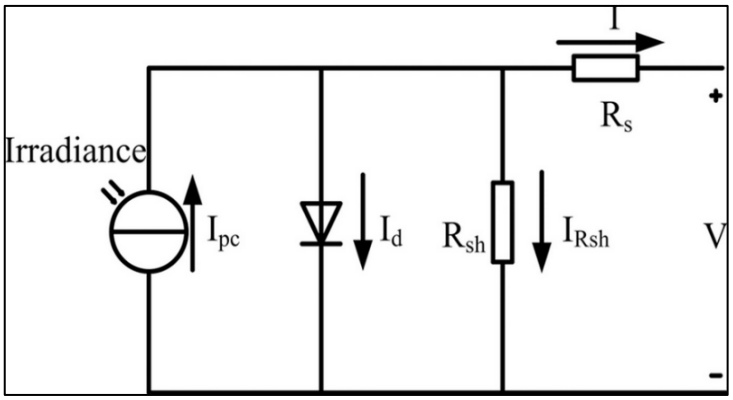

Figure 3.1: Electrical Equivalent Circuit Of A Photovoltaic Module [91].

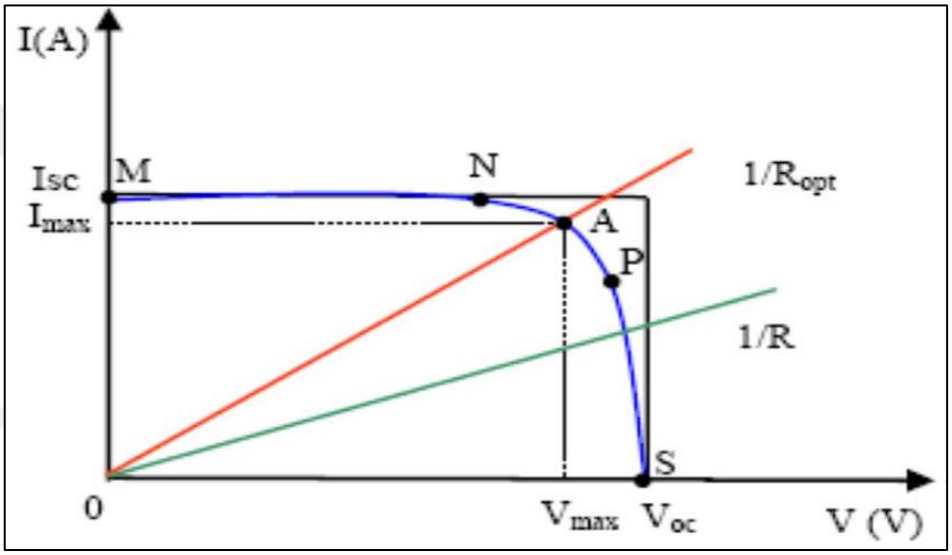

Figure 3.2: A Typical Current-Voltage Curve For Solar Cells.

Figure 3.1 shows the equivalent electrical circuit of a PV cell, where the current is represented at the output terminals. This current equals the light generated current. The internal resistance of the PV cell consists of the series resistance, Rs, and the shunt resistance, Rsh. For an ideal PV cell, Rs = 0, which means that there is no series loss, and Rsh = ∞, which means that there is no leakage to the ground. The short circuit current, ISC, is the highest current that a PV cell can produce when the cell is shorted. Meanwhile, the open circuit voltage, VOC, is the highest voltage at zero current flow when the two terminals of the PV cell are disconnected [92].

On Fig. 3.2, point A, also known as the max out power point, is the functional point (P-max) at which the power is maximized [93]:

$$P_{\max} = I_{\max} V_{\max} \tag{3.2}$$

$$P_{\max} = I_{sc} V_{oc} FF \tag{3.3}$$

Where

$$FF = \frac{P_{\max}}{I_{sc} V_{oc}} \tag{3.4}$$

This formula can be employed to calculate the electrical efficiency of the module at (p max)

$$\eta = \frac{P_{mp}}{GA} \times 100 = \frac{I_{mp} V_{mp}}{GA} \times 100 \tag{3.5}$$

Where A is area of photovoltaic panel [94].

The following equation can be used in the Ansys program to compute the electrical efficiency of solar cells [40].

$$\eta_{\text{cell}} = \eta_{\text{ref}} [1 - \beta (T_{\text{cell}} - T_{\text{ref}})] \tag{3.6}$$

Where reference panel efficiency is given by η ref=15% and β_ref, and temperature coefficient is equal to 25°C, 0.3%, 0.4 %respectively. G indicates the standard solar irradiation: G = 1000 W/m2. For most PV cells, such values are supplied by the manufacturer's product page [95].

A PV module's electrical power production can be evaluated as [96].

$$P_{\text{out}} = \eta_{\text{ref}} [1 - \beta_{\text{ref}} (T_{PV} - T_{\text{ref}})] A G_{\text{module}} \tag{3.7}$$

3.3 COMPUTATIONAL ANALYSIS USING ANSYS PACKAGE

The study of forecasting fluid flow, heat and mass transfer, chemical reactions, and related phenomena by solving numerical solutions to the underlying mathematical equations is known as computational fluid dynamics (CFD). Mass and momentum are both conserved. Energy conservation, species conservation, and body force effects [93]. Computational fluid dynamics studies are carried out to gain a better understanding of the heat flow field

[47], whether for PCM or solar panels. The numerical solution techniques will solve the Cartesian coordinate system to optimize the system's analysis and extract the results of the cooling effect of the solar panels using PCM and Heatsink (x and y). Monocrystalline and polycrystalline panels both have two-dimensional geometry.3D models by SOLIDWORKS programmed version 2021 and ANSYS software are used to create the panel's model. The ANSYS version 2021R2 will be used to design and engineer the system grid as well as to simulate two types of solar panel cooling using two different types of solar panels. The ANSYS version 2021R2 will be used to design and engineer the system grid as well as to simulate two types of solar panel cooling using two different types of solar panels.

3.3.1 Assumptions

The running liquid in the present study is PCM, and the flow parameters are assumed to be:

i. Transient

ii. 2-D

iii. Newtonian

iv. Incompressible

v. Laminar flow

3.3.2 ANSYS Package

The flow equations are resolved by using two parts:

i. The primary module is preprocessor module; a program structure that generates the grid and geometry as in the following:

a. Modeling of geometry.

b. Mesh generation.

ii. The secondary is the Solution module, for solving solidification and melting (which includes continuity, momentum, and energy).

a. Set-up and Boundary conditions.

b. Results.

3.3.2.1 System geometry

The solar panels, the phase-changing material container and the heat sink fins were designed in the Ansys Design Modular. It was taken into account that the design process was conducted out in 2 steps. The 1st step represents the design of the heat sink in a flat and is linked with the solar panel. The complete design geometry of the present system is indicated in the Figure 3.3.

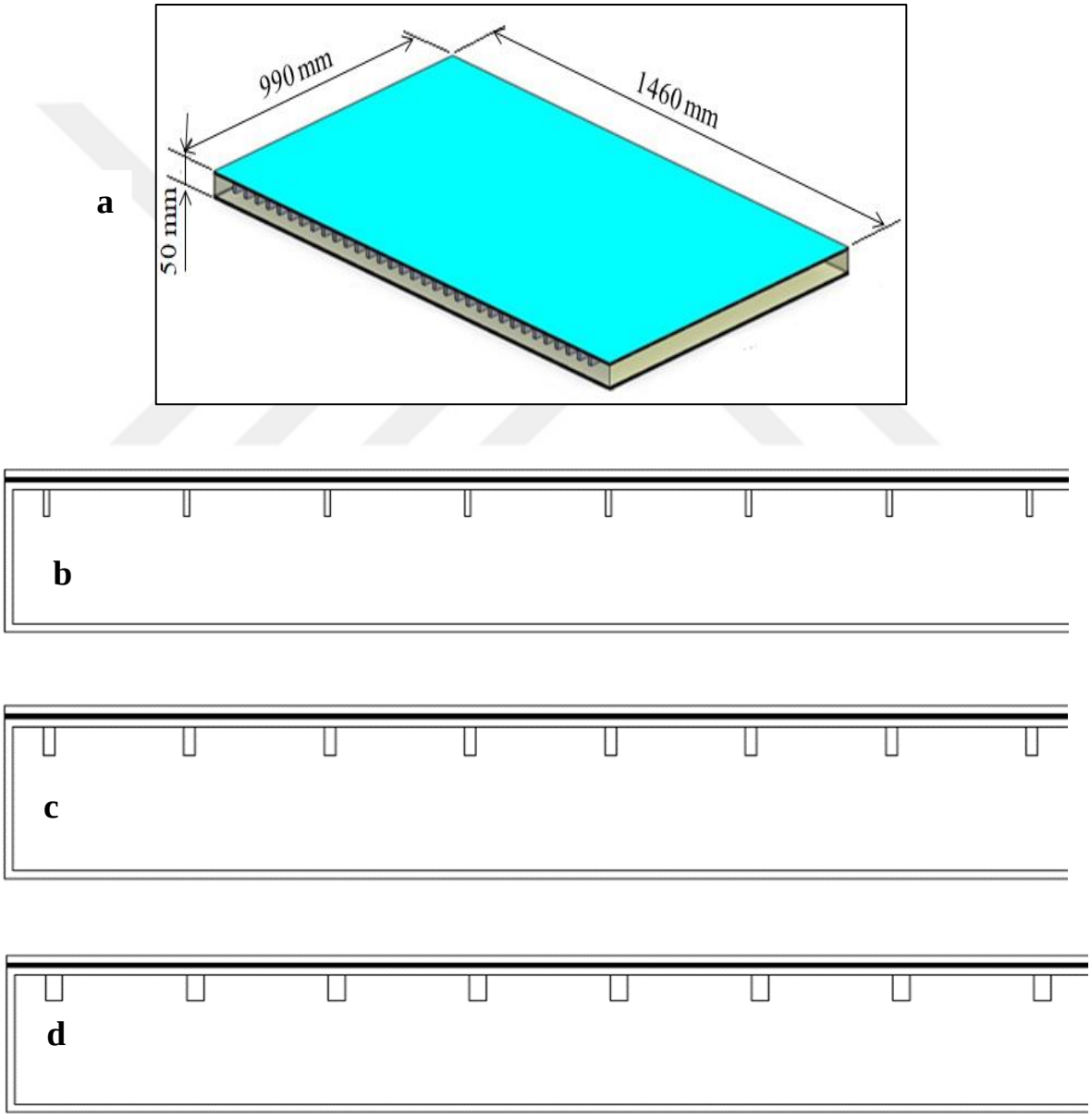

Figure 3.3: A) Overall Design B) (H=10, T=2) Mm, C) (H=10, T=4) Mm, D) (H=10, T=6) Mm.

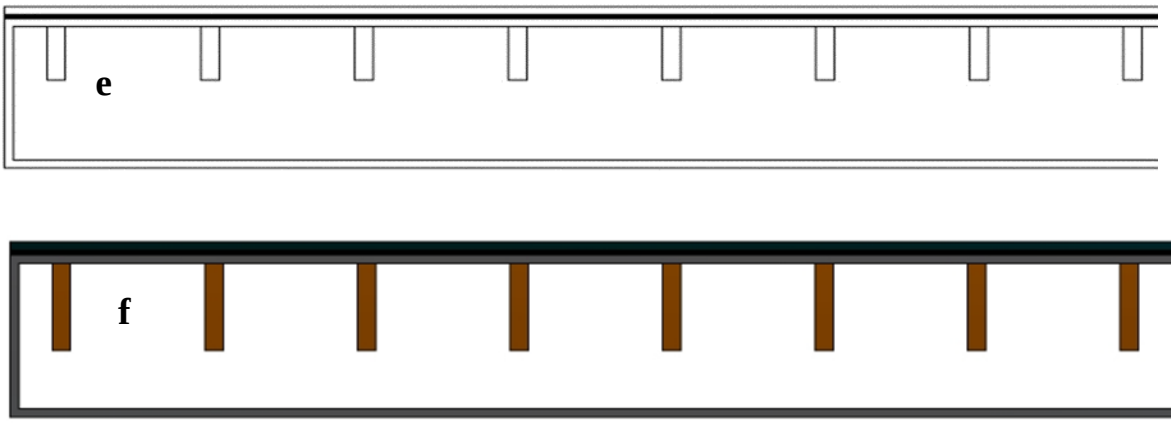

Figure 3.4: E) (H=20, T=6) Mm, F) (H=30, T=6) Mm " Figures Continued ".

Where changing the dimensions of the fins was studied differently, where a different thickness of fins was used for each case 2mm, 4mm, 6mm, which represents the dimension (t), and the distance between one fin and another represented by (d), which is equal to about 46 mm, as for the dimension (h), which represents the length of the fin, three lengths of fins were taken: 10mm, 20mm, and 30mm. Certainly, the change includes the height of the phase changing material to see the effect of height on the results, where three dimensions were taken from the height of the phase changing material 1mm, 3mm, 5mm, 10mm, 20mm, represented by the dimension (H). The thickness of the aluminum container is considered constant as 3mm represented as (δ).

3.3.2.2 Mesh generation

The quality of the mesh plays a significant role in the accuracy and stability of the numerical computation. The attributes associated with mesh quality are node point distribution, smoothness, and skewness. Regardless of the type of mesh used, checking the quality of your grid is essential. Depending on the cell types in the mesh (tetrahedral, hexahedral, polyhedral, etc.) Generally, for the reasons stated above, structured grids are useful for complicated geometries; the structured hexahedron grids were generated and used in the current study, which is depicted in figure 3.5 below. The first thing to do is implement a Grid Independence Study (GIT) so as to get the most relevant mesh cell count and an accurate solution that is not changed as the mesh size is changed. About seven tries have been conducted to choose the optimum mesh, and this is shown below in figure 3.6. The

temperature and power after changing the cell count from 240,000 to 270,000 have not significantly changed, hence the 240,000 cell mesh count was chosen for all the cases.

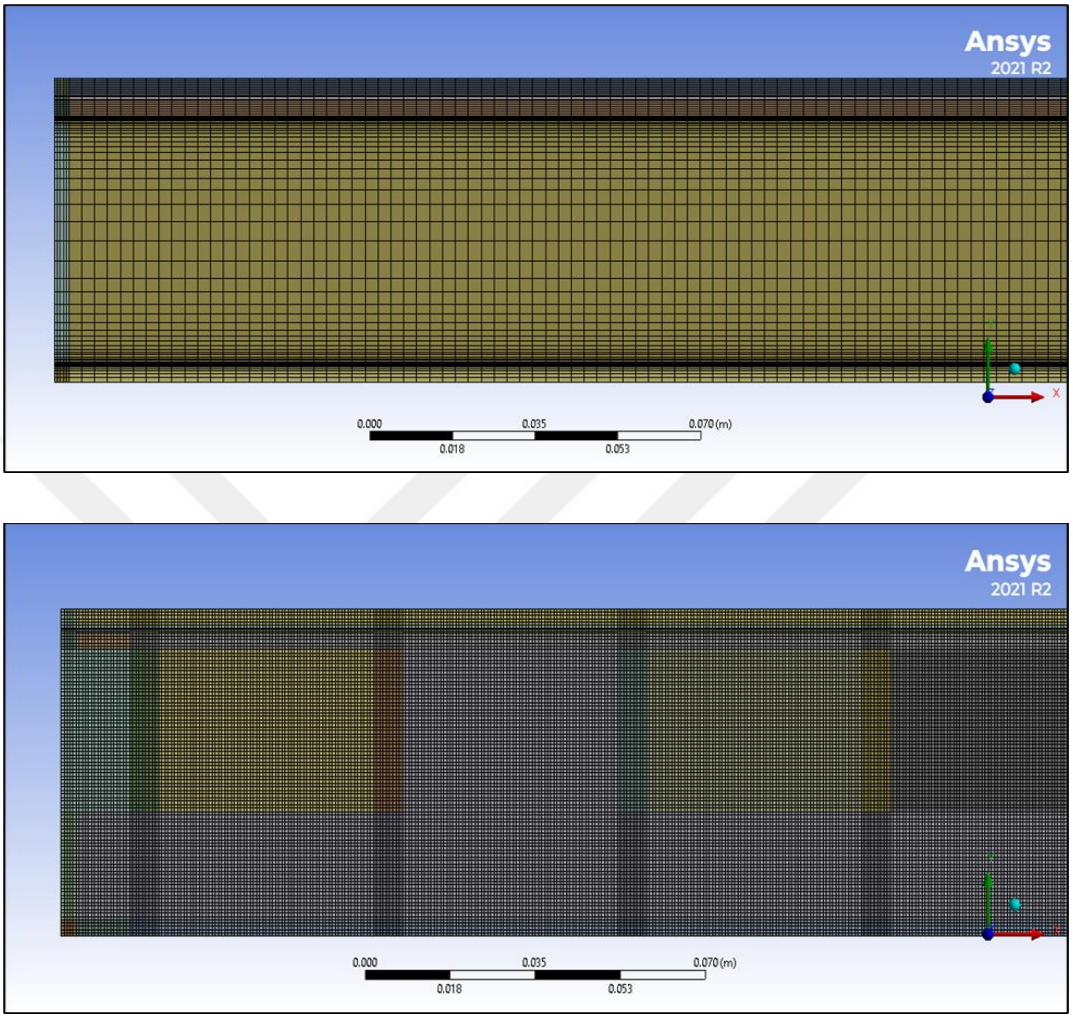

Figure 3.5: Structured Mesh For The PV-PCM Only And The Fincase2.3.

Generally, for the reasons stated above, structured grids are useful for complicated geometries; the structured hexahedron grids were generated and used in the current study, which is depicted in figure 3.5. The first thing to do is implement a Grid Independence Study (GIT) so as to get the most relevant mesh cell count and an accurate solution that is not changed as the mesh size is changed. About seven tries have been conducted to choose the optimum mesh, and this is shown below in figure 3.6. The temperature and power after changing the cell count from 240,000 to 270,000 have not significantly changed, hence the 240,000 cell mesh count was chosen for all the cases.

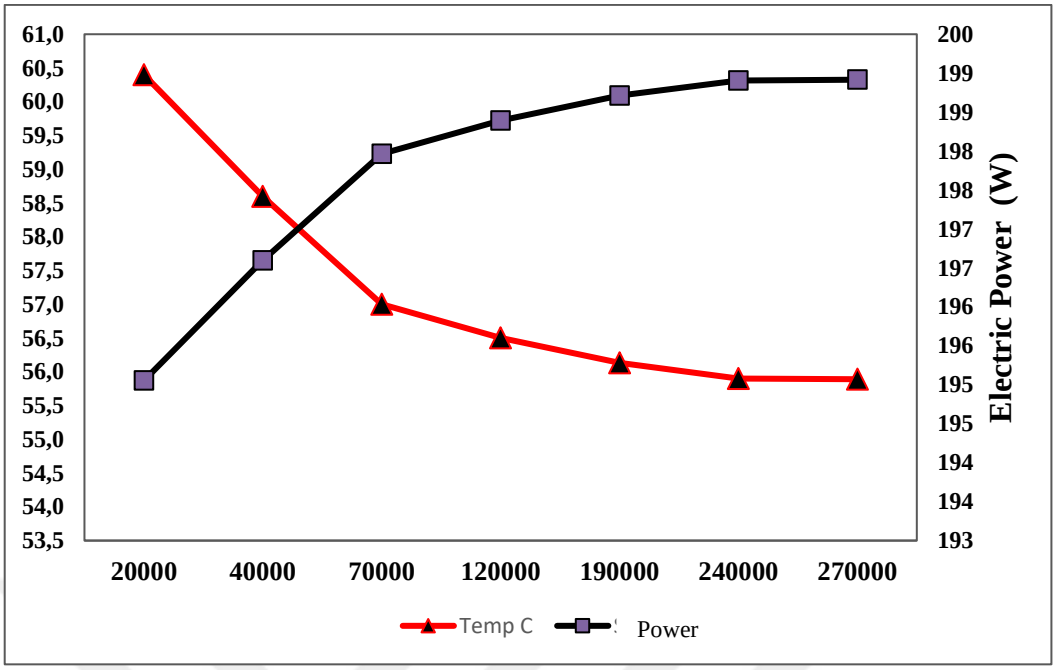

Figure 3.6: GIT For The PV-PCM-Only Case.

3.3.2.3 Boundary conditions of the system

The maximum heat flux falling on the solar panel during the period from 11 to 12 at noon on a particular day in the month of August is 955 W/m^2, according to the meteorological data for that day. For the city of Al-Jadiriyah, Baghdad, Iraq, with a latitude and longitude line of (44.38, 33.28). The system consists of a solid PCM that is maintained at a temp, Tin, that is below the melt point, Tm, of the utilized PCMs at time t = 0. No-slip boundary constraints are also taken into consideration at the solid-fluid interfaces. Furthermore, all existing solid-solid interactions have a boundary condition that is thermally related.

Using Eq. (3-19), the heat obtained as a result of the solar radiation absorbed by each layer in the photovoltaic cells is computed and added to the heat transfer equation as an internal heat generation. In addition, as shown in Figs. 3.6, adiabatic boundary conditions is applied on the upper and lower ends of the PV–PCM system. The thermal boundary situation of the PV cell's top surface is a combination of convection and radiation dissipation. Accurate specifications should be made for the external radiation heat, surface external emissivity, air temperature, and heat transfer coefficient of convection. For the PV-PCM system and for the PV system without the PCM, the external back boundary is prone to convective heat loss as well as convection and radiation losses. (h-conv) for the front side was 10, and half of this

value was utilized for the rear side when simulating the worst-case scenario. The wind speed was 1 m/s. Table 3-1 provides a detailed expression of the applicable boundary conditions for the front and exterior back surfaces.

Table 3.1: Boundary Conditions Of The Present Study.

Surface	Boundary condition
To the front of the Pv panel [84]**:**	$-k_g \frac{\partial T}{\partial y} = h_{\text{conv,g-amb}} (T_{amb} - T_g) + h_{rad,g-sky}(T_{sky} - T_g)$
On the PV-PCM system's back's outer surface:	$-k_{al} \frac{\partial T}{\partial y} = h_{\text{conv},al-amb}(T_{amb} - T_{al})$
On the PV cell's outer rear surface without the PCM:	$-k_T \frac{\partial T}{\partial y} = h_{\text{conv},T-amb}(T_{amb} - T_T) + h_{rad,T-sky}(T_{sky} - T_T)$
h from glass to environment [99]**:** $\boldsymbol{h_{\text{conv, g}-amb} = 5.7 + 3.8V_w}$	
Radiative σ from glass to sky [100]**: and from Tedlar to sky:** $\boldsymbol{h_{rad,g-sky} = \sigma \varepsilon_g \frac{(T_g^4 - T_{sky}^4)}{(T_g - T_{sky})}}$	
The Sky Temperature [100] $\boldsymbol{T_{sky} = 0.0522 T_{amb}^{1.5}}$	

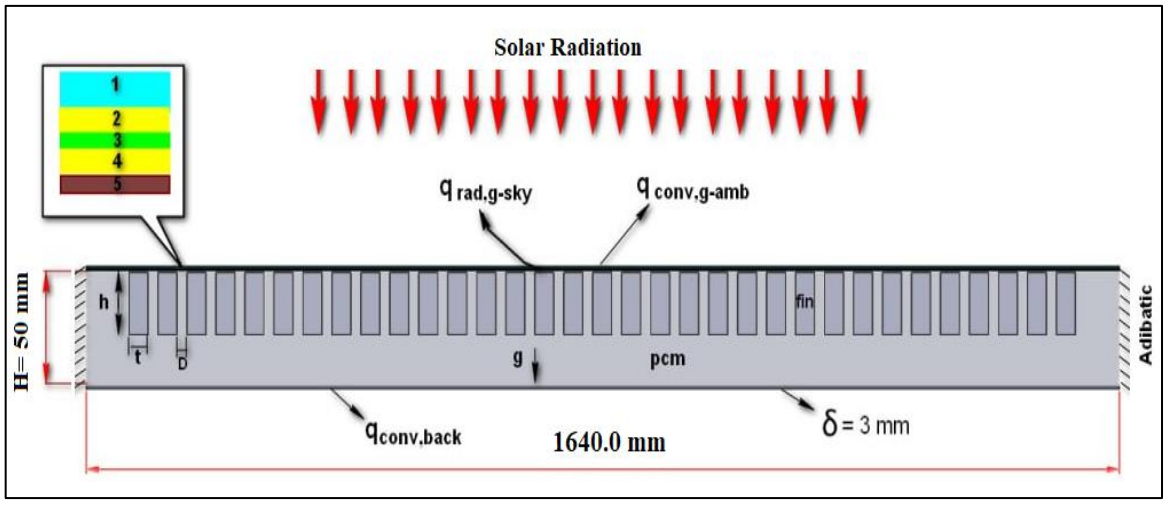

Figure 3.7: PV-PCM-Fin System Schematic.

3.3.3 Governing Equations:

3.3.3.1 Energy equation

Energy equation for solid phase [48]

$$\rho_s \frac{\partial H}{\partial t} = k_s \left(\frac{\partial^2 T}{\partial x^2} + \frac{\partial^2 T}{\partial y^2} \right) \tag{3.8}$$

Energy equation for liquid phase [49]

$$\rho_l \frac{\partial H}{\partial t} + \rho_l u \frac{\partial H}{\partial x} + \rho_l v \frac{\partial H}{\partial y} = k_l \left(\frac{\partial^2 T}{\partial x^2} + \frac{\partial^2 T}{\partial y^2} \right) \tag{3.9}$$

The enthalpy of a substance is calculated as the sum of its apparent enthalpy, h, and its latent heat, ΔH.

$$H = h + \Delta H \tag{3.10}$$

Where:

$$h = h_{ref} + \int_{T_{ref}}^{T} c_p dT \tag{3.11}$$

And the (liquid fraction), β, can be defined as

$$\begin{aligned} &\beta = 0 && \text{if} \quad T < \mathrm{T_{solidus}} \\ &\beta = 1 && \text{if} \quad T > T_{\mathrm{liquidus}} \\ &\beta = \frac{T - T_{\mathrm{solditus}}}{T_{\mathrm{liquidus}}\, T_{\mathrm{soldus}}} && \text{if} \quad T_{\mathrm{solidus}} < \mathrm{T} < \mathrm{T_{liquidus}} \end{aligned} \tag{3.12}$$

Where h and T ref denote the reference enthalpy and temperature, respectively, CP refers to specific heat.

The latent heat component may now be depicted in terms of the material's latent heat. :

$$\Delta H = \beta L \tag{3.13}$$

A material's latent heat content can range from 0 for a solid to L for a liquid. The energy equation for solidification/melting situations is expressed as

$$\frac{\partial}{\partial t}(\rho H) + \nabla \cdot (\rho \vec{v} H) = \nabla \cdot (k \nabla T) + S \tag{3.14}$$

Where H is enthalpy, ρ density, $\vec{V}$ liquid velocity, S source duration.

The resolution for temperature is basically an iteration through energy in the equation (3.14) as well as the liquid fraction equation (3.12). Use formula (3.12) to inform the liquid fraction directly usually leads to poor integration of the energy equation. To inform the melting fraction in fluent, the method suggested by Voller and Swaminathan is used. For pure metals where T-Solidus and T-liquidus are equivalent, (Voller and Prakash's) heat transfer strategy is used instead [97].

3.3.3.2 Mass and momentum equations

The partially cemented zone's mushy zone is considered a porous medium for the momentum equation using the enthalpy porosity approach. The enthalpy-porosity approach treats the solid-liquid mushy zone as a porous medium with porosity equal to the liquid fraction, which causes the velocities in these areas to follow the continuity equation [98]:

$$\frac{\partial u}{\partial x}+\frac{\partial v}{\partial y}=0 \tag{3.15}$$

Momentum equations:

$$\begin{aligned}\rho\frac{\partial u}{\partial t}+\rho u\frac{\partial u}{\partial x}+\rho v\frac{\partial u}{\partial y}&\\ =-\frac{\partial P}{\partial x}+\mu\left(\frac{\partial^2 u}{\partial x^2}+\frac{\partial^2 u}{\partial y^2}\right)+S_x\rho\frac{\partial v}{\partial t}+\rho u\frac{\partial v}{\partial x}+\rho v\frac{\partial v}{\partial y}&\\ =-\frac{\partial P}{\partial y}+\mu\left(\frac{\partial^2 v}{\partial x^2}+\frac{\partial^2 v}{\partial y^2}\right)+F_B+S_y&\end{aligned} \tag{3.16}$$

Where μ is the dynamic viscosity, P is the pressure, u and v are the liquid phase's velocities in the x and y axes, respectively, and ρ is the density. A buoyancy force called FB is provided via the Boussinesq approximation [40].

$$F_B=-\rho_0\big(1-\beta_1(\mathrm{T}-\mathrm{T}_0)\big)g \tag{3.17}$$

The lower porosity of the mushy zone results in a momentum sink that looks like:

$$S=\frac{(1-\beta)^2}{(\beta^3+\varepsilon)}A_{\text{mush}}\left(\vec{v}-\vec{v}_p\right) \tag{3.18}$$

The liquid volume fraction is negligibly small (0.001) in order to prevent division by zero. VP is the solid velocity brought on by attempting to remove solidified material from the zone, where (A mush) is the stable mushy zone (also known as the pull velocity) [95].

The heat converted due to absorbed sun light in each layer of the PV-PCM model may be estimated in the constructed model using Eq. (3.19) and fed to the heat transfer equation as internal heat production, qi

$$q_i = \frac{(1 - \eta_{sc})\, G\, \alpha_i \tau_j\, A_i}{V_i} \tag{3.19}$$

Where qi is the layer 1 internal heat production as a percentage of its volume; η stands for the silicon layer's electrical efficiency in solar cells; all other layers have a value of 0. G stands for solar radiation, whereas α, V and A represent the absorptivity, volume, and area of layer 1, respectively. The layer above has a Transmissivity of τ. I [84].

3.3.4 Solar Models

To assist the comparison procedure, the polycrystalline and monocrystalline solar panels were carefully selected from the Chinese business Ningbo Rarlon Photovoltaic Technology Co. as well as the Max Power Company. The dimensions of the chosen panel are 1640 x 990 x 40 mm, and the cell size is 156 x 156 mm, NO of cells 60 as showed in Figure 3.7.

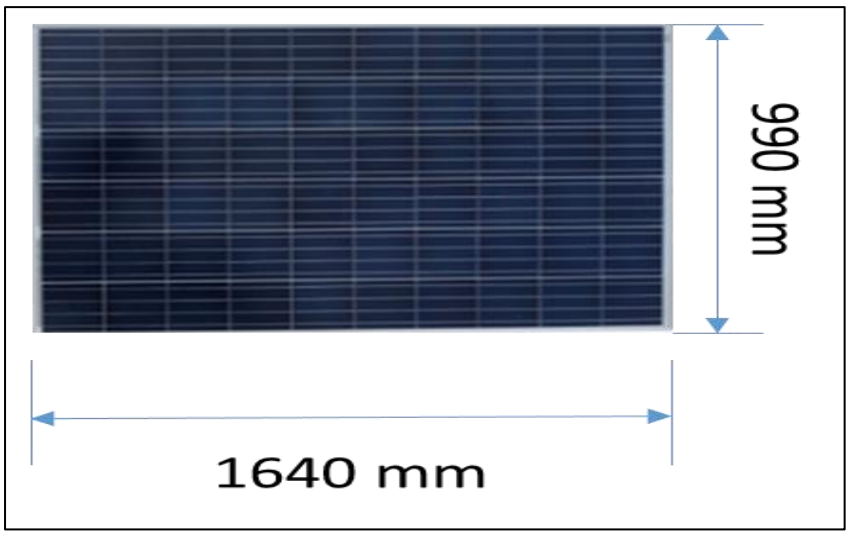

Figure 3.8: Poly Solar Panel.

Table 3.2: Electrical Characteristics Of Solar Panels.

Type	Polycrystalline	monocrystalline
Pmax	250 W	250 W
Vmpp	30.45V	30.72V
Impp	8.21A	8.138A
(Voc)	36.54V	36.91V
(Isc)	9.44A	9.031A
efficiency %	15.3 %	15 .39 %
dimension(L*W)	1640*992 mm	1640*992 mm
B	-0.45 %/°C	-0.35 %/°C

i. Properties of the PV module layers (poly):

Commercial solar panels are made up of several layers, including a transparent top layer of glass and a transparent EVE layer to protect the cells from weather conditions and high temperatures, as well as a lower packing layer of EVE and an aluminum back metal plate to protect the plate from the wind and the cell's edge, As shown in the figure below, which will be used to simulate the layers of the panels using the Ansys software[101].

Table 3.3: Specification Of Poly Layers [65].

Components	ρ kg/m3	t (m)	Cp J/kg K	k W/m.K	ε	α	τ
Glass	3000	0.003	500	2	0.9	0.04	0.92
Si solar cell	2330	0.0002	677	148	-	0.9	-
EVA layer	960	0.0005	2090	0.35	-	0.08	0.90
Tedlar TPT	1200	0.0003	1250	0.2	0.9	-	-

ii. Properties of the PV module layers (mono)

Table 3.4: Specification Of Monocrystalline Layers [102].

Components	ρ kg/m3	t (mm)	Cp J/kg K	k W/m.K
Glass	2300	3	0.50	1
Si cell layer	2330	0.35	0.757	168
EVA layer	960	0.50	2.09	0.35
Tedlar TPT	1500	0.20	1.20	0.20

Furthermore, the transitivity of the glass cover for monocrystalline is τ_g = 0.95, the solar cell absorptivity is αc 0.85, and finally the absorptivity of TPT is α_T = 0.5 [103].

3.3.5 Materials

3.3.5.1 Fins of heat sink

The material used for the heat sink of a solar cell can significantly affect the cell's performance. High operating temperatures also have an impact on the effectiveness of solar panels. A heatsink is used to dissipate the heat generated by solar radiation into the environment. The heat sink's thermal conductivity plays a role in its ability to dissipate heat, and the amount of heat that needs to be dissipated is influenced by the contact area between the heatsink and the environment. Increasing the number of fins on the heatsink can increase the contact area and improve heat dissipation [51]. The material used for the fins used is aluminum due to its frequent use in such works and the ease of its formation as well. Note its properties as in table 3.5 [65].

Table 3.5: Thermo Physical Properties Of Aluminum [65].

Thermo physical properties	Aluminum
ρ kg/m2	2675
K w/k.m2	211
CP kJ/kg.k	0.093

3.3.5.2 PCM

One of the most popular PCMs is paraffin wax, which has several beneficial characteristics. The melting temperature of the paraffin wax utilized in this project is around 57 °C. It was

provided by RUBITHERM and is known by the trade name RT55, as demonstrated in Figure 3-6.

Table 3.6: Thermo Physical Properties Of Paraffin Wax RT55 [104].

Thermo physical properties	RT55
Melting point °C	51-57
Cp (kJ/kg)	170
K (w/k.m2)	0.2
Specific heat capacity (kJ/kg.k)	2

Thermo physical properties	RT55
ρ - Solid kg /m^{-3}	880
ρ - Liquid kg /m^{-3}	770
Volume expansion %	14

3.3.6 Problem Solution

The following stages, which can be employed for solution, comprise a volume of the control-dependent procedure:

i. A grid is created on the field.

ii. By integrating each control volume of the governing equations, sets of equations such as those for velocity, pressure, and conserved scalars are created.

iii. The discretized equations are linearized and solved iteratively.

The governing equations in CFD are non-linear and coupled, which can make finding a converged solution to the problem challenging. ANSYS uses the segregated solution algorithm, which involves dividing the governing equations into smaller pieces and solving them separately, to solve these equations iteratively until a converged solution is obtained. This process may require many iterations before a convergent solution is found.

3.3.7 Solution Parameters

The solution parameters include the following:

a. Precision Solver Type At the end of each solver iteration, the residual sum for each of the conserved variables is computed and stored in Fluent, thus recording the convergence history. On a computer with infinite precision, the residuals would go to zero as the solution converges. On an actual computer, the residuals decay to some small value and then stop changing (level out) [105].

b. Iterations Number: In ANSYS, the iteration process involves solving equations repeatedly to accurately understand the behavior of a system or process. The complexity of the equations and the desired accuracy of the results will impact how many iterations are necessary. Convergence criteria, which are used to determine when a solution is accurate enough, also influence the required number of iterations.

3.3.8 Convergence Criteria

Convergence criteria determine the point at which a simulation solution is considered accurate enough. These criteria specify the acceptable level of error or deviation in the solution, and the solver will continue to perform iterations until the solution meets the criteria or the most iterations are completed. Choosing the right convergence criteria is important for ensuring the accuracy and reliability of the simulation solution. Stricter criteria lead to more accurate solutions but may require more iterations and computational resources. Looser criteria may result in a less accurate solution but may be faster to compute. The result is assumed to be converged when the residuals are below a tolerance limit of 106 for all the fluid flow equations presented above.

4. RESULT AND DUSCUSSION

4.1 INTRODUCTION

ANSYS Fluent, recognized as a leading solution in the field of computational fluid dynamics (CFD), enables engineers to dedicate their time to innovation and enhance product outcomes. The software, which has undergone extensive testing across diverse applications, offers reliability in simulation performance. With ANSYS Fluent, engineers can create sophisticated physical models and examine various fluidic phenomena, all within a flexible and user-friendly interface.

4.2 VALIDATION

To validate a simulation in ANSYS Fluent, the results obtained were compared to experimental data or analytical solutions. This procedure ensures the simulation's correctness and dependability. This is carried out to ensure that the simulation results appropriately reflect the behavior of the system under simulation. By comparing simulation findings to experimental data through charting or statistical analysis, the validation process may be carried out. To verify the simulation setup and the numerical techniques utilized, the simulation results may also be contrasted with analytical answers. The validation procedure aids in enhancing the reliability and accuracy of the simulation findings.

4.2.1 Model Validation

The ANSYS Fluent software was utilized to model the performance of a solar model with and without a cooling method. The cooling system consisted of a phase-changing material and an aluminum frame placed behind the panel. The simulation was run using the same boundary conditions, temperatures, and material properties as in a reference article (Mohamed Emam et al.,[106]) to test the accuracy and predict the melting of the phase-changing material and the surface temperature of the model.

4.2.2 Validation of the Uncooled PV Concentrator Model

The expected results were compared with the experimental results of the reference article, and through simulation, a solar concentration of CR = 5, 10, and 20 was used, which is

equivalent to 50,000, 10,000, and 20,000 w/m2 of incident solar irradiation, and the temperature was compared with the time. As the concentration intensity increases, the heat of the plate's front surface rises over time, and the simulation's boundary conditions are 20 °C atmospheric temperature and 1 m/s wind velocity with a period length of 50 minutes. As shown in Fig.4.1, the predicted findings were substantially equal to the experimental results of the study publication [106], and the greatest error rate was exceptionally low.

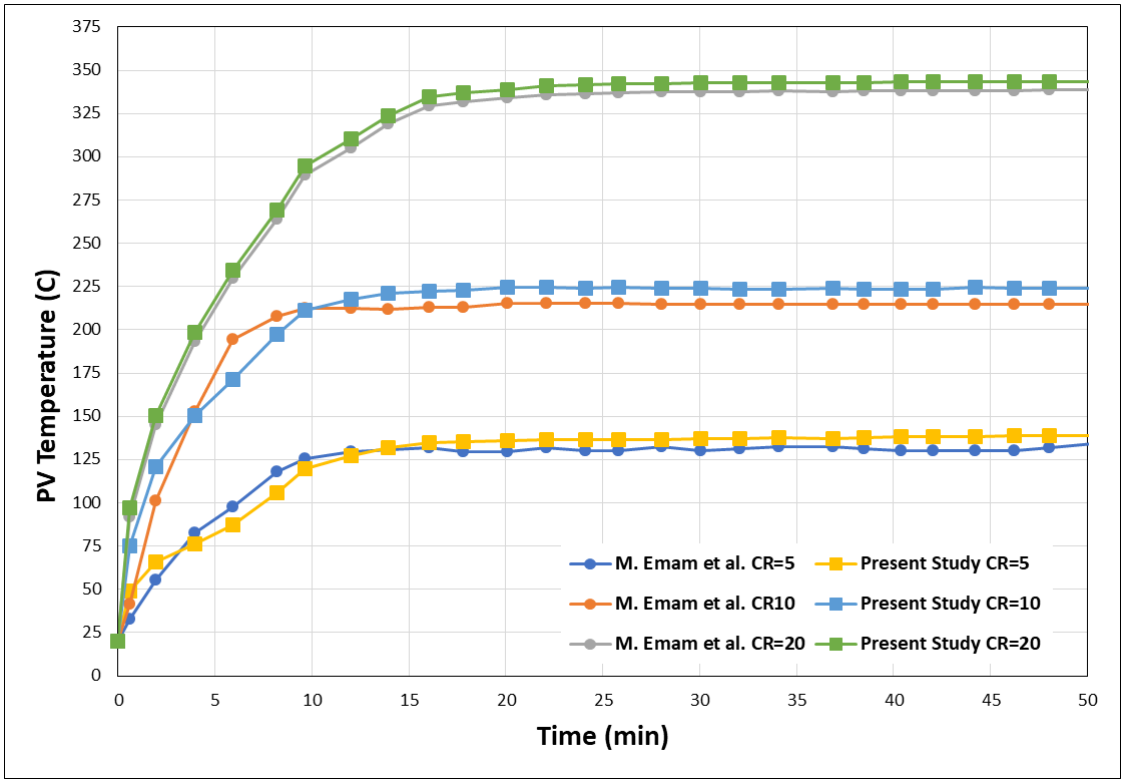

Figure 4.1: Validation For PV Only Without PCM With Reference Article.

4.2.3 Validation of the PV Concentrator Model with PCM

The validity of the expected result for the temperature distribution and solubility of a phase-change material with time has been validated by the research's numerical results. The simulation material is n-octadecane paraffin, which has a melting point of 28 °C and thermal conductivity coefficients of 0.358 and 0.148 (W/m °C) for the solid and liquid situations, respectively. And that the simulation time was only 40 minutes, the concentrated solar radiation is 10, the ambient temperature is 20 °C, and the wind speed is 1m/s, and the results showed the melting of the (PCM) and the temperature of the panel in a manner very similar to the numerical results of the research, and the error rates did not exceed 5% as shown in

figure (4.2), (4.3), (4.4) and (4.5) where they display the predicted validation, solidification, and melting (PV-PCM).

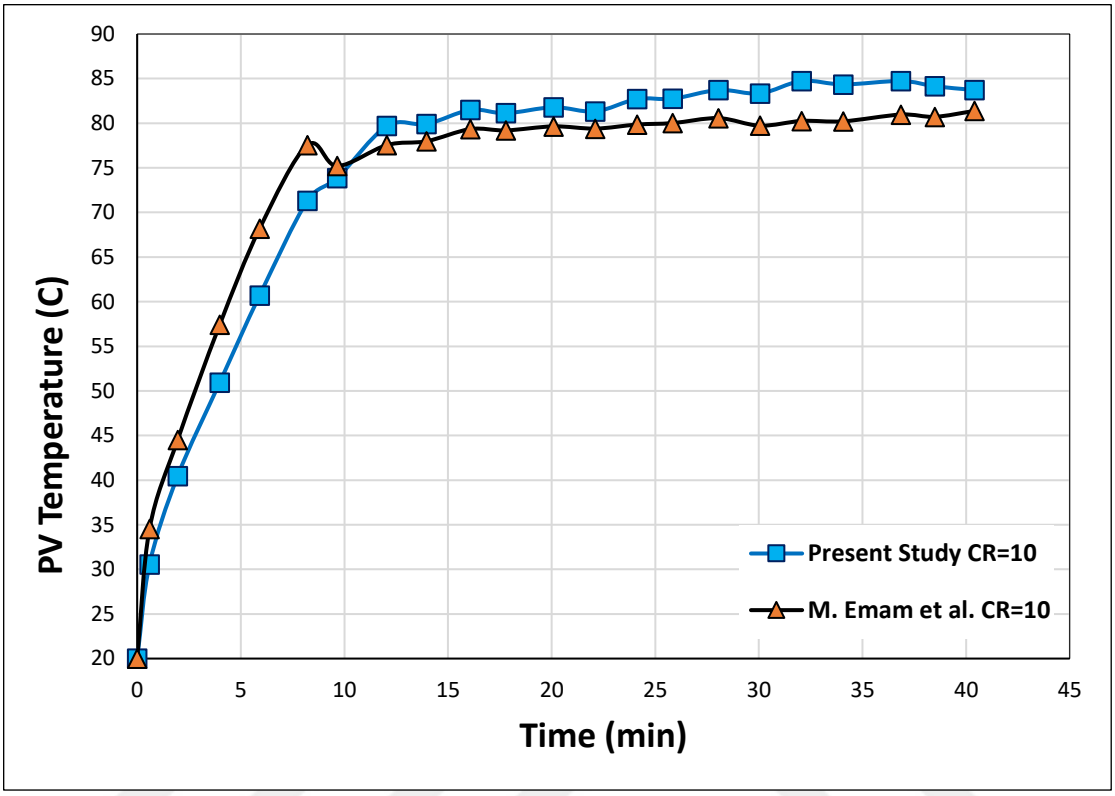

Figure 4.2: Validation For PV-PCM With Reference Article.

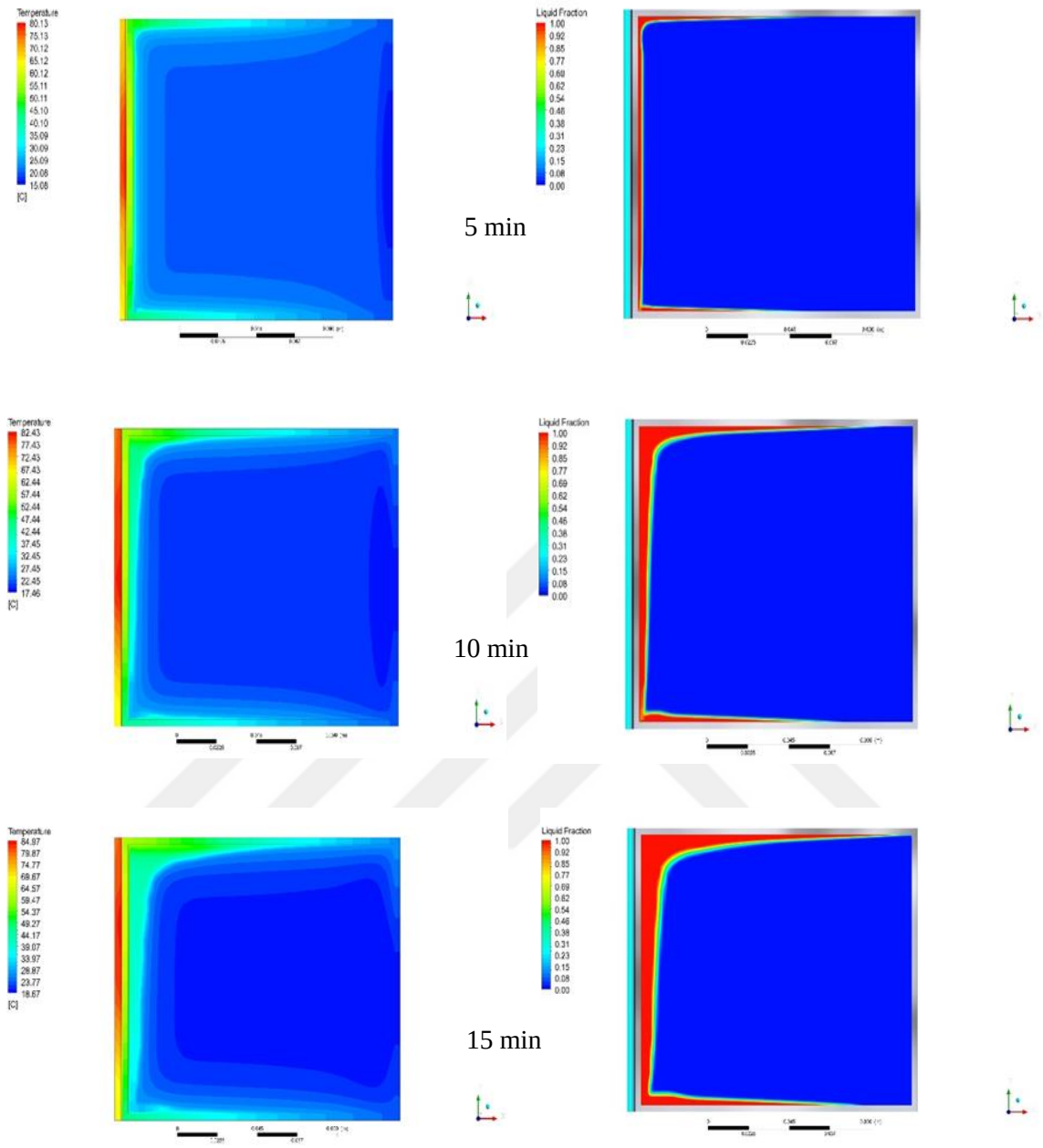

Figure 4.3: The CPV-PCM1 Predicted Isotherms And Analyses Of The Liquid-Solid Interaction, Where Red Represented The Liquid And Blue Represented The Solid. CR=10, 5, 10 And 15 Min.

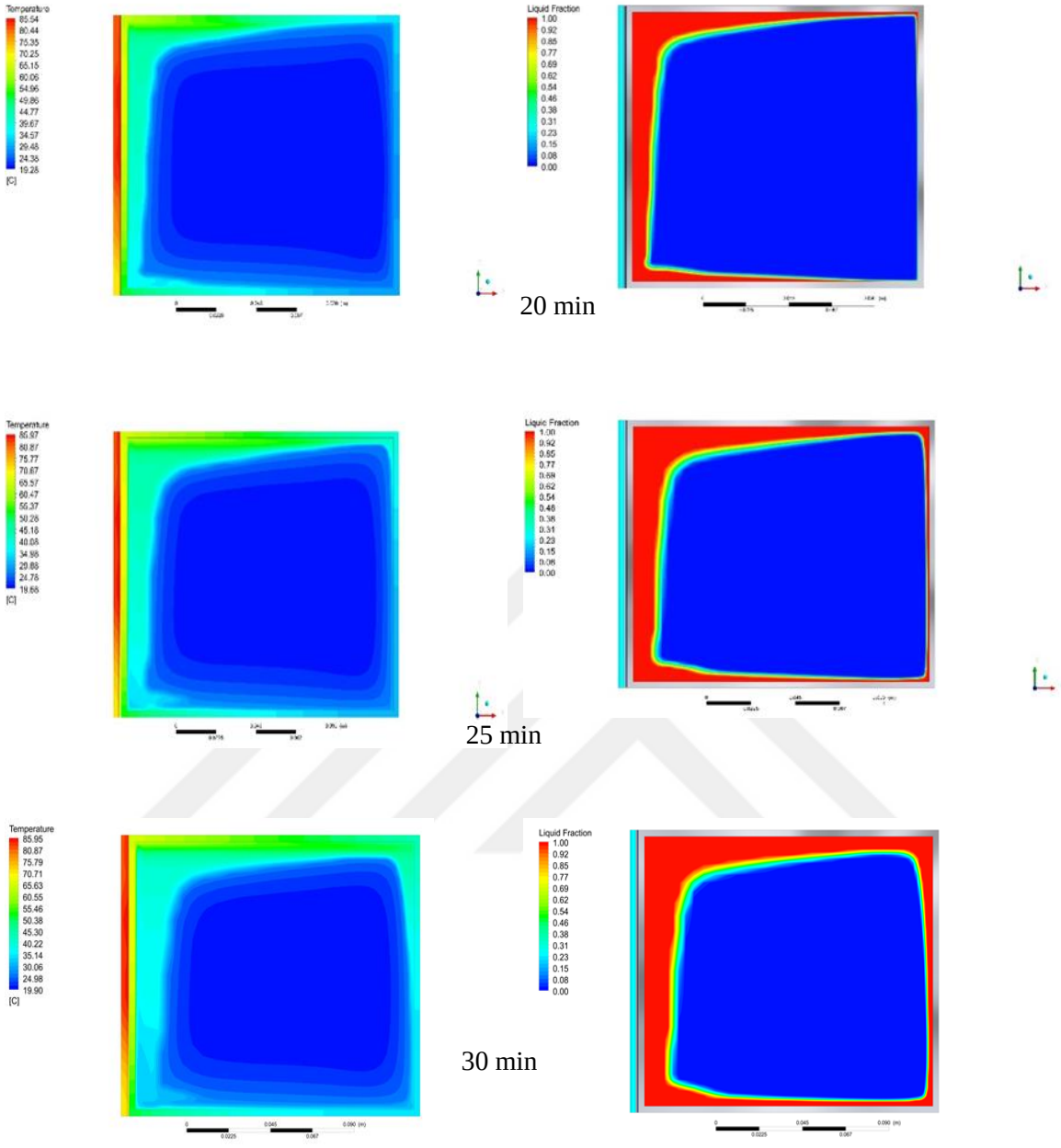

Figure 4.4: The CPV-PCM1 Predicted Isotherms And Analyses Of The Liquid-Solid Interaction, Where Red Represented The Liquid And Blue Represented The Solid. CR=10, From 20, 25and 30 Min.

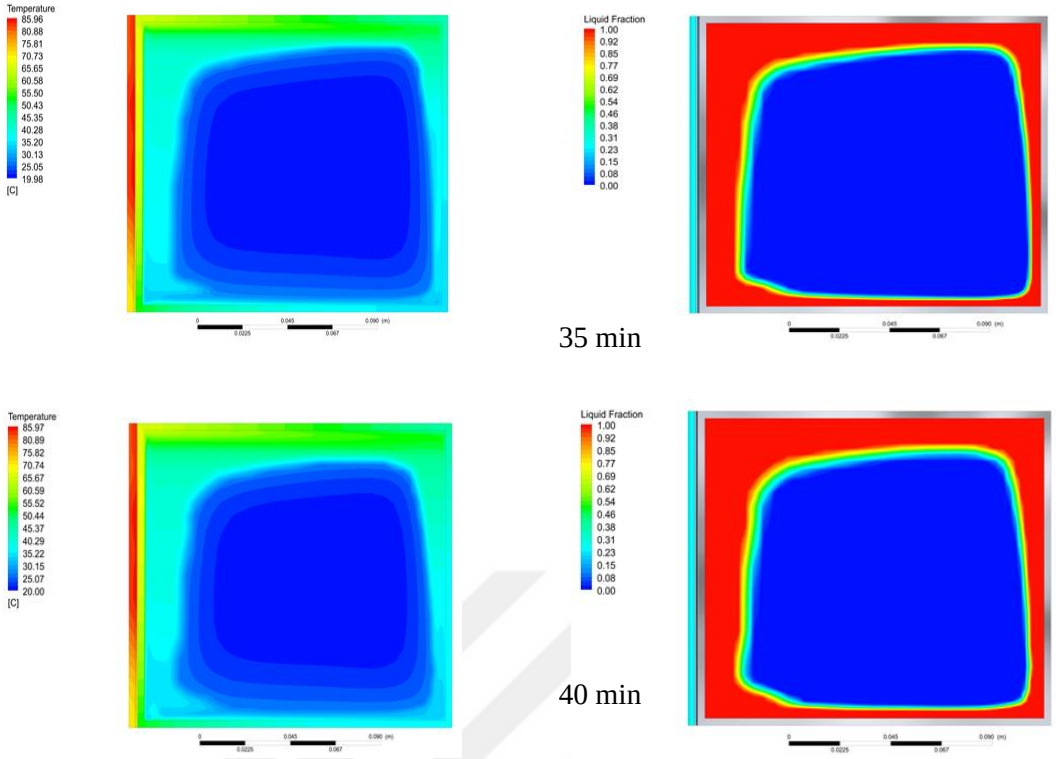

Figure 4.5: The CPV-PCM1 Predicted Isotherms And Analyses Of The Liquid-Solid Interaction, Where Red Represented The Liquid And Blue Represented The Solid. CR=10, 35 And 40 Min

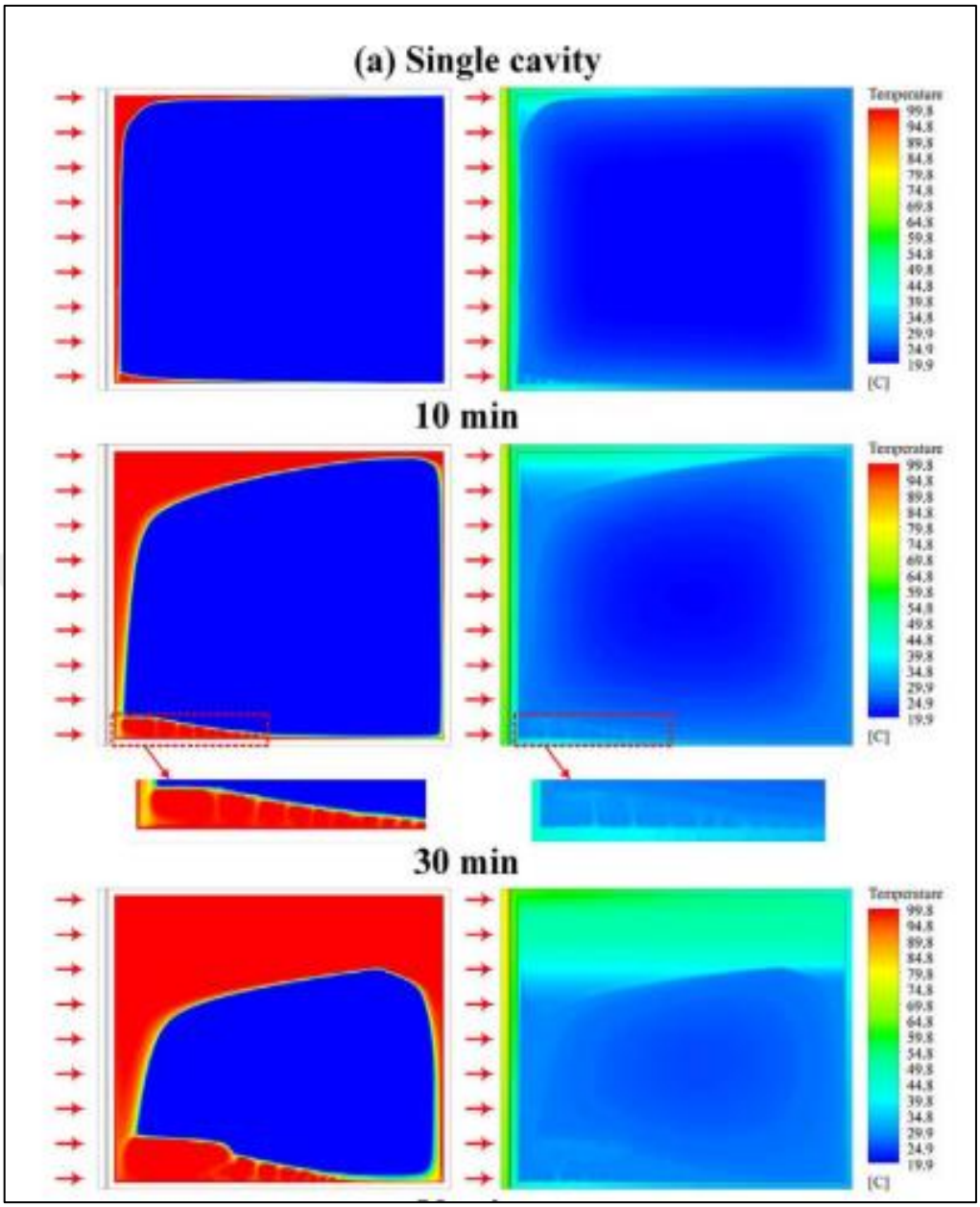

Figure 4.6: The CPV-PCM1 Reference Analysis [106].

4.3 EFFECT OF WAX THICKNESS ON CELL PERFORMANCE

To determine the optimal wax thickness, examine various wax layer heights for 3600 seconds and obtained the following results:

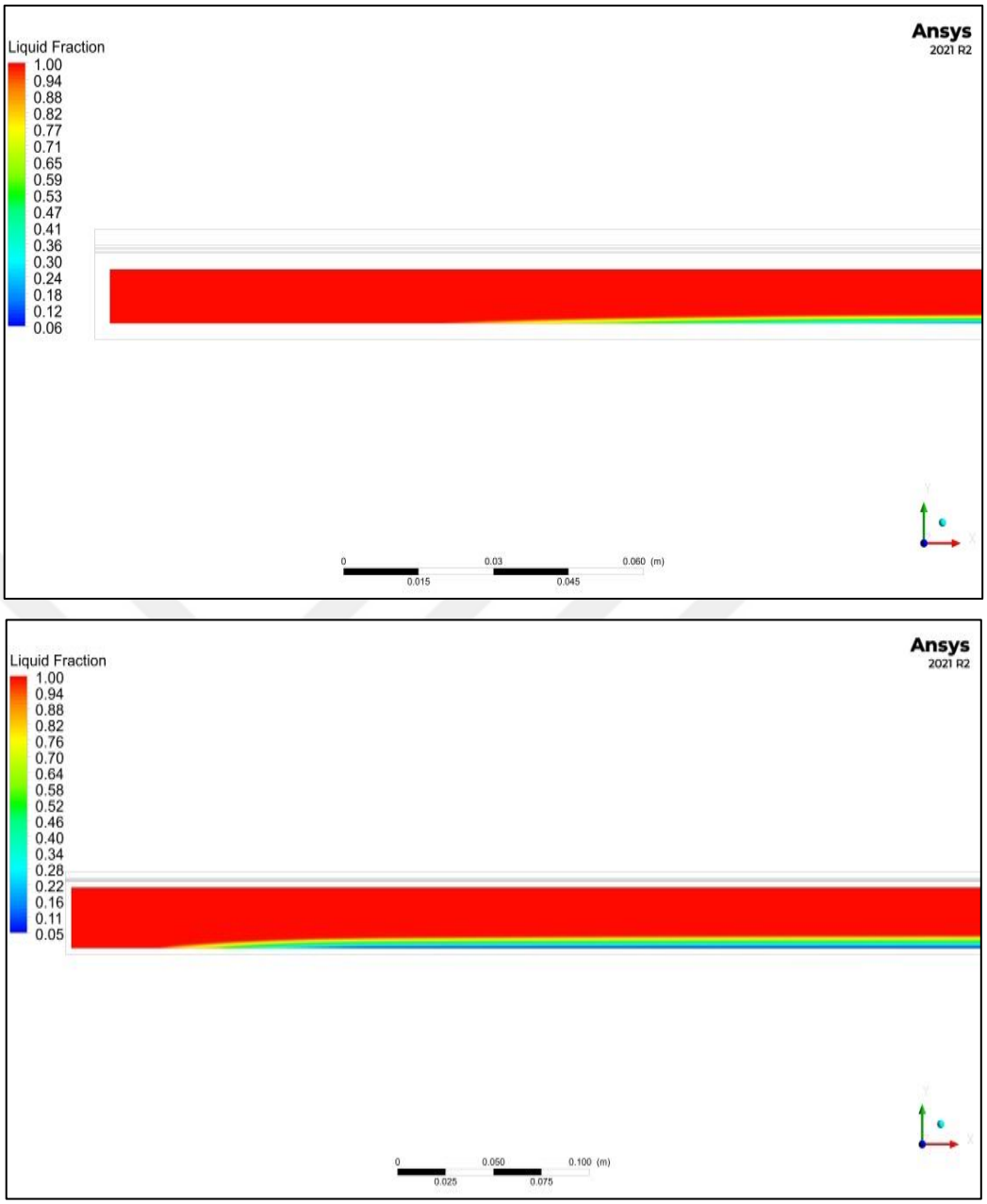

Figure 4.7: Liquid Fraction Wax Layers Of 1 And 3 Cm Thickness For 3600 Seconds**.**

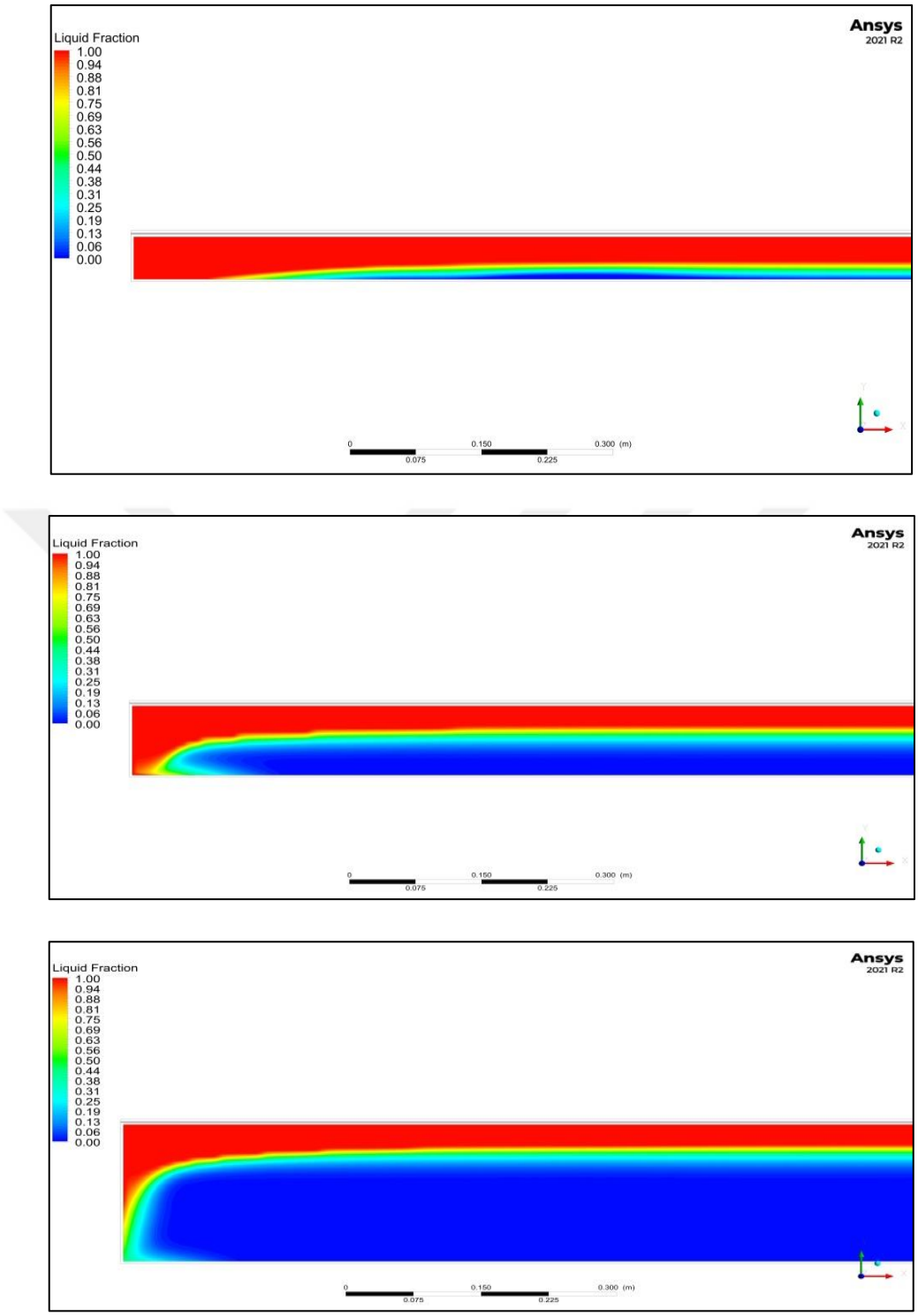

Figure 4.8: Liquid Fraction Wax Layers Of 5, 10 And 20 Cm Thickness For 3600 Seconds "Figures Continued".

Figures 4.7 and 4.8, which depict the liquid fraction interfaces between PCM solid-liquid phases, demonstrate how different locations in the PCM layer behave similarly when phases

change. A tiny piece of the PCM layer begins to melt after 10 minutes, whereas locations that are further from the interior surface take around 20 minutes to reach the liquid state. The quantity of the molten layer increases after 30 minutes. For thicknesses of 1 and 3 cm, the melting process really completes in 60 minutes; however, for thicknesses of 5 and 20, a greater portion of the material is still solid. The tiny thicknesses of 1 and 3 cm are the cause of this. The heated liquid may be transported to the final location using only convection current. Owing to the hot currents' inability to reach certain solid regions due to inadequate buoyancy force, an unmolten portion of the wax may be observed to persist as the wax thickness grows. As a result, these layers take longer to melt. The majority of the PMC layer is already in the molten phase after 60 minutes, and no heat discharge occurs. Red denotes a liquid zone, followed by blue, a solid region, and ultimately green, which denotes the start of a phase shift.

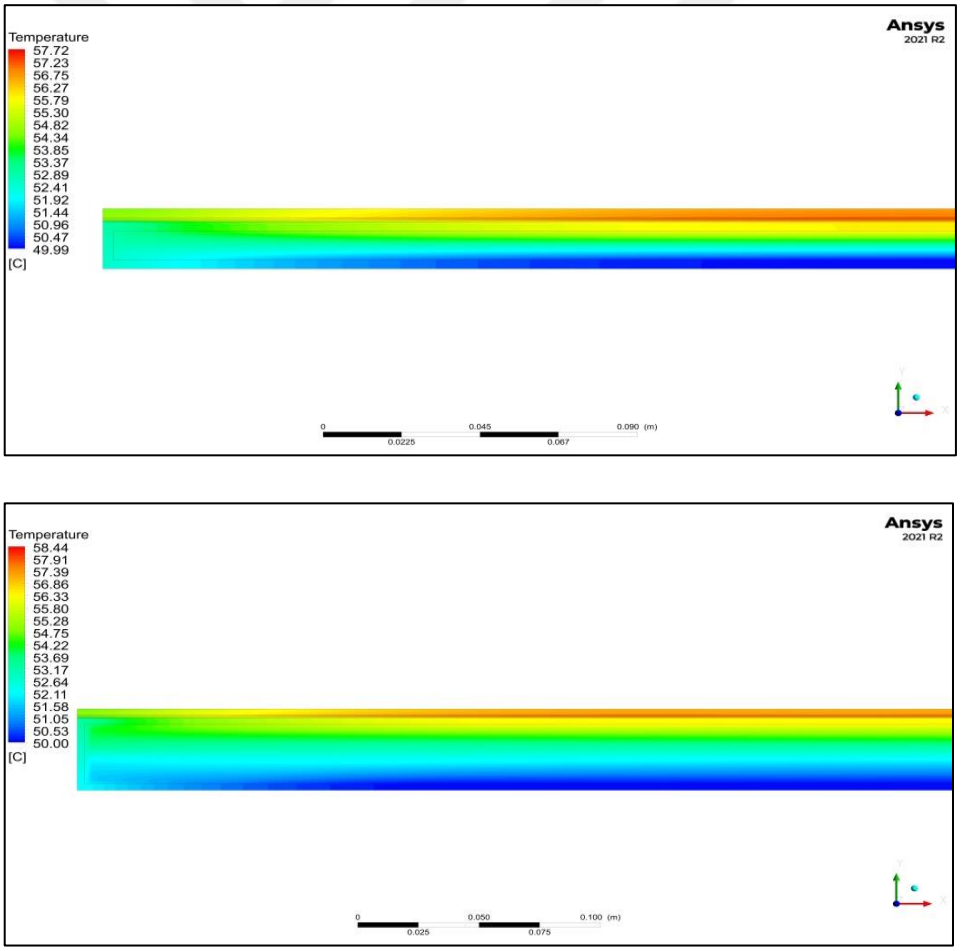

Figure 4.9: Temperature Contour To Wax Layers Of 1and 3 Cm Thickness For 3600 Seconds.

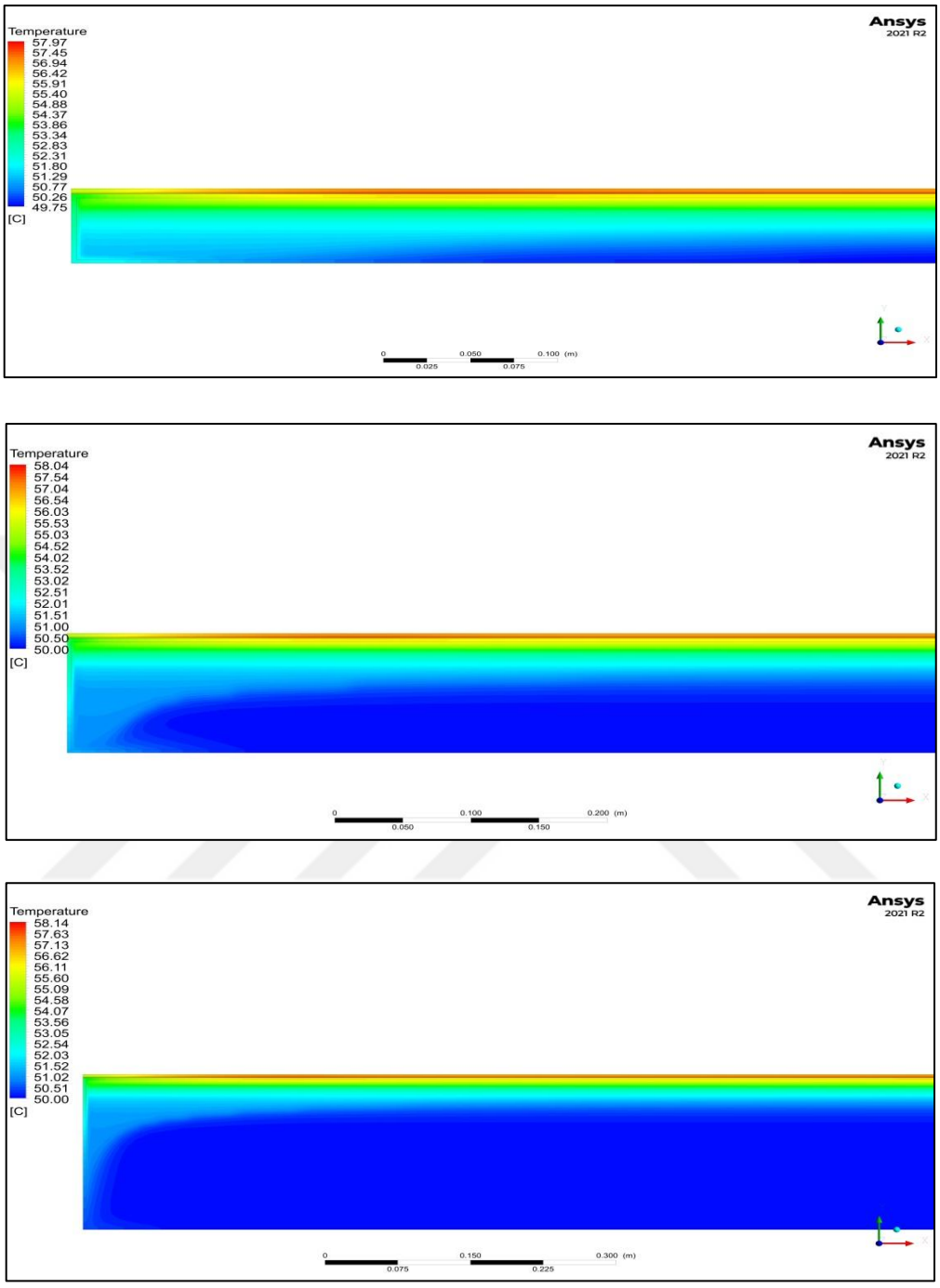

Figure 4.10: Temperature Contour To Wax Layers Of 5, 10 And 20 Cm Thickness For 3600 Seconds.

The temperature contours of a PV-PCM cell during the phase change process are indicated in Figure (4.9) and (4.10). The contours are divided into two regions: a maximum hot region (represented by red color) and a minimum cool region (represented by blue color). At 10 minutes, the maximum temperature of the wax for thicknesses of 1, 3, 5, 10 and 20 cm

recorded as 52.8°C, 52.9°C, 52.82°C, 52.83°C, and 52.85°C, respectively. The melting process did not commence as the temperatures were below the melting point of the wax. The temperatures gradually increased due to the increased convection heat transfer and thermal conductivity of the wax. At 30 minutes, the maximum temperatures recorded 55.04, 55.39, 55.1, 55.14, and 55.2, respectively. As the convection continued, the temperature continued to rise. By 60 minutes, the melting of the wax was complete, and a thermal equilibrium stage began for thicknesses between 1 and 3 cm. The temperatures recorded at this stage were 57.01, 57.7, 57.37, 57.43, and 57.53 °C, respectively.

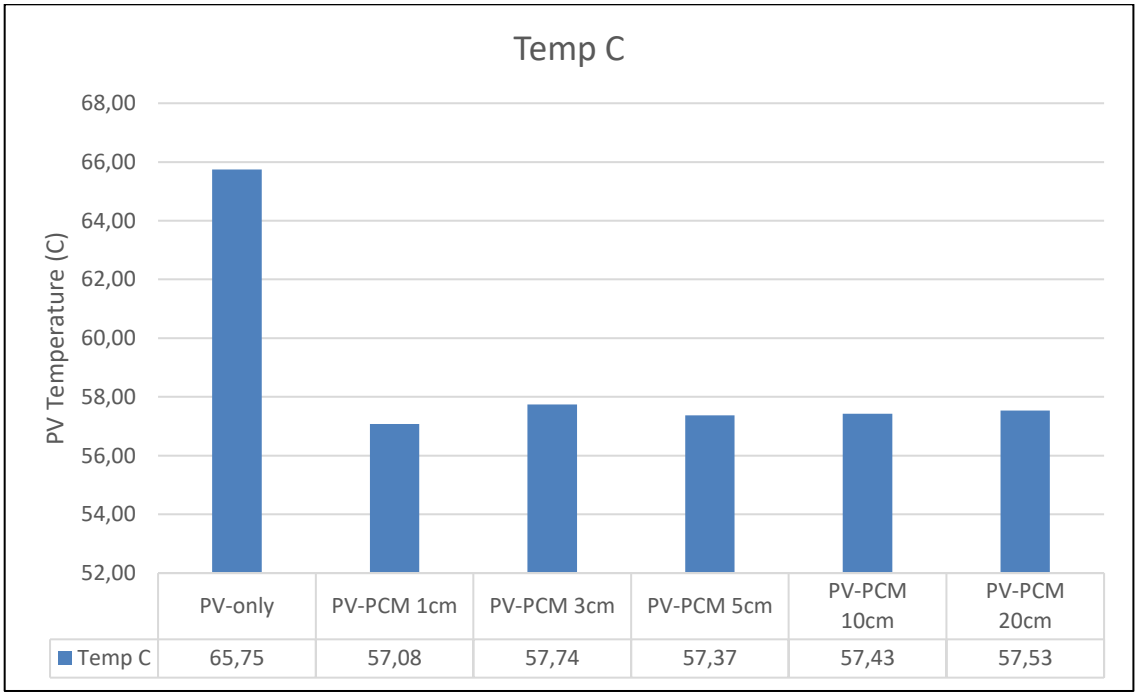

Figure 4.11: PV Temperature With PCM Layers Of 1, 3, 5, 10, And 20 Cm Thickness After 3600 Seconds.

Figure (4.11) PV only without using PCM recorded a maximum value of (65.75), while PV with PCM in 1 cm recorded a minimum value of (57.08). After studying the influence of the thickness, we selected a 5 cm thickness as the optimal thickness for improving the cooling of the board and its performance by adding fins of various sizes and dimensions.

4.4 POLYCRYSTALLINE PV MODULE

Multi-crystalline or polycrystalline photovoltaic (PV) panels are solar panels that are composed of several tiny crystal structures rather than a single, larger crystal structure. To

create them, molten silicon is poured into a square mold and then chopped into smaller, individual wafers.

Figures 4.12 show the temperature distribution through the PV layers (glass to tedlar) when exposed to incident irradiation conditions equal to 955 w/m^2, a wind velocity of 1 m/s, and an environment temperature of 50.1 °C for a period of 3600 seconds. Because of the silicon cell's high transmissivity and high absorption of sunlight, the cell temperature increased, reaching around 65.85 °C inside the silicon layer; thus, the heat inside the cell increased over time, leading to an increase in heat but a lower level in Eva and Tedlar due to heat transfer to the environment. The red color shows the high temperature of the silicone layer, and the light blue color indicates the temperature of both the glass and the Tadler. The rate of rise in the panel's temperature fluctuated between 64 and 65.8 degrees Celsius. Therefore, it became necessary to cool the panels.

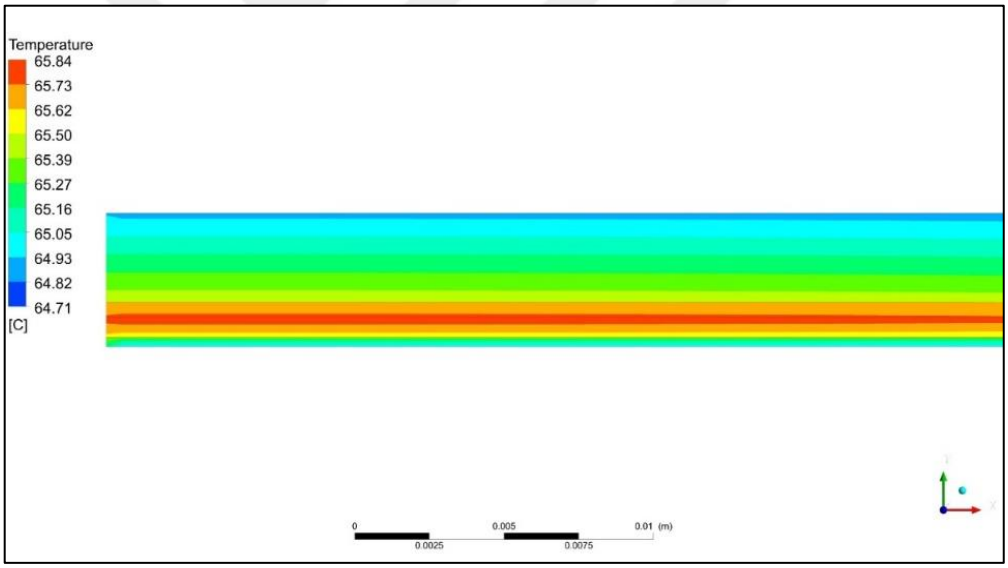

Figure 4.12: Temperature Distribution Of The PV Cell Only.

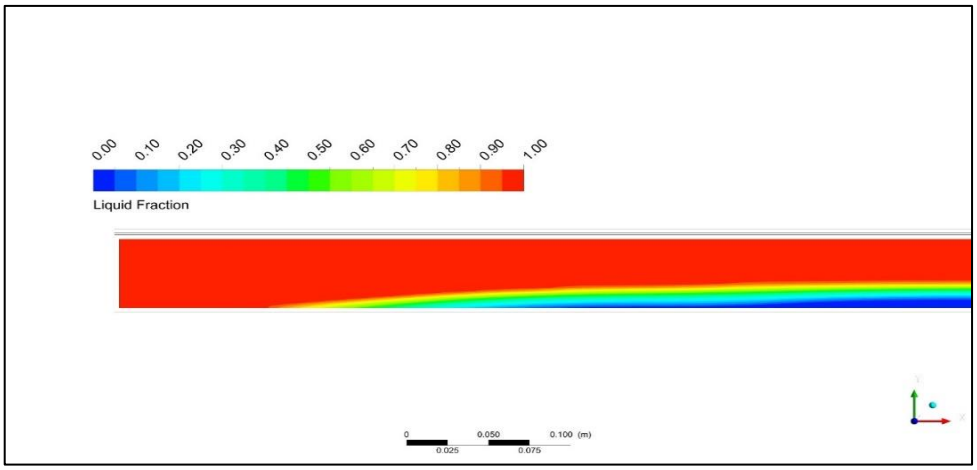

Figure 4.13: Liquid Fraction Distribution PV-PCM.

Figure 4.13 illustrates the process of thermal transfer in a layer of Phase Change Material (PCM) used in a back-cooling device for a solar cell. The heat is transferred from the surface of the silicon cell to the PCM container through a process of convective heat transfer. As the temperature of the PCM increases, it undergoes a phase change, transitioning from a solid to a liquid state.

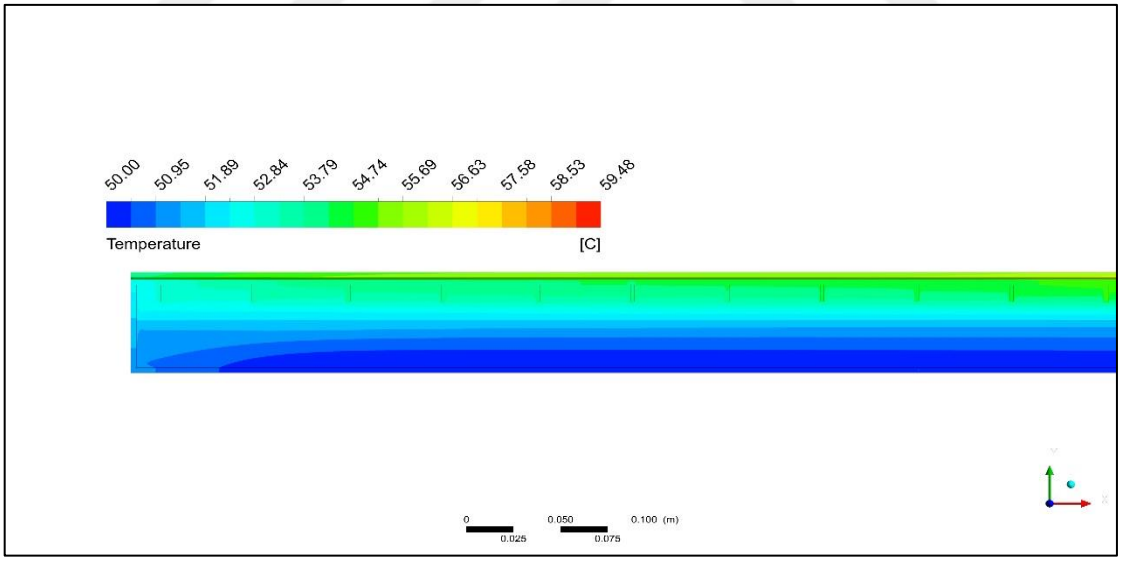

Figure 4.14: Temperature Contour PV PCM- Fins For All Cases.

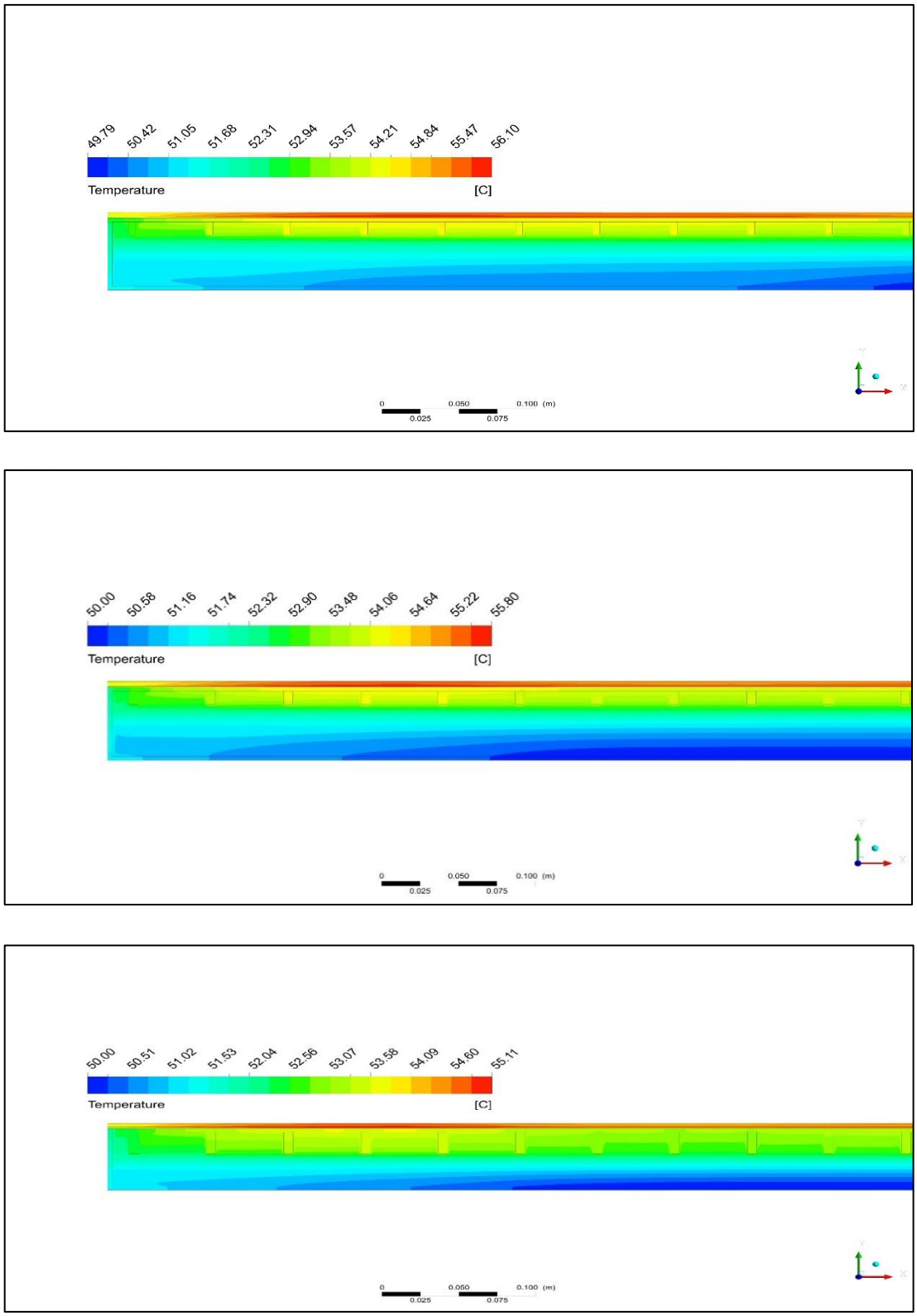

Figure 4.15: Temperature Contour PV PCM- Fins For All Cases “Figures Continued”.

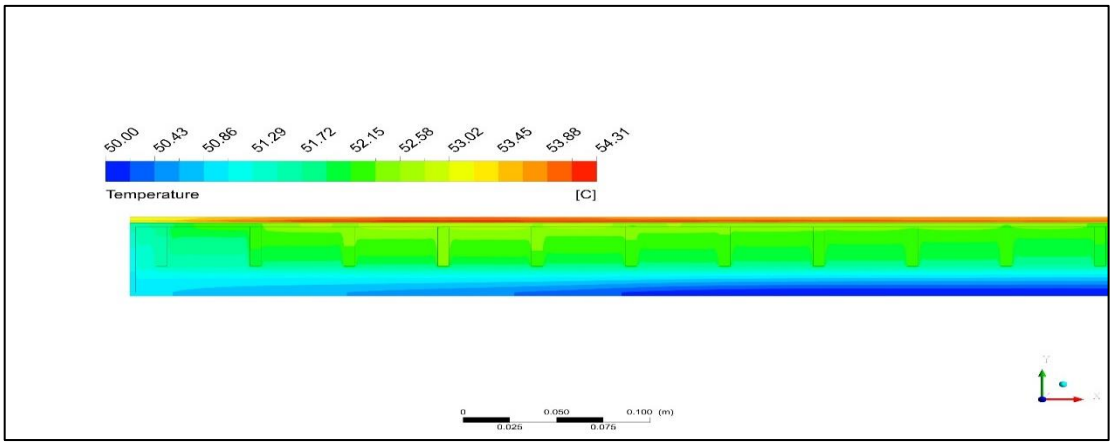

Figure 4.16: Temperature Contour PV PCM- Fins For All Cases “Figures Continued”.

Figures (4.14), (4.15), and (4.16), show temperature dispersion contours for PV-PCMF. Found that the addition of aluminum fins with varying thicknesses of 2, 4, 6, and heights of 10, 20, and 30 mm in combination with a layer of PCM led to a significant decrease in the surface temperature of the panel. Specifically, the cell temperature dropped from 65.8 °C in the PV-only to 53.9 °C in the PCM-F, optimum case 2.3, with a thickness of 6 mm and a height of 30 mm. This reduction is due to the high thermal conductivity of aluminum and the increased heat transfer surface area provided by the fins [107]. The aluminum fins allow for more efficient transfer of heat from the cell to PCM, absorbing heat faster and delivering it to the PCM more effectively.

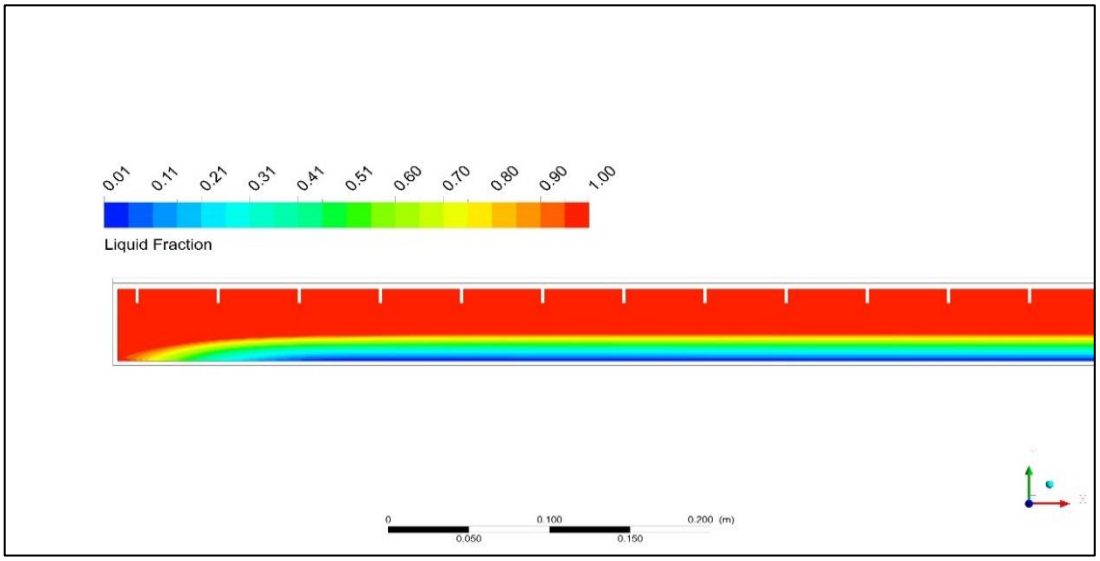

Figure 4.17: Liquid Fraction PV PCM - Fins Case 1.1

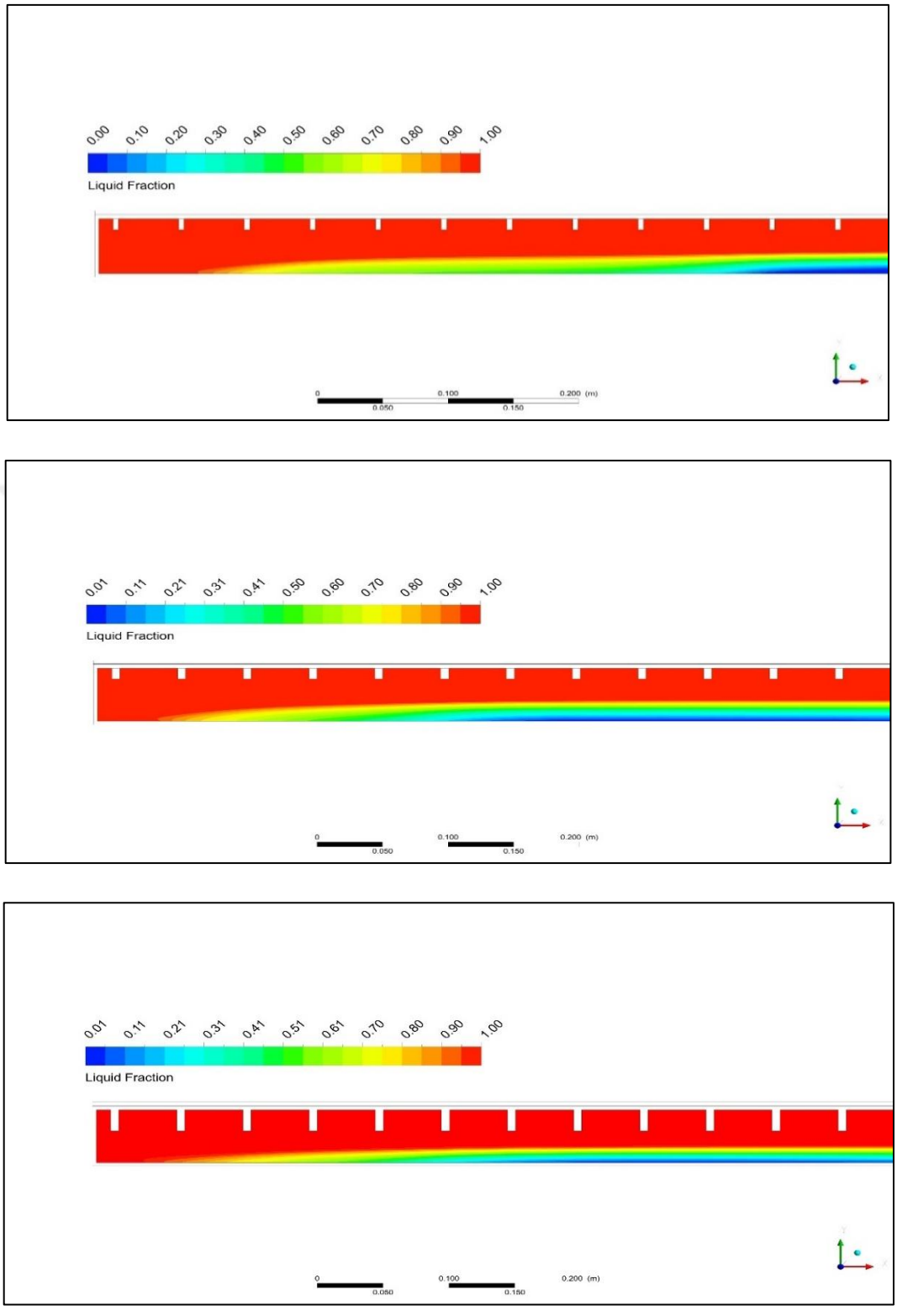

Figure 4.18: Liquid Fraction PV PCM - Fins Case 1.2, 1.3 And 2.1“Figures Continued”.

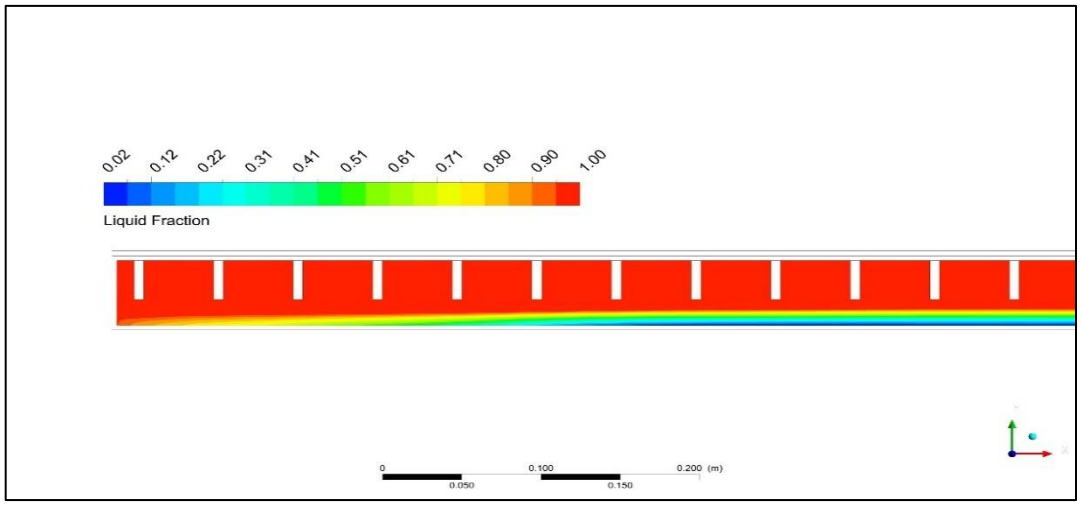

Figure 4.19: Liquid Fraction PV PCM - Fins Case 2.3 “Figures Continued”.

Latent heat is the kind of energy storage used by the PCM. Phase changes in a substance cause latent heat storage. In cases 1.1 and 1.2, the heat that the PCM has stored in its solid form is first released when the temperature rises. Until the temperature rises, the phase absorbs heat and transitions to a liquid state; the temperature then stays constant as the solid substance is completely transformed into a liquid. This process involves the storage of a significant quantity of energy. Heat transmission from the cell layer to the PCM is increased when fins are added to containers. Conduction is the primary mechanism by which temperature is moved from the heated cell surface to melting zone during the early melting stage. As can be observed, the PCM container's top side has a higher liquid percentage than the opposite side. This is mostly due to the fact that PCM density varies as temperature rises. Heat from the back panel is absorbed by fins, which then release it by convection to the PCM. Heat current will therefore grow, especially in the contact region of the fins. Due to the buoyancy effect that drives currents into solid locations, this current will eventually transition into the solid phase [108].

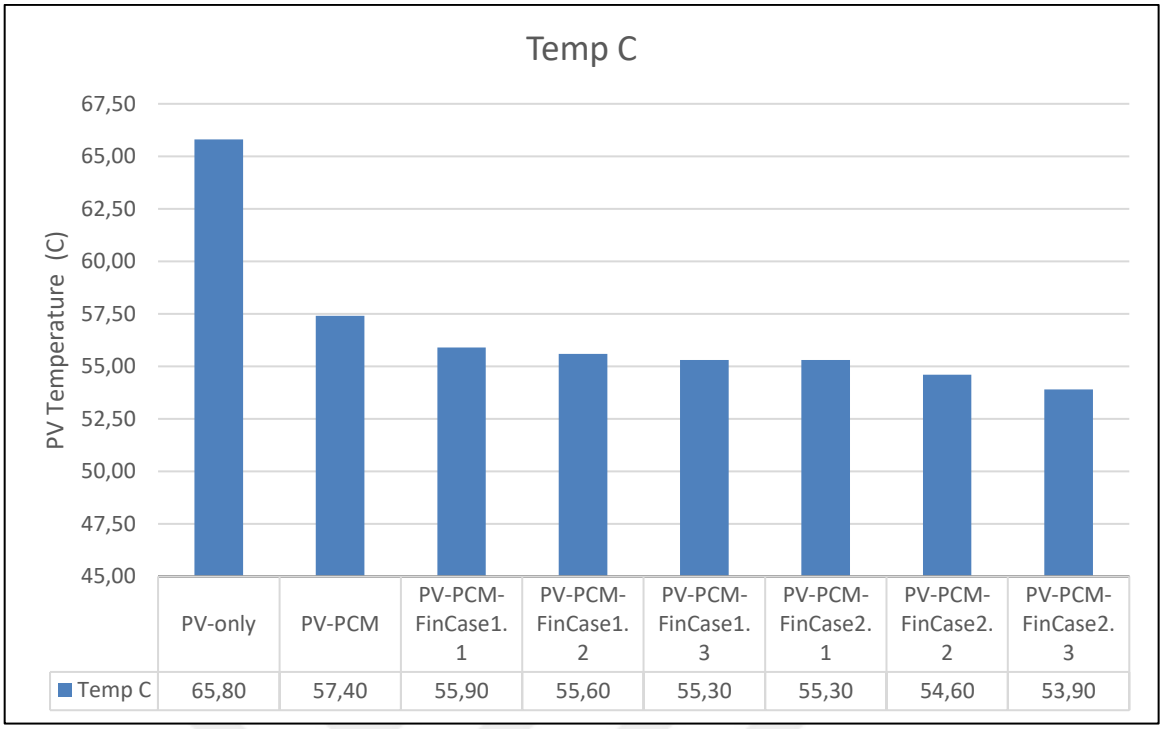

Figure 4.16: Temperature Arrangement PV-PCMF In All Cases.

Figure 4.20 shows the results of a study on the influence of changing the dimensions of the fins and PCM on the surface temperature of a polycrystalline-type module. The figure demonstrates that the best case, 2.3, is able to achieve a temperature of 11.9 °C. This indicates that the cooling system used has an important effect on the model's temperature. Overall, the figure suggests that the size of the fins can be adjusted to optimize the performance of the cooling system and achieve the desired surface temperature for the panel.

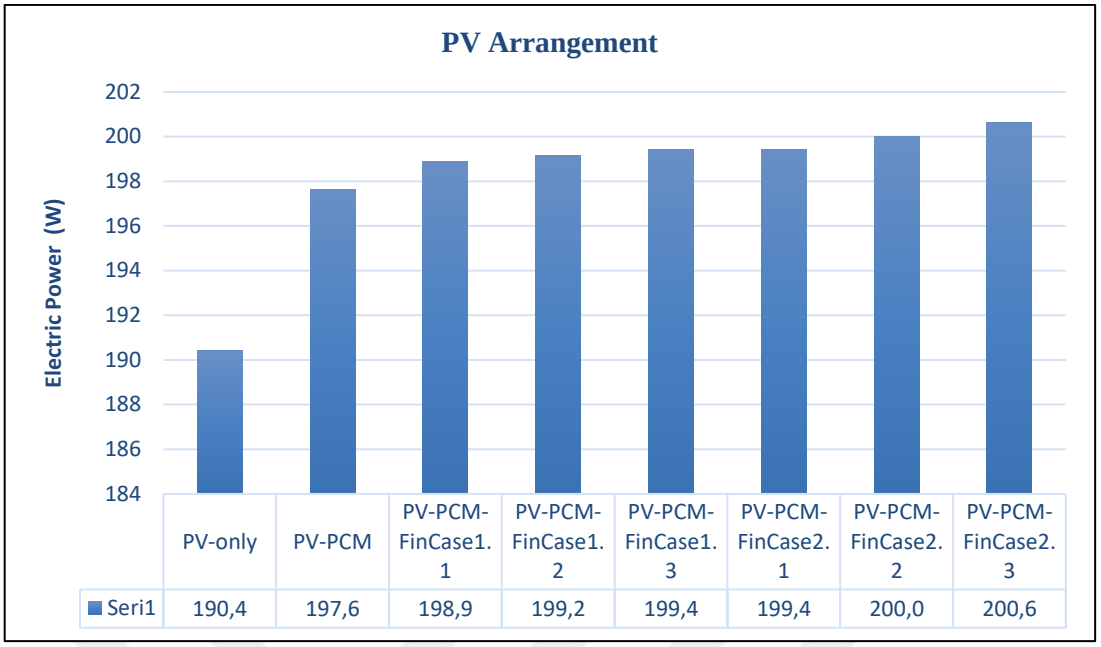

Figure 4.17: Electrical Power Output For PV Arrangements (PV-PCMF).

In Figure 4.21, it was observed that the output power of the panel improved from 190.4 W to 200.6 W after the application of PCM-F (Phase Change Material with fins) in Case 2.3, which was found to be the optimum case. The increase in output power was attributed to the decrease in temperature, which was achieved by the increase in the surface area of the fins. It is known that the performance of a solar panel is affected by temperature. Temperature increases cause a minor rise in current but a drop in voltage. Which in turn leads to a decrease in the panel's output power. However, the application of PCM-F resulted in a low panel temperature, leading to an increase in output power and, as a result, higher electrical efficiency.

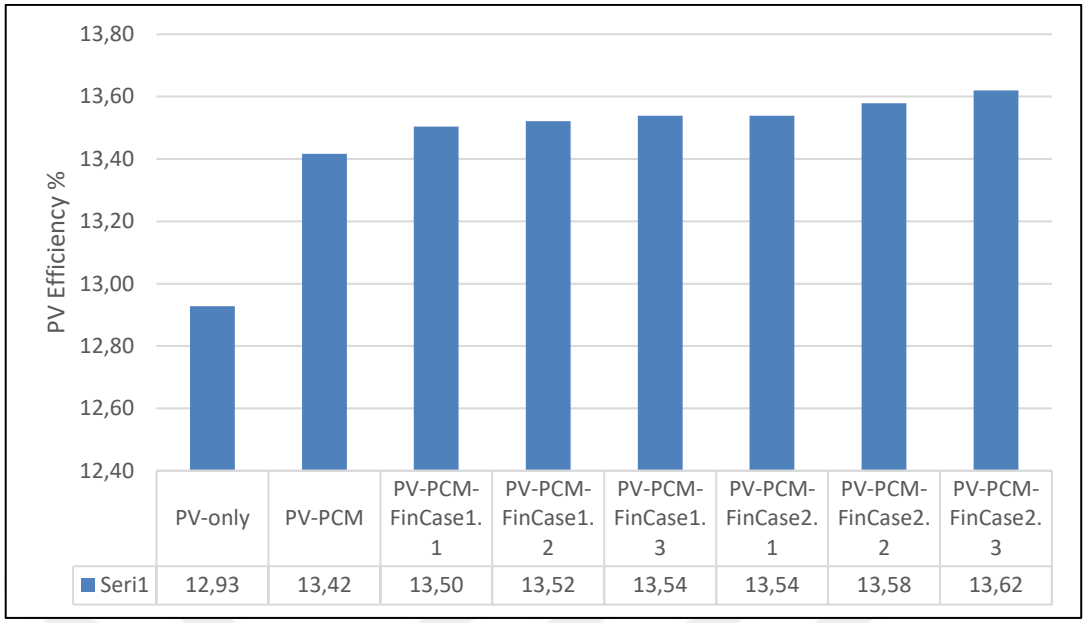

Figure 4.18: Electrical Efficiency PV Arrangement.

The efficiency values of PV-PCMF are presented in Figure 4.22. The electrical efficiency of the PV module was found to be 12.93% with a temperature rise of the cell. After applying PCM, the efficiency improved to 13.42%. The addition of fins further lowered the temperature, leading to an even higher electrical efficiency of 13.62%.

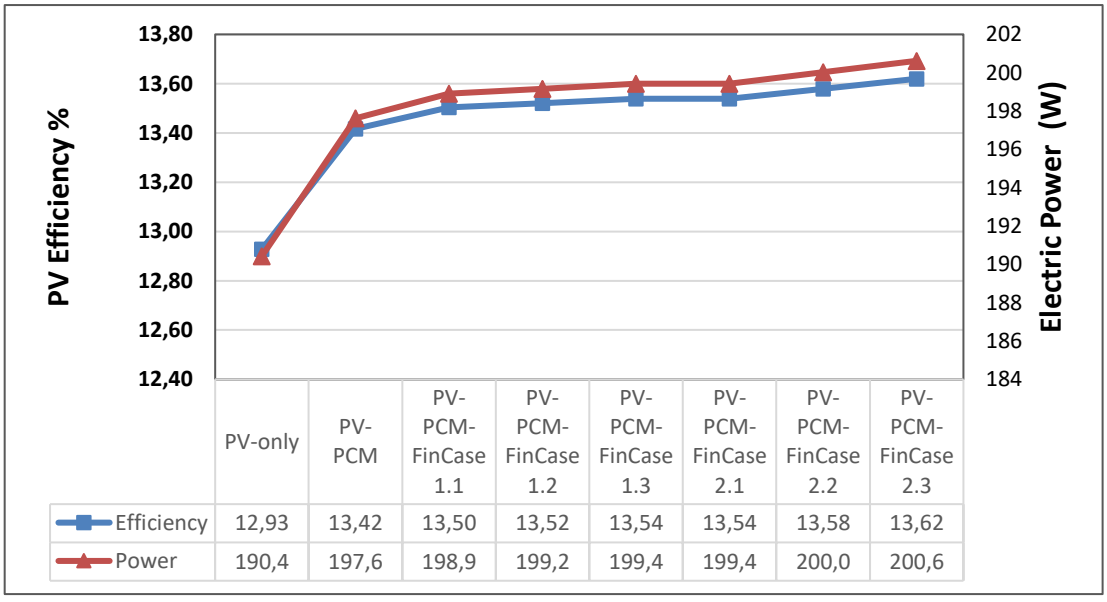

Figure 4.19: Electrical Efficiency And Output Power (W).

4.5 MONOCRYSTALLINE MODULE

Monocrystalline solar cells, made from thin wafers of silicon, are the oldest and most popular type of solar cell technology. They have the highest efficiency, reaching up to 26%, which means that they produce more electricity per unit area of the panel compared to other solar photovoltaic (PV) technologies [109].

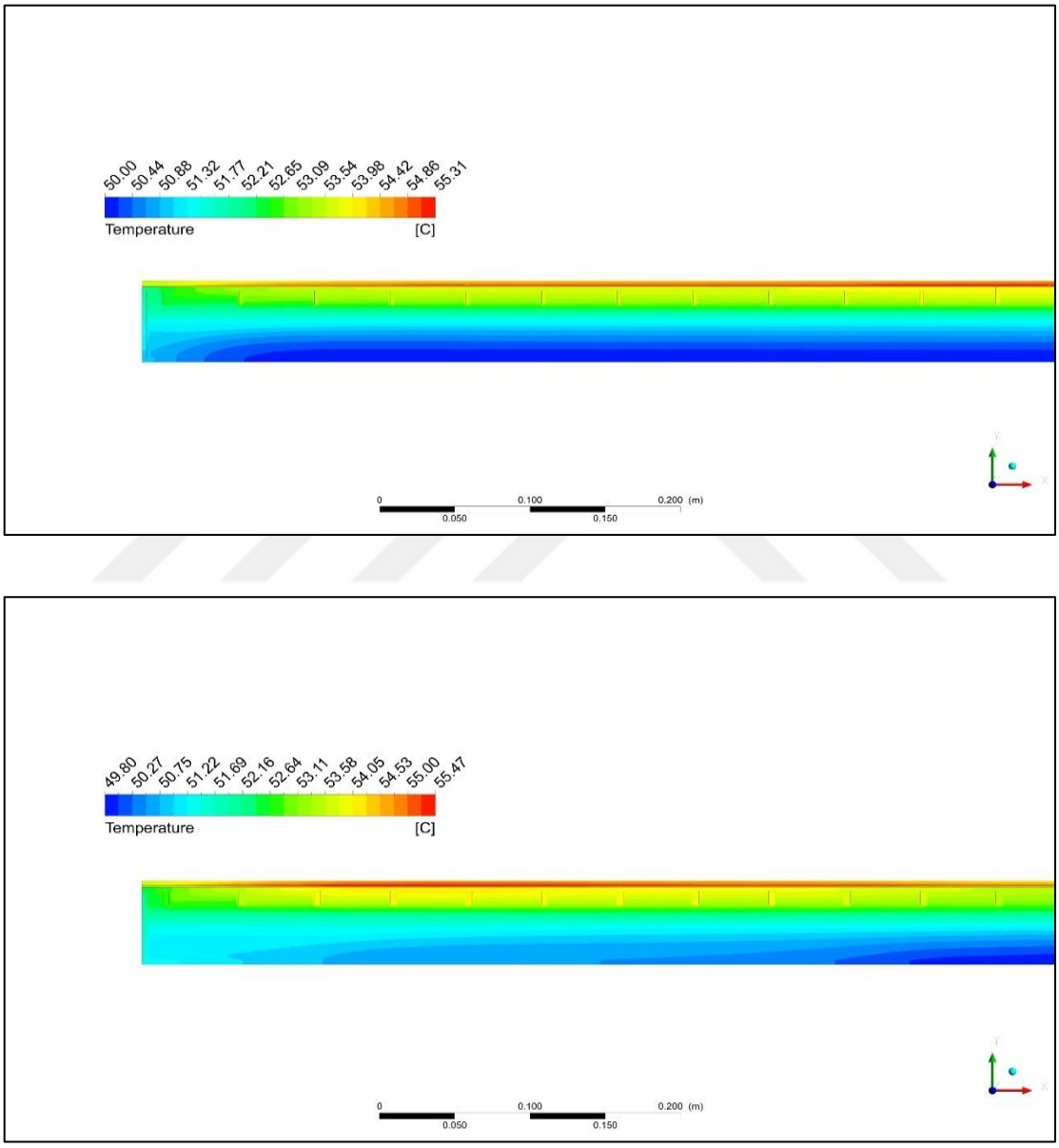

Figure 4.20: Temperature Contour Of The PV –PCM Fins Case1.1 And 1.2.

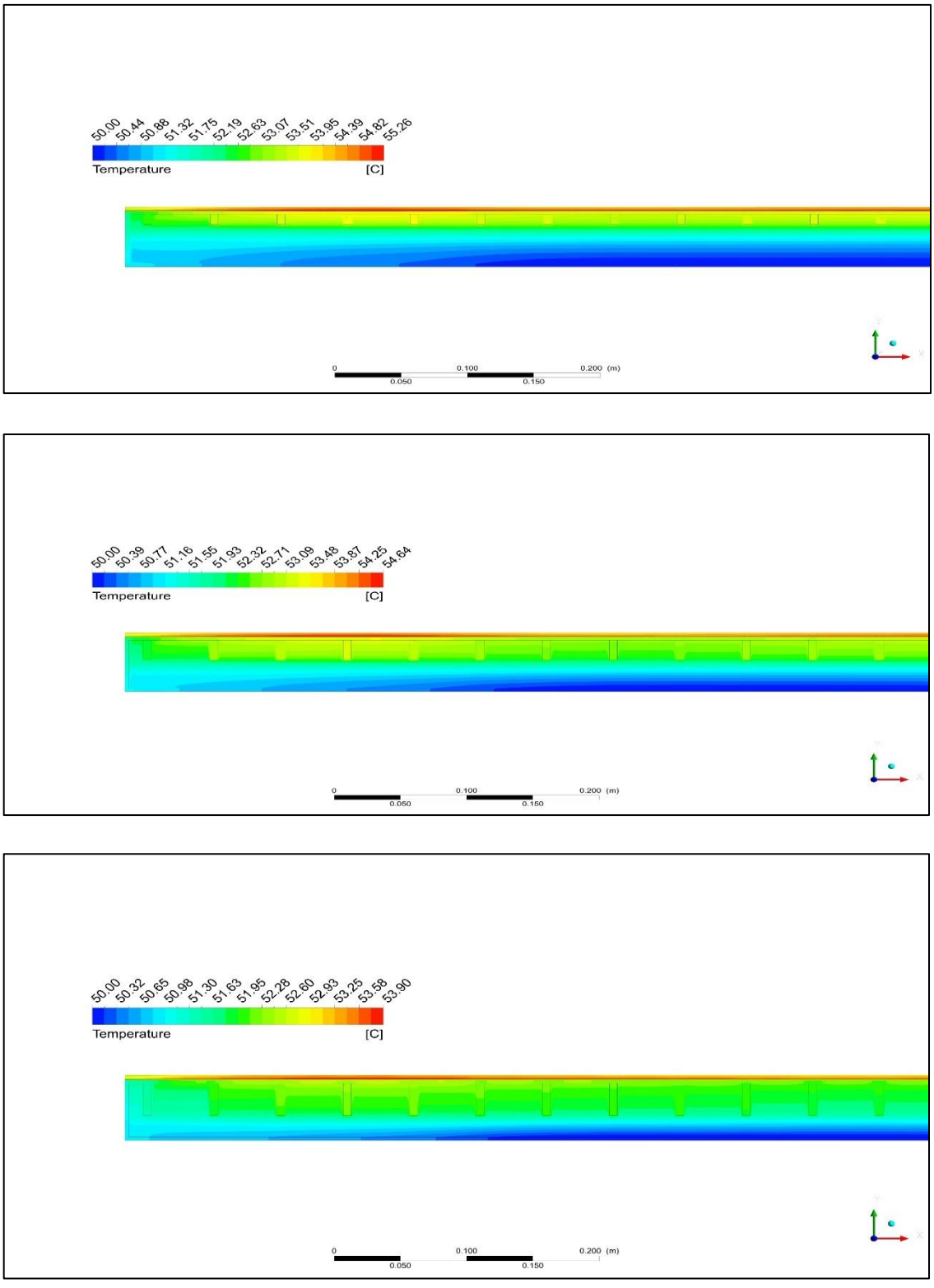

Figure 4.21: Temperature Contour Of The PV –PCM Fins Case (1.3), (2.2) And (2.3)

Figures (4.24) and (4.25) depict the temperature distribution contours for a monocrystalline PV-PCMF (Photovoltaic-Phase Change Material Fin). It can be observed that by

incorporating fins into the PCM, the temperature within the phase change material (PCM) increases due to an enhancement in convection heat transfer. This leads to an increase in the overall thermal activity of the system over time due to the rise in surface area available for heat transfer. The green layer, which represents the regions of high temperature within the PCM, is initially observed to be relatively thin. However, as the size of the fins is changed, as depicted in Cases 2.2 and 2.3, the thickness of this high temperature layer increases accordingly.

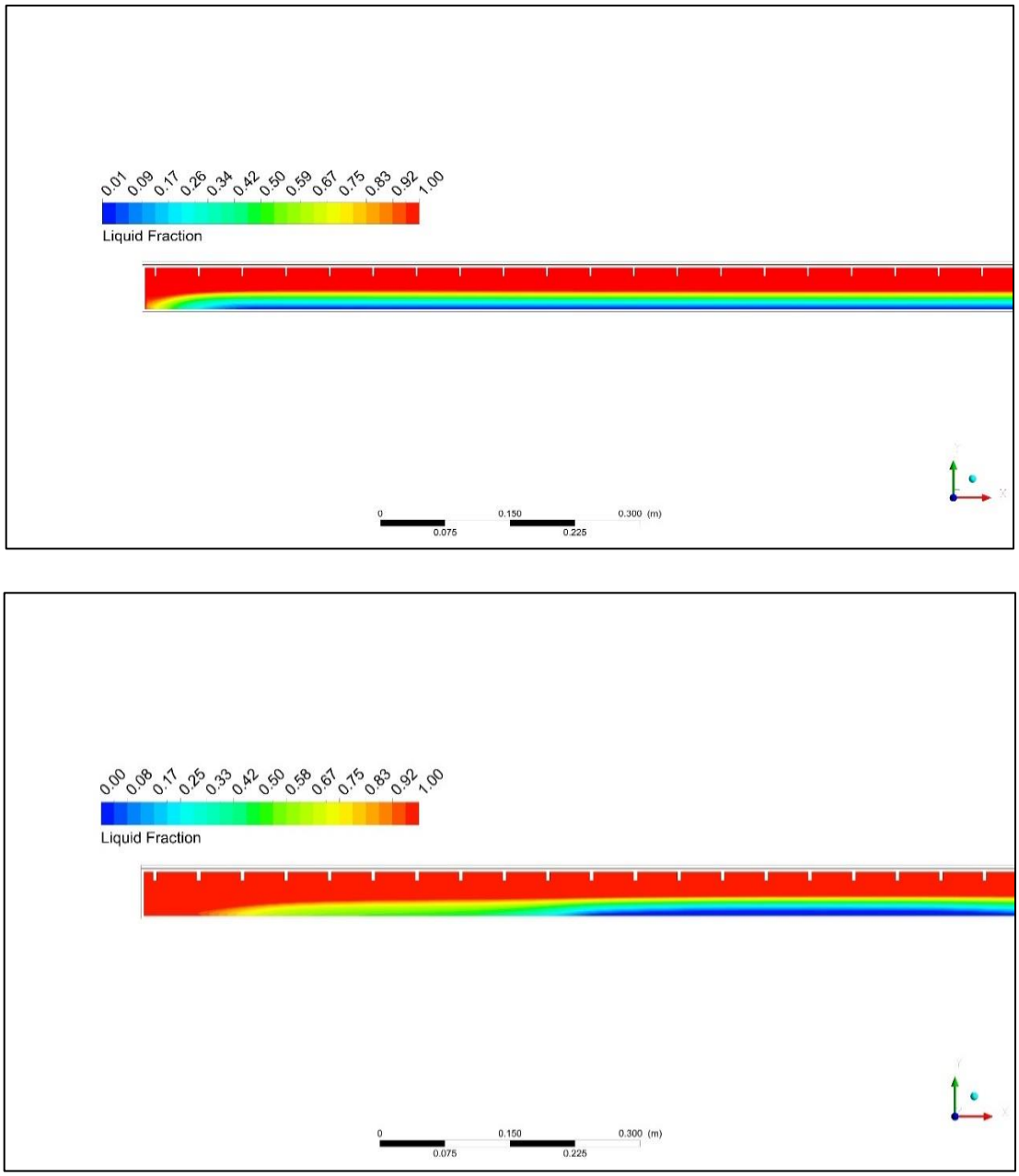

Figure 4.22: Liquid Fraction PV – PCM Fins Case (1.1) (1.2)

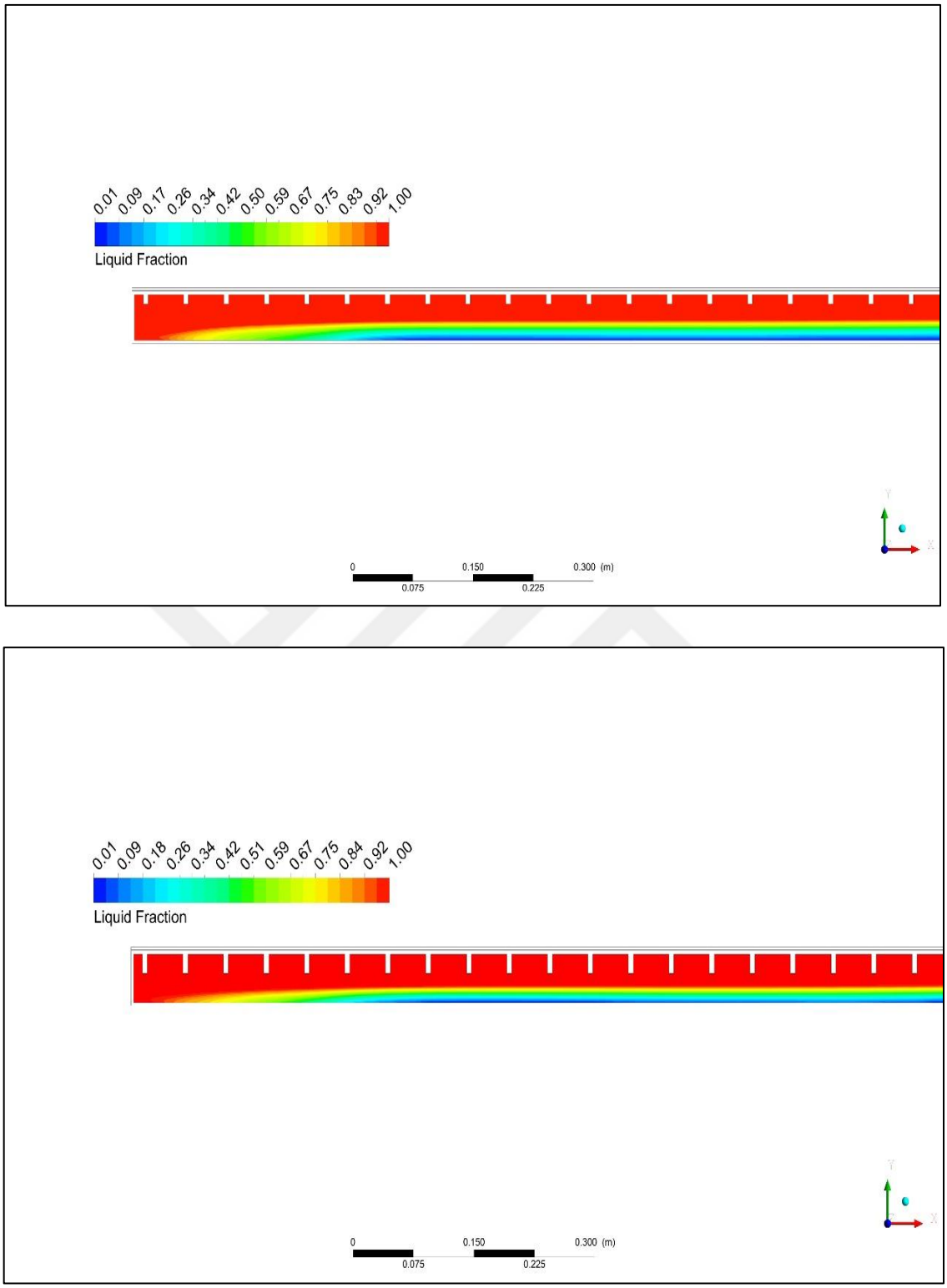

Figure 4.23: Liquid Fraction PV – PCM Fins Case (2.1) And (2.2).

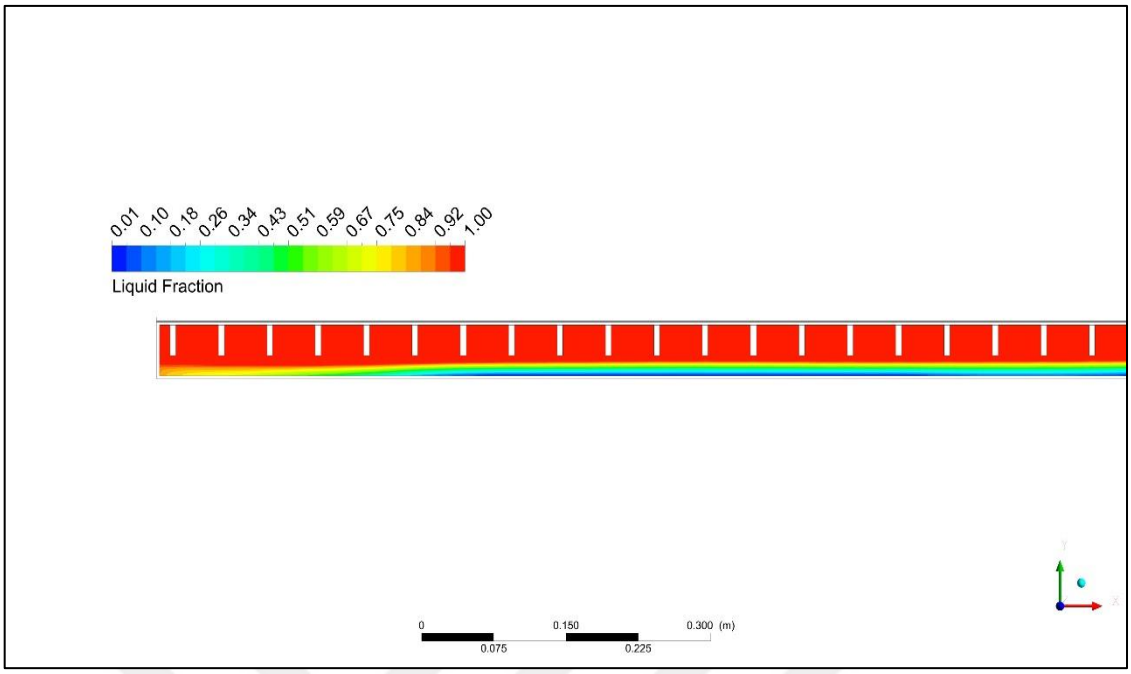

Figure 4.24: Liquid Fraction PV – PCM Fins Case (2.3) "Figures Continued".

Liquid fraction Mono in Figures (4.26), (4.27) and (4.28) the liquid fraction PV-PCMF and phase change for various cases are depicted. In Case 1.1, it can be observed that the red color in the figure represents the thickness of the molten layer that forms at the contact points between the wall of the container and the fins. The molten layer begins to form as a result of the withdrawal of heat from the silicon cell to the wax through conduction, leading to hot currents and an increase in the thickness of the molten layer over time. Additionally, the yellow layer at the left edge of the container indicates the beginning of the phase change due to the heating of the container wall through thermal conductivity.

In Cases 1.2 and 1.3, as the thickness of the fins changed, the amount of heat withdrawn enhanced, leading to a growth in the thickness of the molten layer due to the increase in hot currents flowing toward the solid phase. The increase in the yellow layer in these cases is due to the weak resistance of the solid layer to hot currents.

In Case 2.3, an increase in the length of the fins results in enhanced in heat transfer to the farthest solid area, leading to the fading of the solid area and its appearance as a thin layer. Over time, the wax will completely transition to the liquid phase.

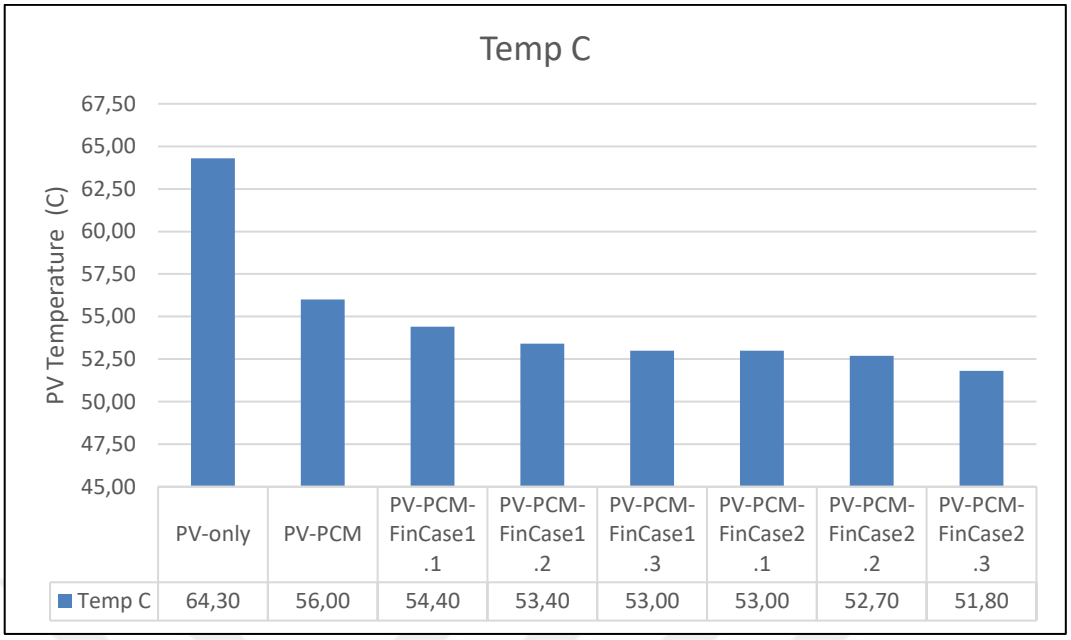

Figure 4.25: Temperature Arrangement Pv-Pcmf In All Cases.

The illustration in figure 4.29 represents the temperature configuration of the PV system utilizing PCMF. It can be seen that, prior to the implementation of the PCM, the temperature of the PV panel was recorded at 64.3 °C. However, after incorporating the PCMF, a reduction in temperature was observed, reaching a value of 56 °C. The addition of fins to the PCM further improves its thermal performance, as depicted in Case 2.3, by increasing the surface area available for heat transfer. This results in a further decline in the temperature of the PV panel, was 51.8 °C, which represents the best-case scenario.

The addition of fins to the Phase Change Material (PCM) in the Photovoltaic system resulted in an improvement in the output power, as indicated in Figure 4.30. The increase in output power was observed to be 200.4 watts, which was attributed to the decline in panel temperature due to the increased surface area of the fins. This reduction in temperature had a positive influence on the performance.

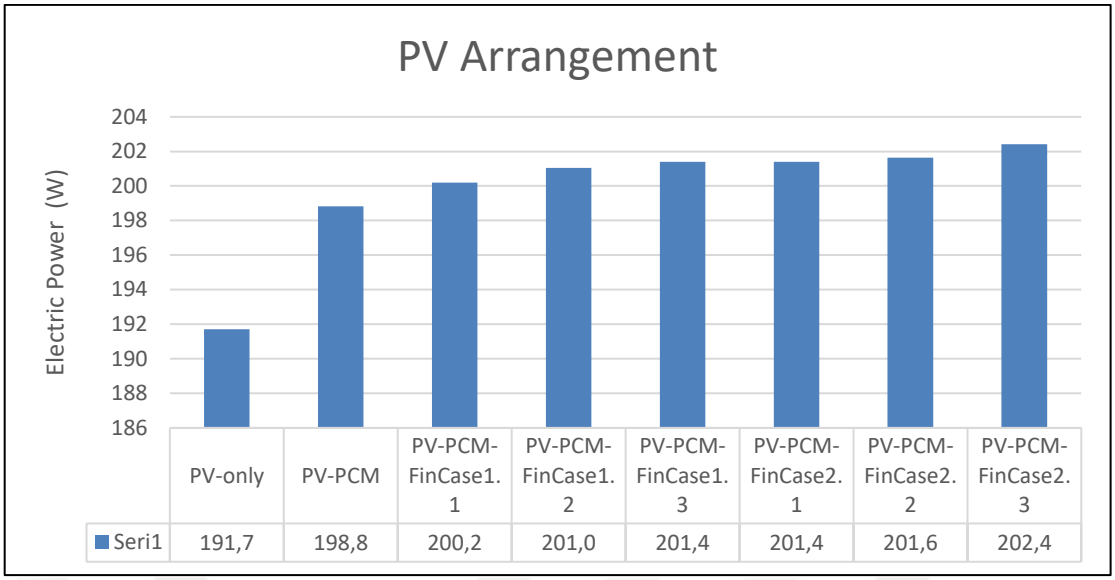

Figure 4.26: Electrical Power Output For PV Arrangements (PV-PCMF).

Figure 4.31 illustrates the PV arrangement and its efficiency. From the figure, it can be seen that Case 2.3 was observed to be the best scenario in terms of improving efficiency. The efficiency of the panel was found to have increased by 13.74%, which was a result of the decline in temperature that was achieved through the implementation of the Phase Change Material (PCM) fins. The lower temperature leads to enhance in the output power and, thus, an improvement in the efficiency of the photovoltaic system.

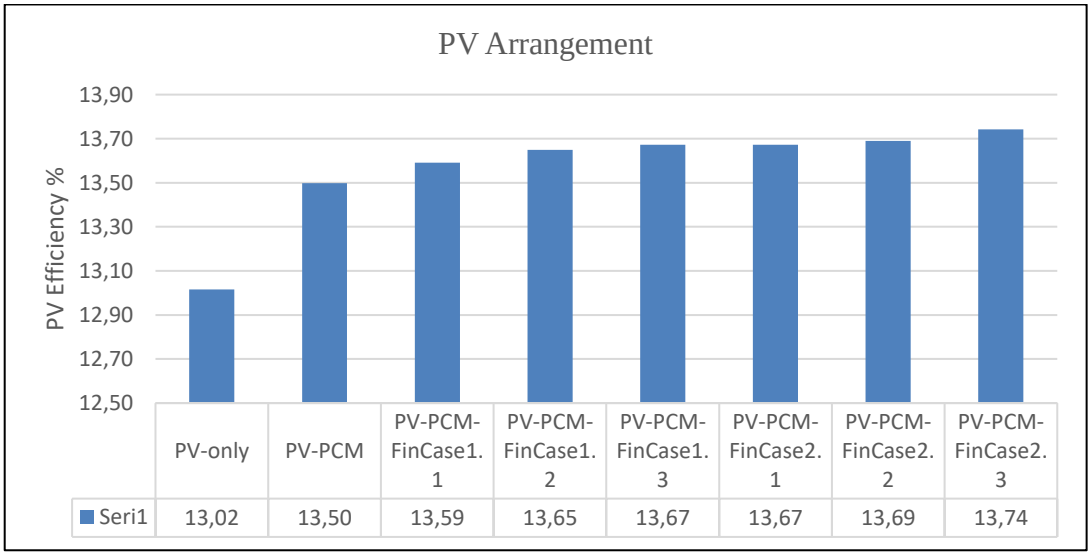

Figure 4.27: Electrical Efficiency PV Arrangement.

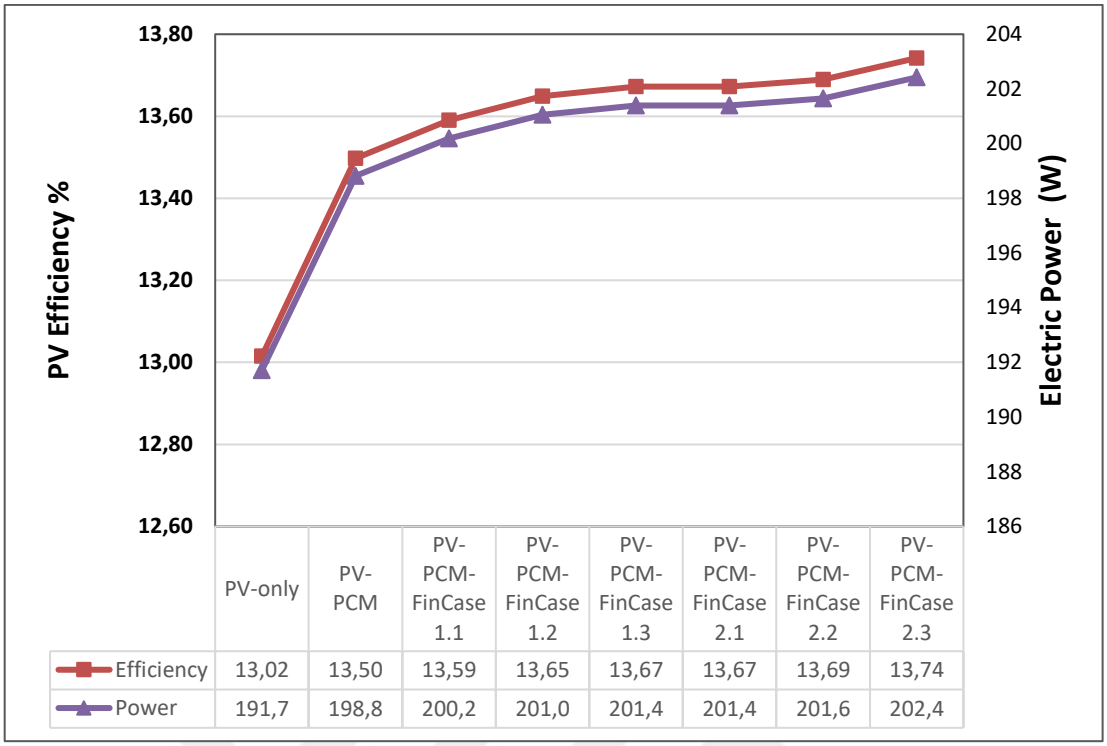

Figure 4.28: Electrical Efficiency And Output Power (W).

4.6 COMPARISON OF POLY-MONOCRYSTALLINE PANELS' PERFORMANCE

Figure 4.33 compares the thermal performances of two types of panels, one monocrystalline and one polycrystalline, with and without cooling. The figure shows that the thermal performance of the monocrystalline panel is slightly better than that of the polycrystalline panel. Due to the fact both the thermal performance coefficient and the thermal conductivity of the monocrystalline panel are better than those of the polycrystalline panel. The poly temperature was measured at 65.8 c without cooling and mono at 64.3 c, after applied PCMFs the temperature notes were 53.9 and 51.8 c, respectively. The monocrystalline panel is more effective at conducting heat and has a higher capacity for thermal performance, leading to better overall thermal performance.

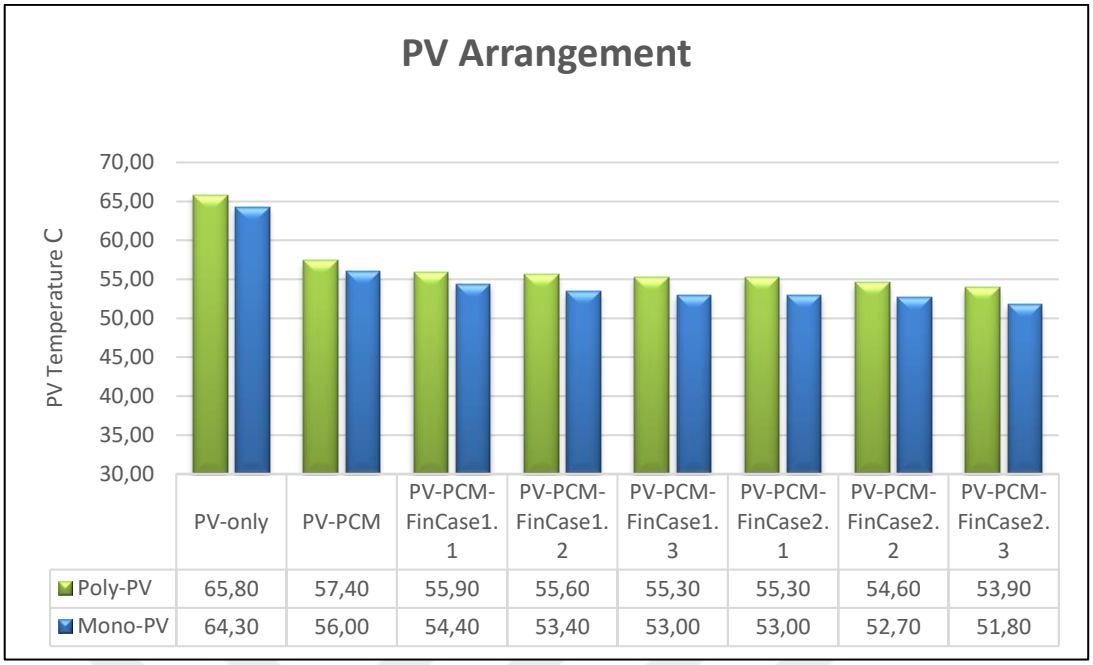

Figure 4.29: Thermal Performance Of Mono-Polycrystalline Panels.

Figure 4.34 compares the electrical performance of monocrystalline and polycrystalline models. The data in the figure suggests that the monocrystalline panel performs electrically better with and without cooling compared with the polycrystalline panel because it recorded a little lower temperature, which leads to enhancement in output power. This is due to the fact that high temperatures can reduce the electrical efficiency. Output power recorded for mono and poly with no cooling applied was 191.7 and 190.4 W, respectively, and with PCMF, it was 202.4 and 200.6 W, respectively, as shown in cases 1.1 and 2.3.

Figure 4.35 illustrates the comparison of the electrical efficiency between poly and monocrystalline photovoltaic cells, with and without cooling. The initial efficiency of the poly model was 12.93%, while the efficiency of the Monocrystalline model was 13.02%. Upon implementing PCMF, the electrical efficiency improved to 13.62% and 13.74% for the poly and monocrystalline models, respectively.

Observed that the monocrystalline model exhibited a slightly better electrical efficiency compared to the poly model. This can be attributed to the lower temperature of the poly model, leading to a marginal increase in output power and efficiency. Thus, it can be concluded that the monocrystalline model performs better in high-temperature conditions.

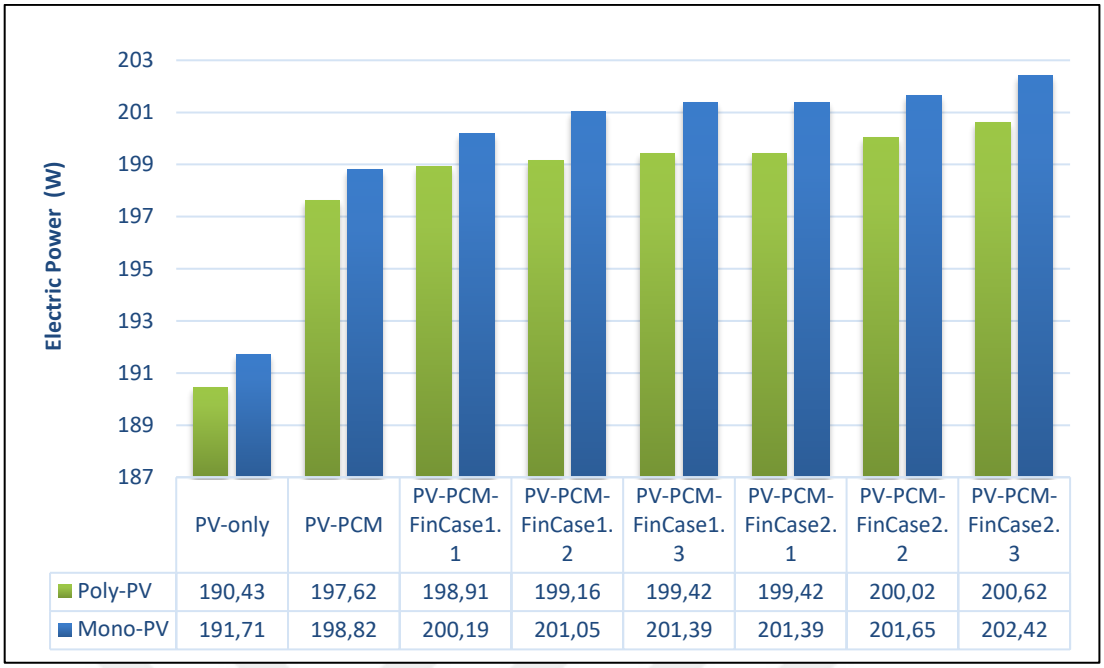

Figure 4.30: Electrical Performance Of Monocrystalline And Polycrystalline Panels.

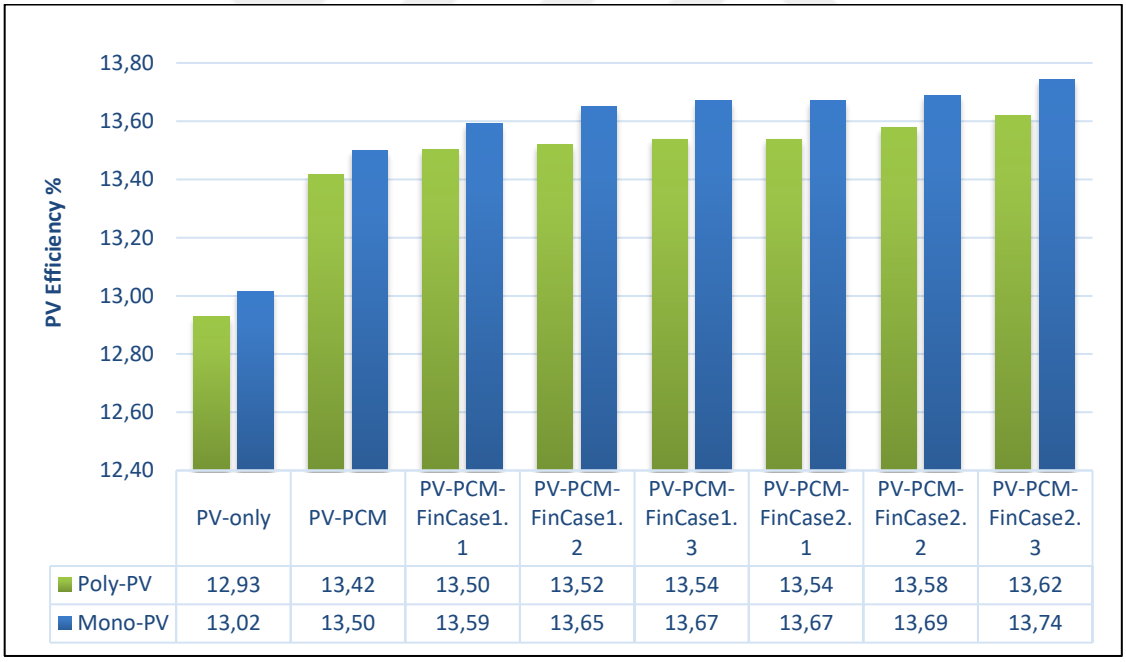

Figure 4.31: Monocrystalline And Polycrystalline Panel Electrical Efficiency.

5. CONCLUSION AND FUTURE SUGGESTION

5.1 CONCLUSION

With a paraffin wax back-cooling system and heatsink, polycrystalline and monocrystalline performance was tested using ANSYS Fluent. The influence of wax thickness was also studied. The aims of this study are to enhance the performance by reducing cell temperature. As high panel temperatures damage decreases its life, and the obtained results of the numerical model can be drawn down as follows:

i. During max solar radiation of 955 w/m2 for an hour, the monocrystalline panel temperature was 1.5 degrees lower than the polycrystalline panel before the application of wax and fins. This suggests that the monocrystalline panel is more resistant to temperature increases when exposed to high levels of solar radiation.

ii. After the applying paraffin wax and fins, the monocrystalline panel demonstrated the best cooling performance compared to the polycrystalline panel, with a temperature that was 2.1 degrees lower. This suggests that the monocrystalline panel is more effective at retaining a lower temperature when cooled using these methods the monocrystalline model output power was higher than the polycrystalline model by 1.3 watts before cooling and by 1.8 watts under the optimal cooling scenario.

iii. Before cooling, the electrical efficiency of the monocrystalline panel was found to be 0.07% higher than that of the polycrystalline panel. After the best cooling strategy was applied, the difference in electrical efficiency between the two panels increased to 0.12%. These results suggest that the monocrystalline panel has a higher inherent electrical efficiency compared to the polycrystalline panel and that this difference becomes more pronounced when cooling methods are used to improve performance.

iv. Thermal reduction, electrical power, and efficiency improvements after cooling are 18%, 19%, 5.2%, 5.3%, 5%, and 5.2% for poly and mono, respectively.

5.2 FUTURE RECOMMENDATION

Cooling photovoltaic (PV) panels is important in order to improve their performance and efficiency. High temperatures can decrease the efficiency of PV panels and reduce their power output. However, the following suggestion could be conducted for future studies as following:

i. Suggested that an alternative organic wax, such as N. Paraffin, be considered as a replacement for the current paraffin wax used.

ii. Different fin configurations, such as perforated fins, or lengthening the fins outside the container exposure to the air, could be used.

iii. Using other metals for fins to enhance thermal conductivity, such as copper.

iv. Addition of nanomaterials to the wax and fins.

REFERENCES

[1] F. Sveučilište u Zagrebu. Fakultet strojarstva i brodogradnje., S. Nižetić, and T. Giuseppe Marco, “Photovoltaic Panels: a Review of the Cooling Techniques,” Transactions of FAMENA, vol. 40, no. SI-1. pp. 63–74, 2000, [Online]. Available: https://hrcak.srce.hr/index.php?id_clanak_jezik=234790&show=clanak.

[2] U.S. EPA, “Part One - The Multiple Benefits of Energy Efficiency and Renewable Energy,” Quantifying Mult. Benefits Energy Effic. Renew. Energy A Guid. State Local Gov., pp. 1–17, 2018, [Online]. Available: https://www.epa.gov/statelocalenergy/quantifying-multiple-benefits-energy-efficiency-and-renewable-energy-guide-state.

[3] N. Yoshino, F. Taghizadeh-Hesary, and M. Otsuka, “Covid-19 and Optimal Portfolio Selection for Investment in Sustainable Development Goals,” Financ. Res. Lett., vol. 38, no. July, p. 101695, 2021, doi: 10.1016/j.frl.2020.101695.

[4] A. Altuwairgi, “Full-spectrum Solar Energy Harvesting for Power and Heat Production using Dichroic Mirror,” no. March, 2022.

[5] N. Kannan and D. Vakeesan, “Solar energy for future world: - A review,” Renew. Sustain. Energy Rev., vol. 62, pp. 1092–1105, 2016, doi: 10.1016/j.rser.2016.05.022.

[6] G. O. G. Löf, J. A. Duffie, and C. O. Smith, “World distribution of solar radiation,” Sol. Energy, vol. 10, no. 1, pp. 27–37, 1966, doi: 10.1016/0038-092X(66)90069-7.

[7] A. M. A. Soliman, D. Hassan, and S. H. Ookawara, “An experimental study of the performance of the solar cell with heat sink cooling system,” Energy Procedia, vol. 162, pp. 127–135, 2019, doi: 10.1016/j.egypro.2019.04.014.

[8] M. Sabry, M. Nahas, and S. H. Al-Lehyani, “Simulation of a standalone, portable steam generator driven by a solar concentrator,” Energies, vol. 8, no. 5, pp. 3867–3881, 2015, doi: 10.3390/en8053867.

[9] A. Saleem, A. Iqbal, K. Mehmood, M. K. Panjwani, F. H. Mangi, and R. M. Larik, “The effect of environmental changes on the efficiency of the PV system,” Indones. J. Electr. Eng. Comput. Sci., vol. 18, no. 1, pp. 558–564, 2019, doi: 10.11591/ijeecs.v18.i1.pp558-564.

[10] B. Moshfegh and M. Sandberg, “Flow and heat transfer in the air gap behind photovoltaic panels,” Renew. Sustain. Energy Rev., vol. 2, no. 3, pp. 287–301, 1998, doi: 10.1016/S1364-0321(98)00005-7.

[11] A. A. Alrobaian, “Performance of PV panel coupled with geothermal air cooling system subjected to hot climatic,” Appl. Therm. Eng., vol. 148, no. November 2017, pp. 1–9, 2019, doi: 10.1016/j.applthermaleng.2018.11.027.

[12] T. M. Razykov, C. S. Ferekides, D. Morel, E. Stefanakos, H. S. Ullal, and H. M. Upadhyaya, “Solar photovoltaic electricity: Current status and future prospects,” Sol. Energy, vol. 85, no. 8, pp. 1580–1608, 2011, doi: 10.1016/j.solener.2010.12.002.

[13] A. Almuwailhi and O. Zeitoun, “Investigating the cooling of solar photovoltaic modules under the conditions of Riyadh,” J. King Saud Univ. - Eng. Sci., no. xxxx, 2021, doi: 10.1016/j.jksues.2021.03.007.

[14] S. Dubey, J. N. Sarvaiya, and B. Seshadri, “Temperature dependent photovoltaic (PV) efficiency and its effect on PV production in the world - A review,” Energy Procedia, vol. 33, pp. 311–321, 2013, doi: 10.1016/j.egypro.2013.05.072.

[15] H. Peng, G. Ding, H. Hu, and W. Jiang, “Effect of nanoparticle size on nucleate pool boiling heat transfer of refrigerant/oil mixture with nanoparticles,” Int. J. Heat Mass Transf., vol. 54, no. 9–10, pp. 1839–1850, 2011, doi: 10.1016/j.ijheatmasstransfer.2010.12.035.

[16] A. Makki, “Innovative Heat Pipe-Based Photovoltaic / Thermoelectric (PV / TEG) Generation System,” 2017.

[17] B. Bradley, “Improving PV Module Efficiency Through Cooling,” Chem. Eng. Undergrad. Honor. Theses, 2020, [Online]. Available: https://scholarworks.uark.edu/cheguht/156.

[18] A. M. P. S. Ni zeti c , F. Grubi si c- Cabo, I. Marini c-Kragi c, “Experimental and numerical investigation of a backside convective cooling mechanism on photovoltaic panels.” p. Energy 111 (2016) 211e225, 2016.

[19] M. Sahli, “Simulation and modelling of thermal and mechanical behaviour of silicon photovoltaic panels under nominal and real-time conditions To cite this version : HAL Id : tel-02520073 Simulation and modelling of thermal and mechanical behaviour of Silicon photovo,” 2020.

[20] J. Y. Usman Jamil Rajput, “Comparison of heat sink and water type PV/T collector for polycrystalline photovoltaic panel cooling,” p. Renewable Energy (2017), doi: 10.1016 /j.renene., 2017.

[21] M. Aghaei et al., “Review of degradation and failure phenomena in photovoltaic modules,” Renew. Sustain. Energy Rev., vol. 159, no. July 2021, p. 112160, 2022, doi: 10.1016/j.rser.2022.112160.

[22] S. Vunnam, M. VanithaSri, and A. RamaKoteswaraRao, “Performance analysis of mono crystalline, poly crystalline and thin film material based 6 × 6 T-C-T PV array under different partial shading situations,” Optik (Stuttg)., vol. 248, no. June, p. 168055, 2021, doi: 10.1016/j.ijleo.2021.168055.

[23] N. S. B. and N. Chander, “Performance comparison of mono and polycrystalline silicon solar photovoltaic modules under tropical wet and dry climatic conditions in east-central India.” pp. 165–177.

[24] T. M. Bruton, “General trends about photovoltaics based on crystalline silicon,” Sol. Energy Mater. Sol. Cells, vol. 72, no. 1–4, pp. 3–10, 2002, doi: 10.1016/S0927-0248(01)00145-3.

[25] M. Katoch, K. Kumar, and V. Dahiya, “Dust accumulation and reduction in electrical performance of solar PV panels,” Mater. Today Proc., vol. 46, no. xxxx, pp. 6608–6612, 2020, doi: 10.1016/j.matpr.2021.04.082.

[26] M. R. Maghami, H. Hizam, C. Gomes, M. A. Radzi, M. I. Rezadad, and S. Hajighorbani, “Power loss due to soiling on solar panel: A review,” Renew. Sustain. Energy Rev., vol. 59, pp. 1307–1316, 2016, doi: 10.1016/j.rser.2016.01.044.

[27] S. Efficiency, “Key Factors for Solar Performance,” Sunpower, [Online]. Available: https://us.sunpower.com/sites/sunpower/files/media-library/white-papers/wp-key-factors-solar-performance.pdf.

[28] A. K. Tripathi, S. Ray, M. Aruna, and S. Prasad, “Evaluation of solar PV panel performance under humid atmosphere,” Mater. Today Proc., vol. 45, no. xxxx, pp. 5916–5920, 2020, doi: 10.1016/j.matpr.2020.08.775.

[29] Q. Zhong and D. Tong, “Spatial layout optimization for solar photovoltaic (PV) panel installation,” Renew. Energy, vol. 150, pp. 1–11, 2020, doi: 10.1016/j.renene.2019.12.099.

[30] A. Rahmatmand, S. J. Harrison, and P. H. Oosthuizen, “An experimental investigation of snow removal from photovoltaic solar panels by electrical heating,” Sol. Energy, vol. 171, no. July, pp. 811–826, 2018, doi: 10.1016/j.solener.2018.07.015.

[31] V. K., “An Overview of Factors Affecting the Performance of Solar PV Systems,” Energy Scan, no. February, pp. 2–8, 2017, [Online]. Available: https://www.researchgate.net/publication/319165448.

[32] A. R. Amelia et al., “Cooling on Photovoltaic Panel Using Forced Air Convection Induced by DC Fan,” Int. J. Electr. Comput. Eng., vol. 6, no. 2, p. 526, 2016, doi: 10.11591/ijece.v6i2.9118.

[33] T. Nabil and T. M. Mansour, “Augmenting the performance of photovoltaic panel by decreasing its temperature using various cooling techniques,” Results Eng., vol. 15, no. August, p. 100564, 2022, doi: 10.1016/j.rineng.2022.100564.

[34] A. M. P. Müslüm Arıcı, Feyza Bilgin, Sandro Nižetić, “Phase change material based cooling of photovoltaic panel: A simplified numerical model for the optimization of the phase change material layer and general economic evaluation.” 2018, doi: 10.1016/j.jclepro.2018.04.057.

[35] S. Maiti, S. Banerjee, K. Vyas, P. Patel, and P. K. Ghosh, “Self regulation of photovoltaic module temperature in V-trough using a metal-wax composite phase change matrix,” Sol. Energy, vol. 85, no. 9, pp. 1805–1816, 2011, doi: 10.1016/j.solener.2011.04.021.

[36] M. Jun Huang, “The effect of using two PCMs on the thermal regulation performance of BIPV systems,” Sol. Energy Mater. Sol. Cells, vol. 95, no. 3, pp. 957–963, 2011, doi: 10.1016/j.solmat.2010.11.032.

[37] P. H. Biwole, P. Eclache, and F. Kuznik, “Phase-change materials to improve solar panel’s performance,” Energy Build., vol. 62, pp. 59–67, 2013, doi: 10.1016/j.enbuild.2013.02.059.

[38] C. J. Smith, P. M. Forster, and R. Crook, “Global analysis of photovoltaic energy output enhanced by phase change material cooling,” Appl. Energy, vol. 126, pp. 21–28, 2014, doi: 10.1016/j.apenergy.2014.03.083.

[39] A. Hasan, S. J. McCormack, M. J. Huang, and B. Norton, “Characterization of phase change materials for thermal control of photovoltaics using Differential Scanning Calorimetry and Temperature History Method,” Energy Convers. Manag., vol. 81, pp. 322–329, 2014, doi: 10.1016/j.enconman.2014.02.042.

[40] K. Kant, A. Shukla, A. Sharma, and P. H. Biwole, “Heat transfer studies of photovoltaic panel coupled with phase change material,” Sol. Energy, vol. 140, pp. 151–161, 2016, doi: 10.1016/j.solener.2016.11.006.

[41] P. Royo, V. J. Ferreira, A. M. López-Sabirón, and G. Ferreira, “Hybrid diagnosis to characterise the energy and environmental enhancement of photovoltaic modules using smart materials,” Energy, vol. 101, no. 2016, pp. 174–189, 2016, doi: 10.1016/j.energy.2016.01.101.

[42] and W. N. I. B. Hasan Mahamudul , Md. Momtazur Rahman, H. S. C. Metselaar, Saad Mekhilef, S. A. Shezan , Rana Sohel, Sayuti Bin Abu Karim, “Temperature Regulation of Photovoltaic Module Using Phase Change Material: A Numerical Analysis and Experimental Investigation.” 2016, doi: https://doi.org/10.1155/2016/5917028.

[43] S. Preet, “Water and phase change material based photovoltaic thermal management systems: A review,” Renew. Sustain. Energy Rev., vol. 82, no. September 2017, pp. 791–807, 2018, doi: 10.1016/j.rser.2017.09.021.

[44] A. K. Suresh, S. Khurana, G. Nandan, G. Dwivedi, and S. Kumar, “ScienceDirect Role on nanofluids in cooling solar photovoltaic cell to enhance overall efficiency,” Mater. Today Proc., vol. 5, no. 9, pp. 20614–20620, 2018, doi: 10.1016/j.matpr.2018.06.442.

[45] M. Nouira, “Numerical study of an inclined photovoltaic system coupled with phase change material under various operating conditions.” pp. 958–975, 2018, doi: https://doi.org/10.1016/j.applthermaleng.2018.06.039.

[46] Z. Li, T. Ma, J. Zhao, A. Song, and Y. Cheng, “Experimental study and performance analysis on solar photovoltaic panel integrated with phase change material,” Energy, vol. 178, pp. 471–486, 2019, doi: 10.1016/j.energy.2019.04.166.

[47] J. Zhao, T. Ma, Z. Li, and A. Song, “Year-round performance analysis of a photovoltaic panel coupled with phase change material,” Appl. Energy, vol. 245, no. January, pp. 51–64, 2019, doi: 10.1016/j.apenergy.2019.04.004.

[48] N. K. Sharma, M. K. Gaur, and C. S. Malvi, “Application of phase change materials for cooling of solar photovoltaic panels: A review,” Mater. Today Proc., vol. 47, no. xxxx, pp. 6759–6765, 2020, doi: 10.1016/j.matpr.2021.05.127.

[49] H. G. Abdulmunem R. Abdulmunem , Pakharuddin Mohd Samin , Hasimah Abdul Rahman , Hashim A. Hussien , Izhari Izmi Mazali, “Numerical and experimental analysis of the tilt angle’s effects on the characteristics of the melting process of PCM-based as PV cell’s backside heat sink.” pp. 520–530, 2021.

[50] S. M. Ciril Arkar , Tej ˇZiˇzak , Suzana Domjan, “Comparative analysis of free cooling of photovoltaics – phase change versus evaporative cooling.” p. 104162, 2022, doi: https://doi.org/10.1016/j.est.2022.104162.

[51] M. R. A. P. and A. R. P. Zainal Arifi, Suyitno Suyitno , Dominicus Danardono Dwi Prija Tjahjana, Wibawa Endra Juwana, “The Effect of Heat Sink Properties on Solar Cell Cooling Systems.” The Effect of Heat Sink Properties on Solar Cell Cooling Systems, 2020.

[52] M. Alzahrani, H. Baig, K. Shanks, and T. Mallick, “Estimation of the performance limits of a concentrator solar cell coupled with a micro heat sink based on a finite element simulation,” Appl. Therm. Eng., vol. 176, no. August 2019, p. 115315, 2020, doi: 10.1016/j.applthermaleng.2020.115315.

[53] P. Atkin and M. M. Farid, “Improving the efficiency of photovoltaic cells using PCM infused graphite and aluminium fins,” Sol. Energy, vol. 114, pp. 217–228, 2015, doi: 10.1016/j.solener.2015.01.037.

[54] J. H. J. Danish Ansari, “A novel variable-height-pinfin isothermal heat sink for densely-packed concentrated photovoltaic systems.” p. 115519, 2022.

[55] R. Salehi, A. Jahanbakhshi, M. Reza Golzarian, and M. Khojastehpour, “Evaluation of solar panel cooling systems using anodized heat sink equipped with thermoelectric module through the parameters of temperature, power and efficiency,” Energy Convers. Manag. X, vol. 11, no. April, p. 100102, 2021, doi: 10.1016/j.ecmx.2021.100102.

[56] A. Ahmed, G. Zhang, K. Shanks, S. Sundaram, Y. Ding, and T. Mallick, “Performance evaluation of single multi-junction solar cell for high concentrator photovoltaics using minichannel heat sink with nanofluids,” Appl. Therm. Eng., vol. 182, no. August 2020, p. 115868, 2021, doi: 10.1016/j.applthermaleng.2020.115868.

[57] H. I. Elqady et al., “Concentrator photovoltaic thermal management using a new design of double-layer microchannel heat sink,” Sol. Energy, vol. 220, no. April 2020, pp. 552–570, 2021, doi: 10.1016/j.solener.2021.02.003.

[58] M. Ibrahim and T. Saeed, “Designing a new heat sink containing nanofluid flow to cool a photovoltaic solar cell equipped with reflector,” J. Taiwan Inst. Chem. Eng., vol. 124, pp. 9–16, 2021, doi: 10.1016/j.jtice.2021.05.015.

[59] E. Johnston, P. S. B. Szabo, and N. S. Bennett, “Cooling silicon photovoltaic cells using finned heat sinks and the effect of inclination angle,” Therm. Sci. Eng. Prog., vol. 23, no. November 2020, p. 100902, 2021, doi: 10.1016/j.tsep.2021.100902.

[60] L. Bilir, Z. Ozcan, M. Gülgün, and S. Ecem, “Cooling channel effect on photovoltaic panel energy generation,” vol. 230, no. November, pp. 943–953, 2021, doi: 10.1016/j.solener.2021.10.086.

[61] A. Abidi, “Evaluation of thermal , electrical and overall efficiency of an air-cooled solar panel equipped with hexagonal pin-fins,” Sustain. Energy Technol. Assessments, vol. 48, no. August, p. 101579, 2021, doi: 10.1016/j.seta.2021.101579.

[62] M. J. Huang, P. C. Eames, and B. Norton, “Phase change materials for limiting temperature rise in building integrated photovoltaics,” Sol. Energy, vol. 80, no. 9, pp. 1121–1130, 2006, doi: 10.1016/j.solener.2005.10.006.

[63] A. Chuttar and D. Banerjee, “Machine learning (ML) based thermal management for cooling of electronics chips by utilizing thermal energy storage (TES) in packaging that leverages phase change materials (PCM),” Electron., vol. 10, no. 22, 2021, doi: 10.3390/electronics10222785.

[64] S. Nižetić, A. M. Papadopoulos, and E. Giama, “Comprehensive analysis and general economic-environmental evaluation of cooling techniques for photovoltaic panels, Part I: Passive cooling techniques,” Energy Convers. Manag., vol. 149, pp. 334–354, 2017, doi: 10.1016/j.enconman.2017.07.022.

[65] M. Emam and M. Ahmed, “Cooling concentrator photovoltaic systems using various configurations of phase-change material heat sinks,” Energy Convers. Manag., vol. 158, no. June 2017, pp. 298–314, 2018, doi: 10.1016/j.enconman.2017.12.077.

[66] S. Khanna, S. Newar, V. Sharma, K. S. Reddy, and T. K. Mallick, “Optimization of fins fitted phase change material equipped solar photovoltaic under various working circumstances,” Energy Convers. Manag., vol. 180, no. October 2018, pp. 1185–1195, 2019, doi: 10.1016/j.enconman.2018.10.105.

[67] R. M., L. S., R. S., A. H., and D. A., “Experimental investigation on the abasement of operating temperature in solar photovoltaic panel using PCM and aluminium,” Sol. Energy, vol. 188, no. February, pp. 327–338, 2019, doi: 10.1016/j.solener.2019.05.067.

[68] S. A. B. Al-Omari, Z. A. Qureshi, E. Elnajjar, and F. Mahmoud, “A heat sink integrating fins within high thermal conductivity phase change material to cool high heat-flux heat sources,” Int. J. Therm. Sci., vol. 172, no. PA, p. 107190, 2022, doi: 10.1016/j.ijthermalsci.2021.107190.

[69] P. Singh et al., “Solar photovoltaic panels with finned phase change material heat sinks,” Energies, vol. 13, no. 10, 2020, doi: 10.3390/en13102558.

[70] T.Wongwuttanasatian and A. S. T. Sarikarin, “Performance enhancement of a photovoltaic module by passive cooling using phase change material in a finned container heat sink T.” pp. 47–53, 2020.

[71] H. G. Teo, P. S. Lee, and M. N. A. Hawlader, “An active cooling system for photovoltaic modules,” Appl. Energy, vol. 90, no. 1, pp. 309–315, 2012, doi: 10.1016/j.apenergy.2011.01.017.

[72] H. C. Sox, “Notice of retraction.,” Ann. Intern. Med., vol. 139, no. 8, p. 702, 2003, doi: 10.7326/0003-4819-139-8-200310210-00017.

[73] P. Valeh-e-sheyda, M. Rahimi, A. Parsamoghadam, and M. M. Masahi, “Ac ce p te cr t,” Energy Build., no. 2014, 2013, doi: 10.1016/j.enbuild.2013.12.052.

[74] A. H. Alami, “Effects of evaporative cooling on efficiency of photovoltaic modules,” Energy Convers. Manag., vol. 77, pp. 668–679, 2014, doi: 10.1016/j.enconman.2013.10.019.

[75] M. S. Abd-Elhady, M. M. Fouad, and T. Khalil, “Improving the efficiency of photovoltaic (PV) panels by oil coating,” Energy Convers. Manag., vol. 115, pp. 1–7, 2016, doi: 10.1016/j.enconman.2016.02.040.

[76] S. Abdo, H. Saidani-Scott, B. Borges, and M. A. Abdelrahman, “Cooling solar panels using saturated activated alumina with saline water: Experimental study,” Sol. Energy, vol. 208, no. April, pp. 345–356, 2020, doi: 10.1016/j.solener.2020.07.079.

[77] A. Homadi, T. Hall, and L. Whitman, “Study a novel hybrid system for cooling solar panels and generate power,” Appl. Therm. Eng., vol. 179, no. May, p. 115503, 2020, doi: 10.1016/j.applthermaleng.2020.115503.

[78] E. B. Agyekum, S. PraveenKumar, N. T. Alwan, V. I. Velkin, and S. E. Shcheklein, “Effect of dual surface cooling of solar photovoltaic panel on the efficiency of the module: experimental investigation,” Heliyon, vol. 7, no. 9, p. e07920, 2021, doi: 10.1016/j.heliyon.2021.e07920.

[79] S. Abdo and H. Saidani-Scott, “Effect of using saturated hydrogel beads with alumina water-based nanofluid for cooling solar panels: Experimental study with economic analysis,” Sol. Energy, vol. 217, no. October 2020, pp. 155–164, 2021, doi: 10.1016/j.solener.2021.01.050.

[80] O. T. Laseinde and M. D. Ramere, “Efficiency Improvement in polycrystalline solar panel using thermal control water spraying cooling,” Procedia Comput. Sci., vol. 180, pp. 239–248, 2021, doi: 10.1016/j.procs.2021.01.161.

[81] S. S. Bhakre, P. D. Sawarkar, and V. R. Kalamkar, “Performance evaluation of PV panel surfaces exposed to hydraulic cooling – A review,” Sol. Energy, vol. 224, no. May, pp. 1193–1209, 2021, doi: 10.1016/j.solener.2021.06.083.

[82] T. Reindl, J. Luther, C. Reise, and Z. Ye, “On PV module temperatures in tropical regions,” vol. 88, pp. 80–87, 2013, doi: 10.1016/j.solener.2012.11.001.

[83] J. Van Deelen, L. Klerk, and M. Barink, “Optimized grid design for thin film solar panels,” Sol. Energy, vol. 107, pp. 135–144, 2014, doi: 10.1016/j.solener.2014.05.028.

[84] J. Zhou, Q. Yi, Y. Wang, and Z. Ye, “ScienceDirect Temperature distribution of photovoltaic module based on finite element simulation,” Sol. ENERGY, vol. 111, pp. 97–103, 2015, doi: 10.1016/j.solener.2014.10.040.

[85] M. S. Naghavi, A. Esmaeilzadeh, B. Singh, B. C. Ang, T. M. Yoon, and K. S. Ong, “Experimental and numerical assessments of underlying natural air movement on PV modules temperature,” Sol. Energy, vol. 216, no. June 2020, pp. 610–622, 2021, doi: 10.1016/j.solener.2021.01.007.

[86] R. E. Pawluk, M. Rezvanpour, Y. Chen, and Y. She, “A sensitivity analysis on effective parameters for sliding/melting prediction of snow cover on solar photovoltaic panels,” Cold Reg. Sci. Technol., vol. 185, no. November 2020, p. 103262, 2021, doi: 10.1016/j.coldregions.2021.103262.

[87] K. Jaiganesh, K. Bharath Simha Reddy, B. K. D. Shobhitha, and B. Dhanush Goud, “Enhancing the efficiency of rooftop solar photovoltaic panel with simple cleaning mechanism,” Mater. Today Proc., vol. 51, no. xxxx, pp. 411–415, 2022, doi: 10.1016/j.matpr.2021.05.565.

[88] J. Kennedy, A. Lo, H. S. Rajamani, and S. Lutfi, “Solar and sand: Dust deposit mitigation in the desert for PV arrays,” Sustain. Energy, Grids Networks, vol. 28, p. 100531, 2021, doi: 10.1016/j.segan.2021.100531.

[89] E. Andenæs, B. P. Jelle, K. Ramlo, T. Kolås, J. Selj, and S. E. Foss, “The influence of snow and ice coverage on the energy generation from photovoltaic solar cells,” Sol. Energy, vol. 159, no. September 2017, pp. 318–328, 2018, doi: 10.1016/j.solener.2017.10.078.

[90] S. Rustemli and F. Dincer, “Modeling of photovoltaic panel and examining effects of temperature in Matlab/Simulink,” Elektron. ir Elektrotechnika, vol. 3, no. 3, pp. 35–40, 2011, doi: 10.5755/j01.eee.109.3.166.

[91] Z. Sun and Z. Yang, “Improved maximum power point tracking algorithm with cuk converter for PV systems,” J. Eng., vol. 2017, no. 13, pp. 1676–1681, 2017, doi: 10.1049/joe.2017.0617.

[92] W. J. Potscavage, A. Sharma, and B. Kippelen, “Critical interfaces in organic solar cells and their influence on the open-circuit voltage,” Acc. Chem. Res., vol. 42, no. 11, pp. 1758–1767, 2009, doi: 10.1021/ar900139v.

[93] J. Dominguez, Solar Energy Engineering Processes and Systems Second Edition. 2014.

[94] H. Hamzah, M. Toifur, and I. Ishafit, “Determination of Fill Factor and Efficiency in Solar Cell Type (99 × 69) mm2 with Arduino Uno R3 Based Drive assisted by Logger Pro 3.14.1,” Indones. Rev. Phys., vol. 2, no. 2, p. 53, 2019, doi: 10.12928/irip.v2i2.1258.

[95] Z. Xu and C. Kleinstreuer, “Concentration photovoltaic-thermal energy co-generation system using nanofluids for cooling and heating,” Energy Convers. Manag., vol. 87, pp. 504–512, 2014, doi: 10.1016/j.enconman.2014.07.047.

[96] E. Skoplaki and J. A. Palyvos, “On the temperature dependence of photovoltaic module electrical performance : A review of efficiency / power correlations,” Sol. Energy, vol. 83, no. 5, pp. 614–624, 2009, doi: 10.1016/j.solener.2008.10.008.

[97] C. Pagkalos, M. G. Vrachopoulos, J. Konstantaras, and K. Lymperis, “Comparing water and paraffin PCM as storage mediums for thermal energy storage applications,” E3S Web Conf., vol. 116, 2019, doi: 10.1051/e3sconf/201911600057.

[98] “User’s guide to safe computing,” Comput. Secur., vol. 11, no. 8, p. 727, 1992, doi: 10.1016/0167-4048(92)90125-b.

[99] M. Ahmed and A. Radwan, “Performance evaluation of new modified low-concentrator polycrystalline silicon photovoltaic/thermal systems,” Energy Convers. Manag., vol. 149, no. May, pp. 593–607, 2017, doi: 10.1016/j.enconman.2017.07.057.

[100] O. Rejeb, M. Sardarabadi, C. Ménézo, M. Passandideh-Fard, M. H. Dhaou, and A. Jemni, “Numerical and model validation of uncovered nanofluid sheet and tube type photovoltaic thermal solar system,” Energy Convers. Manag., vol. 110, pp. 367–377, 2016, doi: 10.1016/j.enconman.2015.11.063.

[101] K. Naumenko and V. A. Eremeyev, “A layer-wise theory for laminated glass and photovoltaic panels,” Compos. Struct., vol. 112, no. 1, pp. 283–291, 2014, doi: 10.1016/j.compstruct.2014.02.009.

[102] S. V. Hudișteanu et al., “Effect of Wind Direction and Velocity on PV Panels Cooling with Perforated Heat Sinks,” Appl. Sci., vol. 12, no. 19, 2022, doi: 10.3390/app12199665.

[103] F. Sarhaddi, S. Farahat, H. Ajam, A. Behzadmehr, and M. Mahdavi Adeli, “An improved thermal and electrical model for a solar photovoltaic thermal (PV/T) air collector,” Appl. Energy, vol. 87, no. 7, pp. 2328–2339, 2010, doi: 10.1016/j.apenergy.2010.01.001.

[104] G. Righetti, L. Doretti, C. Zilio, G. A. Longo, and S. Mancin, “Experimental investigation of phase change of medium/high temperature paraffin wax embedded in 3D periodic structure,” Int. J. Thermofluids, vol. 5–6, p. 100035, 2020, doi: 10.1016/j.ijft.2020.100035.

[105] Joe D. Hoffman, numerical methods for engineers and scientists, vol. 4, no. 1. new york: new york 1992, 2557.

[106] M. A. Mohamed Emam, “Cooling concentrator photovoltaic systems using various configurations of phase-change material heat sinks.” pp. 289–314, 2018.

[107] A. Dmitruk, K. Naplocha, J. Grzęda, and J. W. Kaczmar, “Aluminum inserts for enhancing heat transfer in PCM accumulator,” Materials (Basel)., vol. 13, no. 2, 2020, doi: 10.3390/ma13020415.

[108] J. Zhao, Z. Li, and T. Ma, “Performance analysis of a photovoltaic panel integrated with phase change material,” Energy Procedia, vol. 158, pp. 1093–1098, 2019, doi: 10.1016/j.egypro.2019.01.264.

[109] K. Ranabhat, L. Patrikeev, A. A. evna Revina, K. Andrianov, V. Lapshinsky, and E. Sofronova, “An introduction to solar cell technology,” J. Appl. Eng. Sci., vol. 14, no. 4, pp. 481–491, 2016, doi: 10.5937/jaes14-10879.